JOÃO VINÍCIUS HONÓRIO DA SILVA

EXPOSIÇÃO AO DIMESILATO DE LISDEXANFETAMINA DURANTE A PERIPUBERDADE PROVOCA ALTERAÇÕES EM PARÂMETROS RENAIS E HEPÁTICOS DE RATOS WISTAR

Londrina
2022

JOÃO VINÍCIUS HONÓRIO DA SILVA

EXPOSIÇÃO AO DIMESILATO DE LISDEXANFETAMINA DURANTE A PERIPUBERDADE PROVOCA ALTERAÇÕES EM PARÂMETROS RENAIS E HEPÁTICOS DE RATOS WISTAR

Dissertação apresentada ao Programa de Pós-Graduação em Patologia Experimental, da Universidade Estadual de Londrina - UEL, como requisito parcial para a obtenção do título de Mestre.

Orientadora: Profa. Dra. Glaura Scantamburlo Alves Fernandes.
Coorientador: Prof. Dr. Fábio Goulart de Andrade.

Londrina
2022

Ficha de identificação da obra elaborada pelo autor, através do Programa de Geração Automática do Sistema de Bibliotecas da UEL

da Silva, João Vinícius Honório.

Exposição ao dimesilato de lisdexanfetamina durante a peripuberdade provoca alterações em parâmetros renais e hepáticos de ratos Wistar / João Vinícius Honório da Silva. - Londrina, 2022.
158 f. : il.

Orientador: Glaura Scantamburlo Alves Fernandes.
Coorientador: Fábio Goulart Andrade.
Dissertação (Mestrado em Patologia Experimental) - Universidade Estadual de Londrina, Centro de Ciências Biológicas, Programa de Pós-Graduação em Patologia Experimental, 2022.
Inclui bibliografia.

1. Anfetaminas - Tese. 2. Nefrotoxicidade - Tese. 3. Hepatotoxicidade - Tese. 4. Puberdade - Tese. I. Fernandes, Glaura Scantamburlo Alves. II. Andrade, Fábio Goulart. III. Universidade Estadual de Londrina. Centro de Ciências Biológicas. Programa de Pós-Graduação em Patologia Experimental. IV. Título.

CDU 616

JOÃO VINÍCIUS HONÓRIO DA SILVA

EXPOSIÇÃO AO DIMESILATO DE LISDEXANFETAMINA DURANTE A PERIPUBERDADE PROVOCA ALTERAÇÕES EM PARÂMETROS RENAIS E HEPÁTICOS DE RATOS WISTAR

Dissertação apresentada ao Programa de Pós-Graduação em Patologia Experimental, da Universidade Estadual de Londrina - UEL, como requisito parcial para a obtenção do título de Mestre.

BANCA EXAMINADORA

_____

Orientadora: Profa. Dra. Glaura Scantamburlo Alves Fernandes
Universidade Estadual de Londrina - UEL

_____

Coorientador: Prof. Dr. Fábio Goulart de Andrade
Universidade Estadual de Londrina - UEL

_____

Prof. Dr. Waldiceu Aparecido Verri Junior
Universidade Estadual de Londrina - UEL

_____

Profa. Dra. Graziela Scalianti Ceravolo
Universidade Estadual de Londrina – UEL

Londrina, 6 de junho de 2022.

AGRADECIMENTOS

Antes de tudo, sou extremamente grato a Deus, pelo dom da vida e do conhecimento. Ele foi quem me deu força para não desistir durante o caminho, e me ajudou a se sentir capacitado para me tornar um pesquisador.

Aos meus pais, Tatiana e Claudio, que sempre confiaram e abraçaram meus sonhos e planos. Vocês são meu exemplo de vida e profissionais, meu porto seguro. Espero um dia retribuir tudo que me proporcionaram. Amo vocês!

À Profa. Dra. Glaura Scantamburlo Alves Fernandes, que foi muito mais que uma orientadora, se tornou uma amiga. Obrigado por ter me aceito para compor o seu grupo de pesquisa, acreditando no meu potencial como pesquisador. Se eu estou aqui, é graças as oportunidades que a senhora me possibilitou. Contigo aprendi não somente questões acadêmicas e científicas, como por exemplo escrever um e-mail para colaboradores, técnicas, e escrita científica, mas também aprendi a ser uma pessoa melhor, e um futuro cientista no mínimo excelente.

Ao Prof. Dr. Fábio Goulart de Andrade, ou melhor, somente Fábio, me faltam palavras que consigam descrever tamanho respeito, admiração e gratidão que tenho por ti. Se eu estou defendendo meu mestrado, saiba que grande parcela é devido a oportunidade que você deu no CPCB de 2016. Durante a graduação e mestrado, aprendi contigo sobre questões científicas e isso aumentou ainda mais meu amor pela ciência. Obrigado por acreditar em mim, por escutar meus áudios gigantes, e por cada conversa, café e momentos de alegria ou tristeza que compartilhei contigo durante essa trajetória.

Aos alunos, técnicos e professores que colaboraram para que esse projeto acontecesse, auxiliando para que fosse possível realizar técnicas importantes para este trabalho. Muitos foram os que ajudaram, portanto, para não esquecer o nome de algum, agradeço aos laboratórios: Laboratório de Toxicologia e Distúrbios Metabólicos da Reprodução (profa. Dra. Glaura); Laboratório de Análise Histopatológica (prof. Dr. Fábio); Laboratório de Dor, Inflamação, Neuropatia e Câncer (prof. Dr. Waldiceu); Laboratório de Patologia Animal (profa. Dra. Ana Paula); Laboratório de Neuroendocrinologia (prof. Dr. Ernane); e Laboratório de Imunologia de Transplantes (Prof. Dr. Niels).

À Universidade Estadual de Londrina e ao Programa de Pós-Graduação em Patologia Experimental, pela oportunidade e conhecimento passado aos discentes. Agradeço imensamente também à CAPES (Coordenação de Aperfeiçoamento de Pessoal de Nível Superior) pelo auxílio financeiro.

Aos meus amigos do mestrado (Carol, Beatriz, Luca, Rafaela e Lucas), da graduação (Renan, Letícia, Talissa, Priscila, Júlia e Veridiana), da imuno-USP (Ranieri, Isis e Luís) e da vida (Mari Valezi, Gi Pedrini, Anna Betio, Luana, Beatriz Zanoni, Angela, João Chiesa, Gi Negri, Amanda de Paula), meu muito obrigado por não desistirem da minha amizade, e entenderem minha ausência muitas vezes.

À minha psicóloga e psiquiatra, por toda ajuda oferecida para que eu conseguisse manter minha saúde mental durante esse período.

Agradeço também aos membros da banca, prof. Dr. Waldiceu Aparecido Verri Junior e profa. Dra. Graziela Scalianti Ceravolo, por aceitarem, primeiramente compor a banca de qualificação, e agora compor a banca de defesa de mestrado. É uma honra tê-los novamente avaliando minha dissertação, professores tão qualificados, de renome, e que eu tenho grande admiração e respeito pelos profissionais que são.

E por fim, mas não menos importante, gostaria de deixar um agradecimento especial e necessário, a todos os professores e professoras do mundo, que persistem nessa árdua profissão, principalmente no Brasil onde não é devidamente valorizada a educação. Sou grato a todos os professores que disponibilizaram um pouco do seu conhecimento para que eu chegasse até aqui. Agradeço especialmente, além do Fábio e da Glaura, as professoras Gabriela Cortellete, Geni Zafalon, Andressa Niwa, Bruna Hirata, Maria Angélica Watanabe, Carolina Ariza, Laura Condota, Larissa Bosqui, e ao prof. Phileno, por me inspirarem e incentivarem durante as diferentes etapas da minha caminhada, a seguir e buscar o que eu almejava.

“Conheça todas as teorias, domine todas as técnicas, mas ao tocar uma alma humana, seja apenas outra alma humana.”

Carl Jung

RESUMO

SILVA, João Vinícius Honório da. **Exposição ao dimesilato de lisdexanfetamina durante a peripuberdade provoca alterações em parâmetros renais e hepáticos de ratos Wistar**. 2022. 152 f. Dissertação (Mestrado em Patologia Experimental) – Universidade Estadual de Londrina, Londrina, 2022.

O Transtorno de Déficit de Atenção/Hiperatividade (TDAH) é um transtorno neurocomportamental caracterizado por sintomas como desatenção, hiperatividade ou impulsividade, causando prejuízos à qualidade de vida das pessoas. O dimesilato de lisdexanfetamina (LDX) é um psicoestimulante do sistema nervoso central amplamente recomendado para o tratamento do TDAH e pouco se sabe sobre sua possível toxicidade em órgãos como o fígado e os rins uma vez que o fígado é órgão relacionado no metabolismo da maioria das drogas e está envolvido em diversas funções do organismo, e os rins são responsáveis pela excreção dos fármacos e seus metabólitos. Portanto, o presente estudo tem como objetivo avaliar os efeitos da exposição de LDX na morfofisiologia hepática e renal de ratos Wistar púberes, expostos ao LDX durante o período peripuberal. Para isso, 20 ratos Wistar machos foram distribuídos aleatoriamente em dois grupos experimentais: Grupo LDX (LDX) - recebeu 11,3 mg/kg/dia de LDX diluído em água da torneira; e Grupo Controle (C) - recebeu água da torneira. Os animais foram tratados por gavagem (via oral) do dia pós-natal (PND) 25 a 65. No PND 66, os animais ficaram em jejum de 12 horas, e foram anestesiados e eutanasiados por punção da veia cava inferior. O plasma foi coletado e destinado à dosagem de marcadores de lesão hepática, metabolismo lipídico e função renal. O fígado, rins e tecido adiposo branco foram coletados e pesados. O fígado e rins foram destinados para determinações do perfil inflamatório (atividade de MPO e NAG), biomarcadores de estresse oxidativo (concentração de MDA e GSH, atividade da SOD, GST e CAT), análises histoquímicas (coloração de Picrosirius red, ácido periódico de Schiff, tricrômico de Azan Heidenhain, azul de Toluidina) e morfométricas. Além disso, nos rins foi realizada a imunohistoquímica para Caspase-3 de modo a avaliar o número de células em apoptose. Os resultados mostraram que a administração de LDX causou diminuição do peso do tecido adiposo branco, sem alterar o ganho de peso. A concentração plasmática de ALT e AST aumentaram, indicando lesão hepática por esse fármaco. Além disso, LDX causou aumento na atividade de NAG, indicando indiretamente um aumento do recrutamento de macrófagos para o fígado, e redução da atividade da GST ao avaliar o status de estresse oxidativo. Em relação aos rins, a administração de LDX causou redução no diâmetro médio do túbulo contorcido proximal e distal, e aumento no número de células em processo de apoptose na região cortical. A atividade da NAG e MPO foi aumentada após o uso de LDX, indicando indiretamente maior recrutamento de macrófagos e neutrófilos, respectivamente, para os rins. Além disso, nos rins de animais pertencentes ao grupo LDX houve aumento na atividade de antioxidantes como a CAT e GST, redução na concentração de GSH e níveis normais de MDA. Em conclusão, esses resultados mostram que a administração de LDX em ratos durante o período peripuberal, prejudica o fígado e os rins na idade puberal.

Palavras-chave: anfetamina; nefrotoxicidade; hepatotoxicidade; inflamação; puberdade

ABSTRACT

SILVA, João Vinícius Honório da. **Exposure to lisdexamfetamine dimesylate during peripuberty causes changes in renal and hepatic parameters of Wistar rats**. 2022. 152 p. Dissertation (Master's degree in Experimental Pathology) – Universidade Estadual de Londrina, Londrina, 2022.

Attention-Deficit/Hyperactivity Disorder (ADHD) is a neurobehavioral disorder characterized by symptoms such as inattention, hyperactivity, or impulsivity, causing damage to people's quality of life. Lisdexamfetamine dimesylate (LDX) is a central nervous system psychostimulant widely recommended for the treatment of ADHD. Little is known about its possible toxic effects on organs such as the liver and kidneys, since the liver is involved in the metabolism of most drugs and is involved in several body functions, and the kidneys are responsible for the excretion of drugs and their metabolites. Therefore, the present study aims to evaluate the effects of LDX exposure on hepatic and renal morphophysiology of pubertal Wistar rats exposed to LDX during the peripubertal period. For this, 20 male Wistar rats were randomly assigned to two experimental groups: LDX Group (LDX) - received 11.3 mg/kg/day of LDX diluted in tap water; and Control Group (C) - received tap water. The animals were treated by gavage (orally) from postnatal day (PND) 25 to 65. In PND 66, the animals were fasted for 12 hours, and were anesthetized and euthanized by puncture of the inferior vena cava. Plasma was collected and destined for measurement of markers of liver injury, lipid metabolism and renal function. Liver, kidneys, and white adipose tissue were collected and weighed. The liver and kidneys were destined for determinations of the inflammatory profile (MPO and NAG activity), oxidative stress biomarkers (MDA and GSH concentration, SOD, GST and CAT activity), histochemical (Picrosirius red staining, periodic acid of Schiff, Azan Heidenhain trichrome, Toluidine blue) and morphometric analyzes. In addition, immunohistochemistry for Caspase-3 was performed in the kidneys to assess the number of cells undergoing apoptosis. The results showed that LDX administration caused a decrease in white adipose tissue weight, without altering weight gain. Plasmatic concentrations of ALT and AST increased, indicating liver injury by this drug. Furthermore, LDX caused an increase in NAG activity, indirectly indicating a recruitment of macrophages to the liver, and a reduction in GST activity when assessing oxidative stress status. Regarding the kidneys, the administration of LDX caused a reduction in the mean diameter of the proximal and distal convoluted tubules, and an increase in the number of cells undergoing apoptosis in the cortical region. NAG and MPO activity was increased after the use of LDX, indirectly indicating a major recruitment of macrophages and neutrophils, respectively, to the kidneys. In addition, in the kidneys of animals from the LDX group there was an increase in the activity of antioxidants such as CAT and GST, a reduction in the concentration of GSH and normal levels of MDA. In conclusion, these results show that the administration of LDX in male rats during the peripubertal period, impairs the liver and kidneys at pubertal age.

Key words: amphetamine; nephrotoxicity; hepatotoxicity; inflammation; puberty

LISTA DE FIGURAS

LISTA DE ABREVIATURAS E SIGLAS

-OH	Radicais hidroxila
ADH	Hormônio antidiurético ou vasopressina
ALT	Alanina aminotransferase
ANCA	Anticorpo anti-citoplasma de neutrófilos
APC	Célula apresentadora de antígeno
AST	Aspartato aminotransferase
ATP	Adenosina trifosfato
CAT	Catalase
CCL2	Ligante de quimiocina de motivo CC
CCR7	Receptor de quimiocina de motivo CC
CD1d	Glicoproteína de superfície apresentadora de antígeno
Cl-	Íon cloreto
CX3CR1	Receptor 1 de quimiocina de motivo C-X3-C
DAMPs	Padrões moleculares associados a danos
DC	Ducto coletor
DNA	Ácido desoxirribonucleico
DSM	Manual Diagnóstico e Estatístico de Transtornos Mentais
EROs	Espécies reativas de oxigênio
G6P	Glicose-6-fosfato
GLUT2	Transportador de glicose tipo 2
GM-CSF	Fator estimulador de colônias de granulócitos e macrófagos
GPx	Glutationa peroxidase
Gred	Glutationa redutase
GSH	Glutationa
GST	Glutationa-S-transferase
H2O2	Peróxido de hidrogênio
HCO3+	Bicarbonato
H+	Íon de hidrogênio
IFN-y	Interferon gama
IL	Interleucina
ILC1s	Células linfoides inatas do grupo 1
JNK	Quinase N-terminal c-Jun

K+	Íon potássio
LDX	Dimesilato de lisdexnfetamina
LPS	Lipopolissacarídeo
MAO	Monoamina oxidase
MDSC	Células supressoras derivadas de mieloides
MHC	Complexo principal de histocompatibilidade
Na+	Íon sódio
Na+/K+ ATPase	Bomba de sódio e potássio
NaCl	Cloreto de sódio
NADPH	Nicotinamida adenina dinucleotídeo fosfato
NAG	N-acetil-β-D-glucosaminidase
Nf-κB	Fator nuclear kappa B
NK	Natural killer
NKCC2	Na+-K+-2Cl- cotransportador
NOAEL	Nível Sem Efeitos Adversos Observáveis
NKT	T natural killer
O2-	Ânion superóxido
PAMPs	Padrões moleculares associados a patógenos
PD-L1	Ligante 1 de morte programada
PEPT1	Transportador de peptídeos 1
PGE2	Prostaglandina E2
PRRs	Receptores de reconhecimento de padrão
RNA	Ácido ribonucleico
SNC	Sistema nervoso central
SOD	Superóxido dismutase
SOD1	Cu,Zn-superóxido dismutase
SOD2	Mn-superóxido dismutase
SRAA	Sistema renina angiotensina aldosterona
T-bet	Fator de transcrição T-bet
TBARS	Substâncias reativas ao ácido tiobarbitúrico
TCD	Túbulo contorcido distal
TCP	Túbulo contorcido proximal
TDAH	Transtorno de Déficit de Atenção e Hiperatividade
TGF-β	Fator de crescimento transformador beta

Th1	T helper 1
Th2	T helper 2
Th17	T helper 17
TNF	Fator de necrose tumoral
TNF-α	Fator de necrose tumoral alfa

SUMÁRIO

1 INTRODUÇÃO

1.1 ASPECTOS HISTOFISIOLÓGICOS DO FÍGADO

O fígado é o maior órgão maciço do corpo, seu peso corresponde a 2-5% do peso corporal médio (SI-TAYEB et al., 2010). Encontra-se internamente no quadrante superior direito da cavidade abdominal, abaixo do diafragma (ABDEL-MISIH; BLOOMSTON, 2010).

Sua estrutura tecidual é repleta de diferentes tipos celulares, entre os quais, os hepatócitos, que representam aproximadamente 70% das células hepáticas. As demais células são: colangiócitos, células endoteliais, células endoteliais sinusoidais, células estreladas hepáticas e diversos tipos de células do sistema imunológico, mas principalmente células *natural killer* (NK) do fígado e células de Kupffer (macrófagos residentes do fígado) (SI-TAYEB et al., 2010).

Esses diferentes tipos celulares estão dispostos em torno dos lóbulos, que são a unidade morfofuncional do fígado, onde circula o sangue, recebendo cerca de 25% do débito cardíaco total (FREITAS-LOPES et al., 2017). À primeira vista, sua arquitetura aparenta ser simples, porém é extremamente complexa. Essa estrutura, como observado na Figura 1, consiste em cordões poligonais de hepatócitos, sinusoides, veia central (ou centrolobular) e a tríade portal, composta pela veia porta, artéria hepática e ducto biliar (GORDILLO et al., 2015).

Figura 1. Estrutura de um lóbulo hepático e seus constituintes

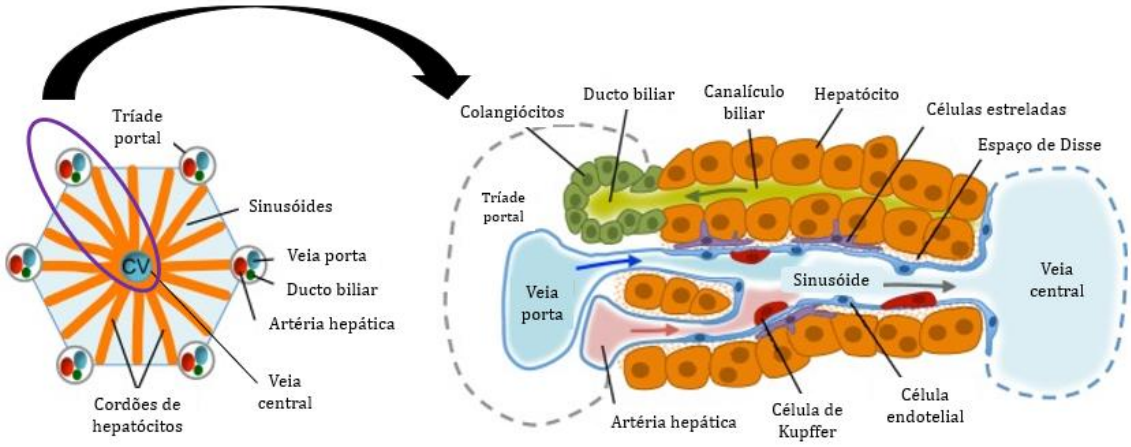

Fonte: Modificado de Gordillo et al. (2015)

Os sinusoides são os menores vasos sanguíneos do fígado,

responsáveis por transportar o sangue no lóbulo hepático, da veia porta e da artéria hepática até a veia central (SI-TAYEB et al., 2010).

O esquema hemodinâmico hepático é único e complexo. Resumidamente, o sangue advindo da circulação portal se unirá com o sangue arterial da artéria hepática, o qual é rico em oxigênio. Este fluirá lentamente entre os sinusoides em direção à veia central, aonde chegará desoxigenado. A arquitetura vascular é extremamente especializada, possibilitando com que haja uma interação eficaz entre a circulação sistêmica e as células hepáticas, permitindo com que o fígado possa realizar suas funções metabólicas (FREITAS-LOPES et al., 2017; TREFTS et al., 2017).

Como há diferença no sangue que sai da tríade portal ao que chega à veia central, a função dos hepatócitos também será diferente conforme sua localização no lóbulo. Por este motivo, o lóbulo é dividido em 3 “zonas metabólicas”, como é possível observar na Figura 2, que facilita a diferenciação funcional e metabólica dos hepatócitos (GRIJALVA; VAKILI, 2013).

Figura 2. Lóbulo hepático dividido em zonas metabólicas

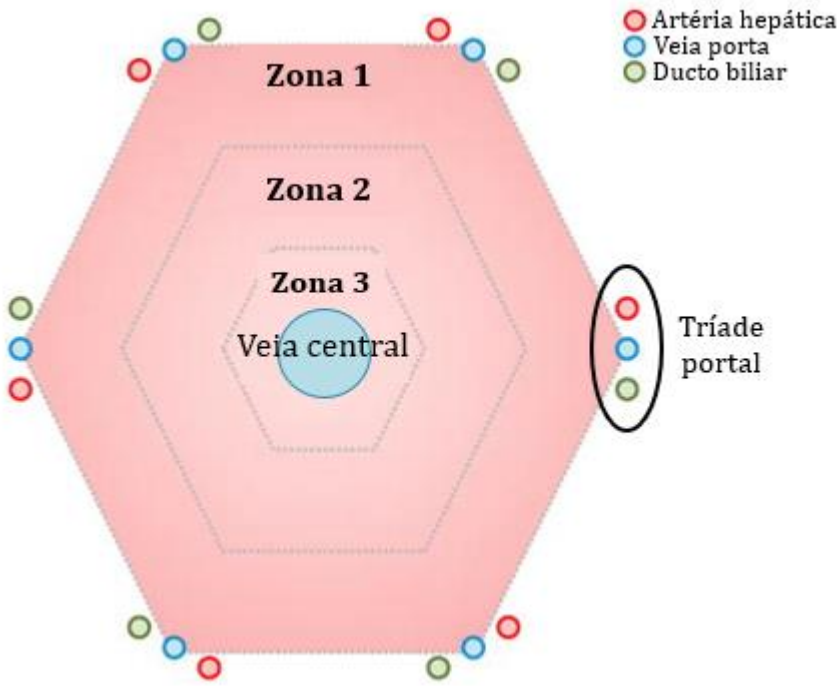

Fonte: Modificado de Trefts et al. (2017)

Os hepatócitos apresentam morfologia cuboide, estão dispostos em

forma de cordões, e executam diversas funções atribuídas ao fígado, principalmente as funções metabólicas (GORDILLO et al., 2015). Nestas células, as superfícies basolaterais encontram-se próximas das células endoteliais sinusoidais fenestradas, que permite que as substâncias produzidas pelos hepatócitos atinjam facilmente a corrente sanguínea (SI-TAYEB et al., 2010). As funções dos hepatócitos diferem de acordo com a localização no lóbulo hepático, portanto, os que estão na zona 1, que é próximo a tríade portal, realizam funções como gliconeogênese e β-oxidação, devido a maior oxigenação tecidual nesta região; na zona 2 os hepatócitos podem apresentar funções semelhantes aos da zona 1 e 3 quando necessário e dependendo de sua proximidade relativa; e por fim, os da zona 3, próximos a veia central, são responsáveis pela síntese de ureia, biotransformação, glicólise, lipogênese e síntese de triglicerídeos (HIJMANS et al., 2014; TREFTS et al., 2017).

Os colangiócitos são células epiteliais biliares, portanto, formam o epitélio do ducto biliar, para transporte e manutenção da bile. As células endoteliais têm como principal função a organização tecidual para facilitar a irrigação, filtração e circulação sanguínea, participando da constituição dos sinusoides e dos demais vasos sanguíneos, como as veias, artérias, vênulas e arteríolas (SI-TAYEB et al., 2010). O principal componente mesenquimal do fígado são as células estreladas hepáticas, que ficam no espaço de Disse, e podem existir tanto em um estado quiescente ou ativado. Quando no estado quiescente, atuam principalmente como reservatório de vitamina A, já em estado ativado, ou seja, quando o fígado está sofrendo alguma injúria, diferenciam-se em células com atividades semelhantes a um miofibroblasto e, portanto, controlam o tônus microvascular, fazem a manutenção da matriz extracelular e secretam citocinas para ocorrer a regeneração tecidual (GORDILLO et al., 2015).

Além das células responsáveis por fazer com que o fígado seja conhecido principalmente pela sua função metabólica, cada vez mais vem sendo descrito como um órgão imunológico, já que abriga uma população complexa de células imunes e tem papel importante na hematopoiese durante o período embrionário (FREITAS-LOPES et al., 2017; MAFRA et al., 2019).

Outra característica morfológica importante do fígado é sua ampla inervação, sendo muito estudada por estar intimamente relacionada as diferentes funções hepáticas. Portanto, a inervação hepática acaba sendo responsável por ações como regular o apetite, monitorar mudanças na osmolaridade sanguínea, regular a função do sistema biliar e do epitélio biliar, sensor de glicose, lipídios, alguns

hormônios gastrointestinais (ex. incretinas) e interleucinas (IL), por exemplo (JENSEN et al., 2013).

Compreendendo a anatomia e a constituição tecidual do fígado, torna-se mais fácil o entendimento de suas diversas funções, dado que este é a maior glândula do corpo e apresenta funções endócrinas e exócrinas (SI-TAYEB et al., 2010).

O fígado é extremamente conhecido por realizar a síntese e liberação de proteínas plasmáticas (ex. albumina e proteínas da coagulação), metabolismo de glicose, ácidos graxos, ureia e colesterol, síntese biliar, secreção de diferentes hormônios, armazenamento de glicogênio, biotransformação para desintoxicação de xenobióticos, além das funções imunológicas (SI-TAYEB et al., 2010).

As proteínas plasmáticas sintetizadas pelo fígado compreendem aproximadamente 85-90% do volume de proteínas circulantes, sendo a albumina a mais abundante. Além de sintetizar, também consegue quebrá-las e metabolizar os aminoácidos, o que auxilia na produção de energia para as células realizarem suas funções. Entretanto, esse processo gera muitos resíduos nitrogenados, que precisam ser eliminados e, por este motivo o fígado também é responsável pelo ciclo da ureia (TREFTS et al., 2017).

A bile é produzida a partir do colesterol e secretada pelos hepatócitos. É então drenada através dos canalículos biliares até chegar ao ducto hepático comum, responsável por transportá-la para a vesícula biliar, onde é armazenada (FREITAS-LOPES et al., 2017). Apresenta grande importância na absorção intestinal de determinados compostos e na digestão de gorduras (MARIN et al., 2015).

O fígado também realiza a desintoxicação de xenobióticos. Com a participação das enzimas do citocromo P450, realiza a biotransformação/metabolização dos xenobióticos, transformando-os em metabólitos de fácil excreção (GRIJALVA; VAKILI, 2013).

Outra função extremamente importante, como já citado, é a sua relação com os processos metabólicos, principalmente no metabolismo energético, utilizando glicose, aminoácidos e ácidos graxos. Esses processos são rigidamente controlados por diversos fatores de transcrição e correguladores (TREFTS et al., 2017).

A glicose sanguínea ao chegar no fígado, entrará nos hepatócitos por meio do transportador de glicose tipo 2 (GLUT2), e será principalmente fosforilada

para gerar glicose-6-fosfato (G6P). A G6P é responsável por diversos mecanismos metabólicos celulares, uma vez que pode atuar estimulando a glicólise gerando piruvato, para produzir ATP (adenosina trifosfato); fornecer substratos para a síntese de glicogênio (glicogênese); e gerar NADPH. O piruvato e o NADPH produzidos, são moléculas importantes no processo de lipogênese. Muitos desses processos dependem do estado alimentar do indivíduo, se está alimentado, em jejum ou em fase pós-prandial. Por exemplo no estado de jejum, a fim de atender as necessidades energéticas do organismo, ocorre a glicogenólise, via responsável por hidrolisar o glicogênio (RUI, 2014).

Além da glicose, o fígado também consegue utilizar os ácidos graxos como fonte energética através de oxidação. Nesta via metabólica é possível sintetizar colesterol como fonte de energia não somente para o fígado, mas para outros tecidos; e glicerolipídios, como os fosfolipídios que compõem a estrutura da membrana plasmática. (PONZIANI et al., 2015).

1.1.1 Fígado e Inflamação

Muito se tem discutido, sobre a importância do fígado como um órgão imunológico complexo, desmistificando aquela visão de ser principalmente um órgão envolvido em atividades metabólicas (CRISPE, 2009; MAFRA et al., 2019).

Além das células de Kupffer, que são os macrófagos residentes do fígado, há outras células do sistema imune inato e adaptativo no fígado: células dendríticas, células supressoras derivadas de mieloides (MDSC), células T ($CD8^+$ e $CD4^+$), células B, células NK, células T *natural killer* (NKT) e células T reguladoras (Treg) (BOGDANOS et al., 2013; ROBINSON et al., 2016).

As células de Kupffer se encontram ancoradas no endotélio sinusoidal. Já a maior parte da população linfoide e das células dendríticas, em condições fisiológicas, encontram-se próximas à tríade portal, e há um número menor espalhado por todo o parênquima (BOGDANOS et al., 2013).

Por ser um órgão extremamente vascularizado, e que recebe uma grande demanda de sangue, é extremamente exposto a antígenos, que podem ser inofensivos, como os componentes dietéticos e produtos bacterianos da microbiota intestinal (ex. LPS), ou nocivos, como xenobióticos, patógenos e células cancerosas. Diante disso, as células imunológicas do fígado apresentam mecanismos que

asseguram a tolerância imunológica, liberando por exemplo IL-10 e PGE_2, e expressando PD-L1, mas que durante um processo danoso, patológico, podem assumir mecanismos para gerar uma resposta inflamatória (ROBINSON et al., 2016).

Em um ambiente fisiologicamente estável, as células de Kupffer e os hepatócitos, agem identificando, por meio de PRRs (receptores de reconhecimento de padrão) em sua superfície, os PAMPs (padrões moleculares associados a patógenos) e DAMPs (padrões moleculares associados a danos), que posteriormente serão removidos por estas mesmas células através da fagocitose (ROBINSON et al., 2016). Por este motivo, encontram-se majoritariamente ancoradas nas células endoteliais no interior dos sinusoides, para facilitar o contato com a circulação sanguínea e assim captarem os microrganismos invasores e responderem efetivamente frente a ameaças, estabelecendo a homeostase tecidual (MAFRA et al., 2019). Esse processo, quando em situação patológica ou de lesão, pode levar a produção exacerbada de citocinas pró-inflamatórias, que recrutam outras células imunes, e ativação do sistema complemento (KUBES; MEHAL, 2012).

Outra função importante dos macrófagos residentes do fígado, ocorre na sua diferenciação para um fenótipo “M2” (pró-resolutivo), quando sintetizam IL-10, TGF-β e outros componentes da matriz extracelular (MANTOVANI et al., 2004), com o intuito de realizar reparo e remodelamento tecidual, ao eliminarem restos celulares (HOLT et al., 2008; JAESCHKE, 2011).

Por sua vez, a função das células dendríticas no fígado tem sido objeto de estudo. Acredita-se que vai muito além da apresentação de antígeno para ativar e recrutar leucócitos (FREITAS-LOPES et al., 2017). Algo que está elucidado, é a capacidade destas células em auxiliar na tolerância imunológica local, sintetizando IL-10 e TGF-β (HASTINGS et al., 2020).

Em relação aos granulócitos, como os neutrófilos e eosinófilos, podem ser recrutados frente a infecções no fígado e lesão hepática induzida por drogas, respectivamente (FREITAS-LOPES et al., 2017). Quimiocinas liberadas por células imunes e sinais de ATP liberados por células necróticas, conseguem alterar a microvasculatura hepática e realizar a quimiotaxia de neutrófilos ao local injuriado, respectivamente, a fim de realizar a resolução e a reparação da lesão (MCDONALD et al., 2010). Porém, essa resposta pode exacerbar, matando os hepatócitos, causando estresse oxidativo e disfunção proteica (JAESCHKE et al., 1999; KATO, 2016). A atividade dos eosinófilos frente à inflamação no fígado ainda é controversa,

se é favorável para a resolução (BJÖRNSSON et al., 2007) ou contribui para a lesão induzida por drogas (PHAM et al., 2001).

Ainda como componentes do sistema imune inato no fígado, há células NK, que agem efetivamente contra células tumorais (ISHIYAMA et al., 2006), na defesa antiviral matando hepatócitos infectados (BOGDANOS et al., 2013) e regeneração tecidual após dano e atividade citotóxica frente a células tumorais (PENG et al., 2016).

Na resposta imune adaptativa, atuam especialmente as células linfoides, intimamente associadas à indução de tolerância imunológica, respostas antimicrobianas e antitumorais (ROBINSON et al., 2016). Neste grupo, encontram-se as células NKT, que expressam tanto marcadores de células T como de células NK, e representam 10-15% dos linfócitos do fígado de humanos, dentre seus vários subtipos já conhecidos. Fisiologicamente, têm papel semelhante às células NK hepáticas e atuam também na lesão hepática aguda, na fibrose e na regeneração tecidual (GAO et al., 2009).

Assim como no sangue, as células T $CD4^+$ no fígado podem se diferenciar em fenótipos Th1, Th2 ou Th17 e desempenharem, portanto, funções pró-inflamatória e anti-inflamatórias, dependendo do estímulo o qual o órgão for exposto (HEYMANN; TACKE, 2016). Em condições fisiológicas, essa condição é suprimida pela maioria das células residentes hepáticas, mantendo uma hiporresponsividade, e consequentemente a tolerância imunológica (KUBES; JENNE, 2018).

Na imunidade humoral, as células B agem através da produção de anticorpos ao se tornarem plasmócitos, apresentando antígenos como uma APC (célula apresentadora de antígenos), e secretando citocinas (ex. IFN-γ e TNF-α) para ativar outras células imunes no fígado, portanto apresentam um potencial mais pró-inflamatório no ambiente hepático (ZHANG et al., 2013).

Por fim, outro tipo celular linfoide hepático importante, são as células T γδ, que fazem parte do grupo de células T não convencionais. Tais células são ativadas mais rapidamente do que os outros tipos de células T, pois além de reconhecerem antígenos por MHC (complexo principal de histocompatibilidade), também reconhecem antígenos sem precisarem ser apresentados por MHC, e são ativadas por citocinas. Suas funções podem ser patogênicas ou protetoras, quando se acumulam no fígado após uma condição inflamatória ou de fibrose (HAMMERICH; TACKE, 2014). Atuam matando células lesionadas ou infectadas via apoptose

(HUBER et al., 2002) e pela produção de IFN-γ, e as células T γδ produtoras de IL-17 atuam regulando a inflamação hepática e provavelmente contribuindo para a progressão da fibrose hepática (HAMMERICH; TACKE, 2014), visto que a IL-17, quando liberada por outras células no fígado, exacerba o processo fibrótico (MENG et al., 2012).

Sabe-se também que as células T γδ podem produzir mais uma série diversas de moléculas, como IL-6, GM-CSF, IL-4, IL-13, IL-10 e TGF-β (BONNEVILLE et al., 2010).

1.1.2 Fígado e Estresse Oxidativo

O estresse oxidativo se refere a um desequilíbrio entre os agentes pró-oxidantes e antioxidantes, o que pode resultar em danos celulares. Os principais alvos do estresse oxidativo são proteínas, lipídios e DNA/RNA, resultando em alterações estruturais e funcionais das células, podendo muitas vezes serem danos irreversíveis (HUSSAIN et al., 2016; JONES, 2008).

Os radicais livres são exemplos de moléculas pró-oxidantes, pois contêm um ou mais elétrons desemparelhados no orbital de valência, conferindo sua alta-reatividade (BURTON; JAUNIAUX, 2011). Como exemplo temos a geração de oxigênio molecular na forma de espécies reativas de oxigênio (EROs), que compreendem principalmente o ânion superóxido (O_2^-), o peróxido de hidrogênio (H_2O_2) e radicais hidroxila (^-OH) (JAESCHKE et al., 2012). As EROs atuam como mensageiros secundários, envolvidos no mecanismo de transdução de sinais gerados em resposta a citocinas, hormônios e ATP, portanto, acabam por auxiliar na regulação dos processos biológicos e fisiológicos (FINKEL, 2011). Porém, quando a produção de EROs é exacerbada, descontrolada, há maior risco de ocorrer oxidação de proteínas, alterando estrutura e função proteica, peroxidação lipídica e danos ao material genético, explicando seu envolvimento em processos patológicos (KEHRER, 1993).

Para combater e equilibrar o estado redox, o organismo possui um sistema antioxidante, enzimático e não enzimático, sensível a essas alterações (BURTON; JAUNIAUX, 2011).

São exemplos de defesas do sistema enzimático, a superóxido dismutase (SOD), catalase (CAT) e glutationa peroxidase (GPx) (ZHANG et al., 2018).

Durante o processo de desintoxicação, estas enzimas que possuem um metal de transição em seu núcleo, conseguem fazer com que esse metal assuma diferentes valências à medida que transferem elétrons (BURTON; JAUNIAUX, 2011). A SOD atua removendo o superóxido, ao catalisar a transferência de um elétron de uma molécula de superóxido por outra, exemplo cobre/zinco (SOD1) ou manganês (SOD2), produzindo H_2O_2 (JAESCHKE et al., 2012). Esse H_2O_2 poderá ser reduzido pela GPx no citosol e mitocôndrias, porém é dependente da glutationa (GSH), que serve como doador de elétron (WATSON et al., 2004). O H_2O_2 também pode ser reduzido pela CAT, mas principalmente os H_2O_2 gerados nos peroxissomos (CALABRESE; CANADA, 1989).

Compondo o sistema antioxidante não enzimático, há como exemplo: vitamina C, vitamina E, beta-caroteno e GSH (CICHOŜ-LACH; MICHALAK, 2014). O GSH, é um tiol não proteico envolvido em reações enzimáticas e não enzimáticas, que apresenta papel vital na desintoxicação de xenobióticos, na regulação da progressão do ciclo celular e apoptose, modulação das funções do sistema imune, entre outros (LU, 2013).

O fígado, por apresentar alta atividade metabólica e de desintoxicação, acaba por gerar muitas moléculas pró-oxidantes. Em contrapartida, a resposta antioxidante é altamente efetiva para manter o equilíbrio redox (ANDRADE et al., 2015).

Entretanto, em lesões hepáticas, há um desequilíbrio redox, resultando no estresse oxidativo, como causa, consequência ou progressão da doença (ZHU et al., 2012). Durante a fosforilação oxidativa nas mitocôndrias, resposta inflamatória com recrutamento de neutrófilos e macrófagos, toxicidade induzida por drogas, estresse do retículo endoplasmático afetando as enzimas do citocromo P450, por exemplo, ocorre aumento na produção de EROs (ANDRADE et al., 2015).

O mecanismo de morte celular mais comum no contexto de lesão hepática induzida por EROs é a peroxidação lipídica (JAESCHKE et al., 2012), pois ocorre aumento de substâncias reativas ao ácido tiobarbitúrico (TBARS) nessas condições (HSU et al., 2008; KÜPELI et al., 2006).

Os sinais gerados, como mediadores lipotóxicos e sinais intracelulares, são responsáveis por ativar as células de Kupffer, que iniciam e auxiliam na progressão da resposta inflamatória (CONTRERAS-ZENTELLA; HERNÁNDEZ-MUÑOZ, 2016). Quando ativadas, as células de Kupffer, por meio da

via de transcrição NF-κB, produzem diversas citocinas pró-inflamatórias, como TNF-α, IL- 1β, IL-6 e IL-18 (NAKAMOTO; KANAI, 2014), e ativam o complexo enzimático NADPH-oxidase (MOORE et al., 2013), amplificando a resposta inflamatória tecidual. O NADPH pode acabar por estimular a produção de EROs pelos hepatócitos, promovendo ainda mais a lesão (ANDRADE et al., 2015). Em um contexto de doença crônica, as EROs também podem contribuir para o início da fibrogênese, ao promover a suprarregulação de genes envolvidos nesta condição (MORMONE et al., 2011).

1.2 Aspectos Histofisiológicos dos Rins

O aparelho urinário é composto por dois rins (direito e esquerdo), dois ureteres, uma bexiga e uma uretra.

Os rins são órgãos retroperitoneais, de coloração castanho-avermelhada, devido ao grande fluxo sanguíneo que recebem (25% do débito cardíaco), possuem formato semelhante ao de um feijão (oval), com uma borda côncava e uma convexa, e são relativamente pequenos, com uma média de 0,65% do peso corporal médio (RADI, 2019).

Ao redor de cada rim, há uma cápsula fibrosa e uma camada de tecido adiposo, o tecido adiposo perirrenal, os quais conferem uma relativa proteção ao órgão frente a impactos, traumas e pressão. Internamente, é possível observar ainda macroscopicamente, as regiões do parênquima, constituído pelo córtex, medula (interna e externa), papila e pelve renal (RADI, 2019).

O fluxo sanguíneo nos rins é intenso, cerca de 180 litros de sangue são filtrados por dia pelos rins (FARIA et al., 2019). O sangue rico em oxigênio chega pela artéria renal ao hilo, onde se ramificará em artérias interlobares, artérias arqueadas e artérias interlobulares. Estas últimas originam as arteríolas aferentes, que adentram a cápsula de Bowman para formar um conjunto de capilares glomerulares anastomosados, denominado glomérulo, cuja função é filtrar o plasma sanguíneo (GUEUTIN et al., 2012; RADI, 2019).

Após a filtração, o sangue sai do glomérulo pela arteríola eferente, que se ramifica em capilares peritubulares, até a região medular, onde darão origem aos vasos retos. A tensão de oxigênio no sangue diminui ao longo do seu trajeto. Quando chega na veia interlobular, dirige-se para as veias arqueadas onde se encontram com as veias interlobares. Estas últimas irão confluir para a veia renal, na

região do hilo renal (GUEUTIN et al., 2012; RADI, 2019).

São funções dos rins: a filtragem do sangue, preservando a homeostase dos fluídos teciduais; regulação da pressão sanguínea através da síntese de renina, que possui papel importante no sistema renina angiotensina aldosterona (SRAA); controle da produção de eritrócitos através da síntese de eritropoietina; e controle dos níveis circulantes de cálcio, através da ativação do calcitriol (FARIA et al., 2019; MCMAHON, 2016).

A nível microscópico, o rim apresenta uma arquitetura histológica extremamente complexa, especializada e organizada, como é possível observar especialmente na unidade funcional renal denominada de néfron (MCMAHON, 2016).

O néfron é organizado em diferentes regiões, incluindo glomérulo, túbulo contorcido proximal (TCP), alça de Henle e túbulo contorcido distal (TCD), nessa ordem respectivamente (Figura 3) (FARIA et al., 2019). O túbulo e ducto coletor (DC) não são considerados parte do néfron, porque ao se observar o desenvolvimento embriológico do rim, determina-se que estes se originam do broto ureteral (STARUSCHENKO, 2012). Essa unidade funcional e o sistema de ductos coletores, juntamente com as células que a constituem e os vasos sanguíneos, são responsáveis pelas funções renais (FARIA et al., 2019).

Figura 3. Organização do néfron

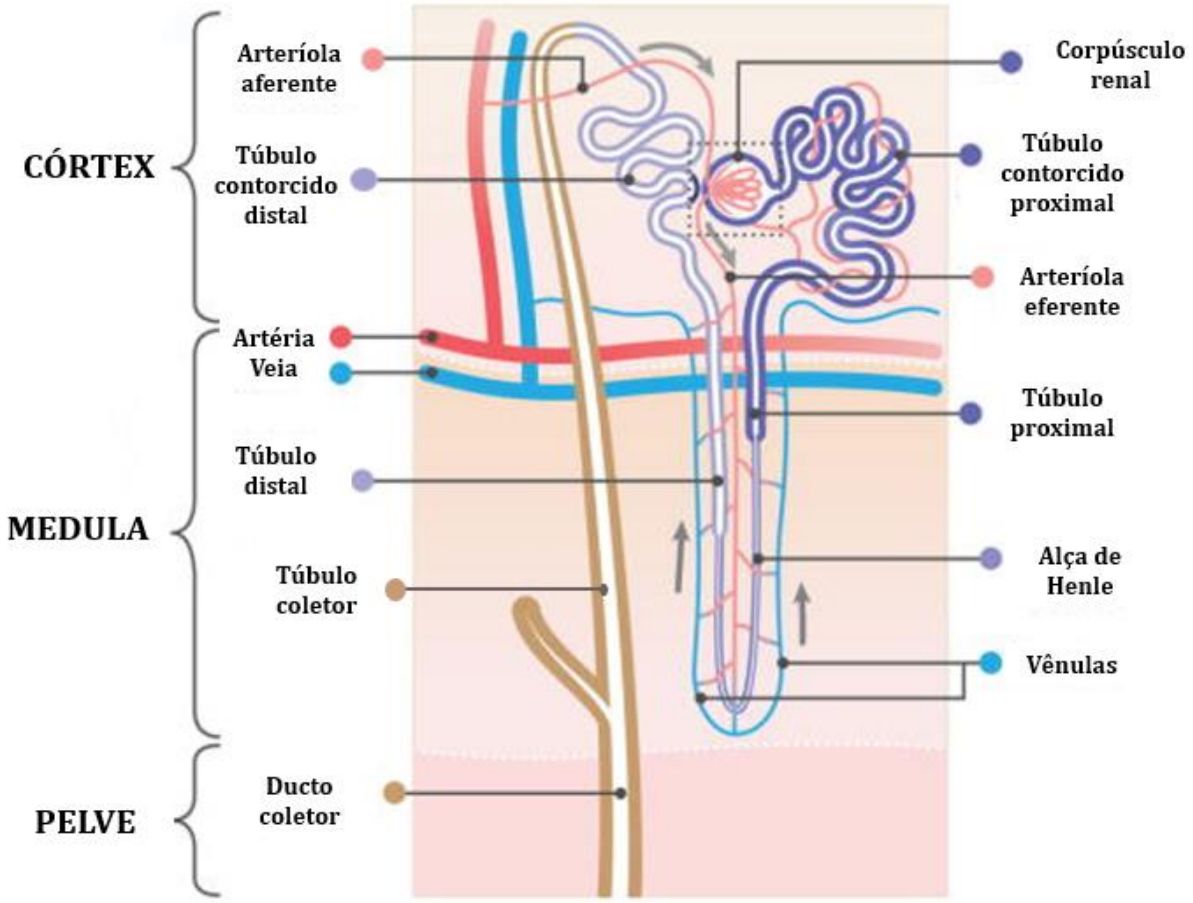

Fonte: Modificado de McMahon (2016)

No córtex renal, dando início ao néfron, há o corpúsculo renal responsável pela filtração do sangue, consistindo na primeira etapa para formar um ultrafiltrado, que posteriormente formará a urina (GREKA; MUNDEL, 2012). O corpúsculo renal é constituído pelos glomérulos, cujos capilares fenestrados são envoltos por células musculares lisas e pela membrana basal glomerular. Estas estruturas fornecem o suporte estrutural deste tufo glomerular e formam uma barreira de filtração seletiva em conjunto com células endoteliais, células mesangiais e os podócitos (Figura 4). As células endoteliais e mesangiais auxiliam na filtração, mantendo a integridade e porosidade da vasculatura, regulando a passagem do que deve ser eliminado do plasma sanguíneo, dependendo do tamanho e da carga das moléculas (GUEUTIN et al., 2012; JOURDE-CHICHE et al., 2019). Já os podócitos, são células extremamente importantes na permeabilidade seletiva, pois possuem processos semelhantes a pés, que vão interagindo com os processos de outros podócitos, formando os diafragmas de fenda, e acabam por cobrir inteiramente a

membrana basal glomerular, servindo então como a última barreira de filtração do glomérulo (GREKA; MUNDEL, 2012).

Figura 4. Estrutura do corpúsculo renal

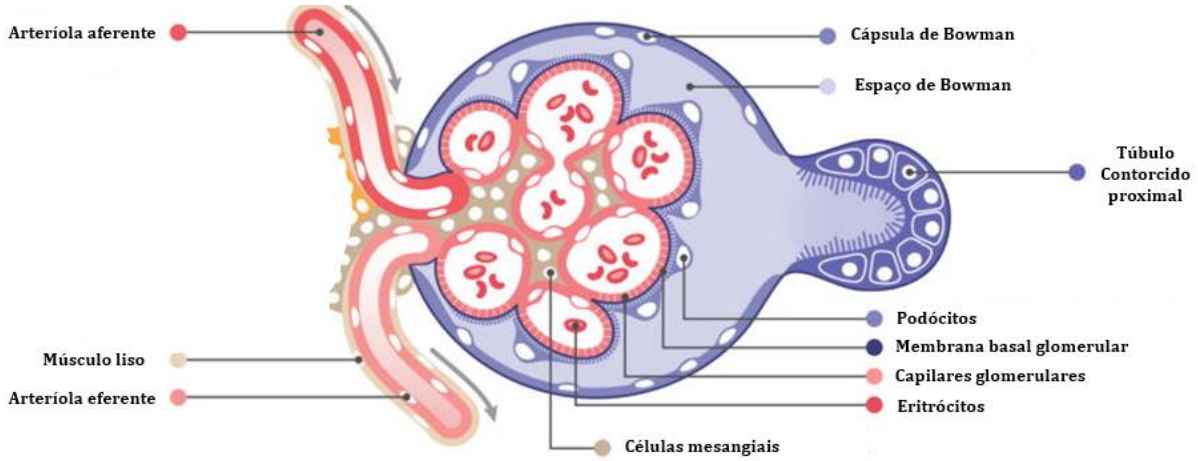

Fonte: Modificado de McMahon (2016)

O glomérulo é delimitado pela cápsula de Bowman, havendo um espaço entre eles, denominado espaço de Bowman, que recebe o ultrafiltrado produzido e o conduz ao TCP, e o que não compõe o filtrado, como por exemplo proteínas carregadas negativamente, retornará pela arteríola eferente (GUEUTIN et al., 2012).

O primeiro segmento do néfron que recebe o filtrado logo após a filtração glomerular é o TCP, principalmente localizado no córtex renal. As células epiteliais constituintes dos TCP apresentam formato cuboide e microvilosidades apicais, criando uma “borda em escova”. Estas células apresentam uma alta capacidade de endocitose, com a participação dos receptores multiligantes megalina e cubilina. Este atributo na superfície apical contribui para que ocorra a maior parte da reabsorção de água, e uma parte significativa de sódio (Na^+) (conduzido pela Na^+/K^+ ATPase), potássio (K^+), cloreto (Cl^-), bicarbonato (HCO_3^-) (com auxílio da anidrase carbônica), fosfato e glicose. Além disso, ocorre reabsorção de proteínas de baixo peso molecular (GUEUTIN et al., 2012; NIESKENS; WILMER, 2016; RADI, 2019).

O TCP também realiza a depuração de compostos residuais e xenobióticos que não foram filtrados, sendo secretados para o lúmen tubular. Esta propriedade demonstra que é um segmento do néfron que pode facilmente sofrer toxicidade renal induzida por drogas (NIESKENS; WILMER, 2016).

O próximo segmento do néfron é a alça de Henle, que possui duas porções, uma porção ascendente e outra descendente, formando um “U” e se encontra quase que totalmente na medula renal. Sua principal função é realizar a concentração da urina, recuperando grande parte do Na^+ e da água filtrada pelo glomérulo (MCMAHON, 2016). Para isso, é necessário gerar um gradiente osmótico intersticial, decorrente de um sistema complexo de multiplicação em contracorrente, tornando o ambiente hiperosmótico. Assim, o segmento delgado descendente é completamente permeável a água, e o segmento ascendente é impermeável a água, já que carece de aquaporinas. Entretanto, este segmento é permeável ao Na^+ e outros solutos como a ureia e Cl^-, que são ativamente bombeados para fora da alça através da Na^+/K^+ ATPase, retornando à circulação sanguínea através dos vasos retos (RADI, 2019). Outro fator importante para este mecanismo de contracorrente, é o cotransportador NKCC2 (Na^+-K^+-2Cl^- cotransportador) no ramo ascendente espesso, que se encontra na membrana apical e medeia a reabsorção de cloreto de sódio (NaCl) (GUEUTIN et al., 2012).

O ramo ascendente desemboca no TCD. O TCD é o segmento onde ocorre a reabsorção de cerca de 5-10% de Na^+ e Cl^-. Esse transporte é regulado principalmente pela aldosterona, cujos efeitos são aumentar a quantidade de Na^+/K^+ ATPase na membrana basal das células do TCD, consequentemente aumentando a reabsorção de NaCl; secretar K^+; regular a homeostase sistêmica do cálcio e do magnésio, reabsorvendo quando necessário; secretar íons H^+, auxiliando no equilíbrio ácido básico (MCCORMICK; ELLISON, 2015; RADI, 2019).

Um fato importante deste segmento, é que parte dele irá se aproximar do corpúsculo renal (polo vascular) deste mesmo néfron, e se modificará a nível estrutural, celular e funcional, passando essa região a se chamar de mácula densa. Esta se comunica com as células justaglomerulares formando o aparelho justaglomerular, constituindo unidade sensorial e de resposta funcional do sistema renina-angiotensina (GOMEZ; SEQUEIRA-LOPEZ, 2018).

As células da mácula densa são responsáveis por realizar o feedback tubuloglomerular, isto é, monitorar as alterações na composição do líquido tubular distal, principalmente de NaCl. Caso necessário, estimulam a secreção de renina pelas células justaglomerulares. Esse sistema acaba por controlar a pressão arterial e regular a taxa de filtração glomerular, além de manter a homeostase fluido-eletrolítica (GOMEZ; SEQUEIRA-LOPEZ, 2018; MCMAHON, 2016).

Os DC são os controladores finais e principais da excreção urinária de Na^+ e K^+, regulando o volume e a osmolaridade da urina. Eles possuem 2 tipos celulares principais, as células principais e as intercaladas. As células principais expressam em sua membrana basolateral receptores para ADH (hormônio antidiurético ou vasopressina) e aldosterona, os quais ajudam a regular a retenção de Na^+ ou água, mantendo o equilíbrio fisiológico (MCMAHON, 2016; RADI, 2019). Já as células intercaladas, que se encontram entre as células principais, têm como função fazer o equilíbrio ácido-básico, regulando o pH sanguíneo ao reabsorver K^+ e HCO_3^- filtrado no TCP, e secretar íons H^+ (ROY et al., 2015).

A urina formada então é drenada para os túbulos da papila renal, que drenam para estruturas chamadas cálices renais menor e maior, respectivamente. Posteriormente, a urina é drenada para a pelve renal. Quando a urina sai dos rins, os ureteres serão responsáveis por transportá-la para a bexiga urinária, que a armazena até a micção (HICKLING et al., 2015).

1.2.1 Rins e Inflamação

A inflamação é uma resposta do organismo frente à algum estímulo, como patógenos infecciosos ou moléculas endógenas, com o intuito de proteger o organismo e reestabelecer a homeostase. Entretanto, em determinadas situações, a resposta inflamatória pode exacerbar e se tornar um fator determinante para o início ou progressão de algum processo patológico. É caracterizada por sinais como calor, dor, rubor/vermelhidão e inchaço/edema (NETEA et al., 2017).

Nos rins foram identificadas as seguintes células imunes residentes: macrófagos, mastócitos, células dendríticas (convencionais e plasmocitoides), células NK, células NKT, células T e B (STEWART et al., 2019).

Juntamente com os macrófagos, as células dendríticas constituem as células imunes mais abundantes no ambiente intrarrenal, uma vez que ambos os tipos celulares fazem parte da rede de fagócitos mononucleares residentes. Contudo, mesmo havendo funções sobrepostas, os macrófagos são descritos como mais efetores na imunidade inata, e as células dendríticas na indução da imunidade adaptativa (KURTS et al., 2020).

As células dendríticas renais apresentam capacidade e facilidade de entrar e sair do rim, o que é fundamental para desempenhar suas funções (KURTS et

al., 2020). Em estado de homeostasia, encontram-se em grande quantidade no espaço tubulointersticial, porém não estão presentes nos glomérulos, de acordo com Krüger et al. (2004), em estudo avaliando rim de camundongos.

Durante a inflamação, as células dendríticas são ativadas e diferenciadas para migrarem até o linfonodo renal de drenagem, onde vão induzir a ativação das células T. A expressão aumentada de CCR7, CCL19 e CCL21, por exemplo, são imprescindíveis no tráfego desses leucócitos. No caso de rins saudáveis, as células dendríticas também migrarão até o linfonodo, porém, apresentarão autoantígenos captados do microambiente renal para as células T, resultando em tolerância imunológica nos rins (MARTÍN-FONTECHA et al., 2003).

Na glomerulonefrite causada por vasculite associada ao ANCA (anticorpo anti citoplasma de neutrófilos), Brix et al. (2015) observaram como um possível biomarcador desta doença, a CCL18, que é secretada por células dendríticas mieloides e macrófagos nos rins. Seus níveis se encontraram elevados nesta condição, favoreceram a inflamação e o comprometimento funcional dos rins. Esta observação é sustentada quando avaliaram que, nos animais *knockout* para CCR8, receptor desta quimiocina em células mononucleares, havia um curso melhorado da doença.

As células dendríticas também podem por atuar na fibrose renal. Quando ativadas juntamente com as células T, podem produzir citocinas como IL-1, TGF-β e TNF, que estimulam fibroblastos, e consequentemente vão conduzir à fibrose renal (LONNEMAN et al., 1995; ZEISBERG et al., 2008).

Já os macrófagos residentes dos rins encontram-se presentes principalmente na cápsula de Bowman e na região medular, além dos macrófagos derivados de monócitos, que são recrutados para os rins. Estão intimamente relacionados à regulação da homeostase renal, e na resposta à lesão renal aguda e crônica (BASSO et al., 2021).

Durante a resposta inflamatória frente a uma lesão renal aguda, macrófagos proliferam e chegam rapidamente, com a ajuda do CCL2 e CX3CR1 por exemplo, ao compartimento glomerular e tubulointersticial, acumulando nestas regiões renais. Estímulos locais podem induzir o desenvolvimento de um fenótipo M1 (pró-inflamatório) nesses macrófagos, que serão então capazes de ativar outros leucócitos e produzir citocinas pró-inflamatórias, como IL-1, IL-6, IL-12 e IL-23, contribuindo muitas vezes para a piora da lesão (TANG et al., 2019). Quando na fase

crônica desta inflamação, o fenótipo destes macrófagos pode se tornar predominantemente M2, que é mais voltado para a reparação tecidual (VINUESA et al., 2008) ou fibrose renal (KUSHIYAMA et al., 2011).

Outra célula imune importante para compreensão da fibrose renal é o mastócito. Ainda que que poucos mastócitos residam no microambiente renal, há aumento do número destas células em doenças renais crônicas (MADJENE et al., 2015), geralmente associados à piora da condição em diversas glomerulopatias (EL-KORAIE et al., 2001; RÜGER et al., 1996).

As células NK residentes nos rins apresentam características semelhantes aos das ILC1s (células linfoides inatas do grupo 1), como produzir IFN-γ e serem parcialmente dependentes do fator de transcrição T-bet para sua função e desenvolvimento (TURNER et al., 2019). Estas células apresentam, no entanto, efetiva capacidade citotóxica (ZHANG et al., 2008), e provavelmente têm grande participação na homeostase renal (TURNER et al., 2019).

Em relação as células NKT estarem envolvidas em doenças renais, a maioria das informações que temos é baseada em estudos com camundongos. Sabe-se que a alfa-galactosilceramida, ativa as células NKT nos rins, levando à atividade citotóxica e lesionando as células endoteliais vasculares e epiteliais tubulares, resultando em lesão renal aguda (UCHIDA et al., 2018). Entretanto, Yang et al. (2008) demonstraram em um modelo de glomerulonefrite induzida em camundongos, que a ausência de células NKT $CD1d^+$ acelerou a condição quando comparado ao grupo *wild type* (selvagem), indicando um possível efeito protetor das células NKT em determinadas situações.

Na resposta imune adaptativa, há grande influência das células T, pois apresentam maior diversidade fenotípica e funcional entre os leucócitos. Portanto, dependendo do estímulo e do microambiente em que estão, as células T $CD4^+$ e T $CD8^+$, podem se diferenciar em seus subconjuntos especializados, para uma resposta mais efetiva, reparação tecidual ou simplesmente para continuar mantendo o equilíbrio imunológico local (BASSO et al., 2021).

Na resposta imune adaptativa humoral, as células B podem produzir citocinas, anticorpos e apresentar antígenos que podem ativar outras células imunes, para estimular a resposta inflamatória, como também secretar citocinas regulatórias. Estas células também podem produzir autoanticorpos patogênicos, ativando células T autorreativas e desencadeando a autoimunidade nos rins (OLEINIKA et al., 2019).

1.2.2 Rins e Estresse Oxidativo

Assim como a inflamação, já há um consenso sobre a influência do estresse oxidativo no desenvolvimento das doenças renais, e sua relação muitas vezes direta com a inflamação nos rins (DAVIES; TOURNIER, 2012; ELMARAKBY; SULLIVAN, 2012; GRIVEI et al., 2020).

As principais fontes comuns de EROs nos rins, são a NADPH-oxidase e a cadeia respiratória mitocondrial, já que os rins são ricos em mitocôndrias. Em estado inflamatório, as células imunes recrutadas contribuem para uma piora do estresse oxidativo local, e da lesão renal (SURESHBABU et al., 2015).

As EROs podem ativar a JNK (quinase N-terminal c-Jun), proteína da família das MAPK. Essa via de sinalização EROs/JNK, dependendo do estímulo que recebe, induz a apoptose, podendo resultar em lesão renal (CHEN et al., 2018b; FU et al., 2006). A ativação da JNK está associada na mediação da apoptose e na produção de citocinas pró-inflamatórias (DAVIES; TOURNIER, 2012).

Em estudo realizado por Sverrisson et al. (2015), foi demonstrado que a produção de citocinas pró-inflamatórias, como IL-1β, TNF-α e IL-6, estimulada pelos EROs, tem papel importante em alterações da permeabilidade glomerular e consequentemente na função de filtração glomerular.

O TCP é o principal segmento do néfron gerador de EROs, devido à alta quantidade de mitocôndrias que suas células apresentam para desempenhar funções como o transporte ativo de substâncias e, por isso, está constantemente sujeito a sofrer danos oxidativos (RATLIFF et al., 2016). Fato importante a se considerar, é que em estudo realizado em células de TCP de ratos, por Visarius et al. (1996), foi observado que as células desse segmento possuem capacidade biossintética limitada para GSH, porém, são dependentes da GSH circulante para a proteção antioxidante.

Em condição crônica da doença renal, é relatado forte influência de diferentes isoformas da NADPH-oxidase, na piora da disfunção vascular e na produção de citocinas que estimulem a fibrose tecidual (SEDEEK et al., 2013). A atividade elevada da NADPH-oxidase também foi observada durante a hipertensão, onde o aumento de EROs tem sido implicado em diversas características patológicas desta condição, como vasoconstrição renal, uma vez que aumenta a contração e proliferação das células do músculo liso vascular, disfunção das células glomerulares,

liberação de renina e proteinúria (ARAUJO; WILCOX, 2014).

Fato interessante, é que células do TCP, principalmente, são capazes de sintetizar dopamina renal, a qual possui papel importante na manutenção dos fluídos, equilíbrio hidroeletrolítico e pressão arterial (ARMANDO et al., 2011). Além dessas funções, alguns receptores de dopamina renal também participam protegendo o rim frente ao estresse oxidativo, inibindo a atividade da NADPH-oxidase, reduzindo a produção de EROS, e estimulando a produção de antioxidantes (CUEVAS et al., 2013).

Além dessa associação das moléculas oxidantes com condições patológicas renais, sabe-se que em baixos níveis, algumas dessas moléculas, como as EROs, são essenciais para o bom funcionamento renal, auxiliando na filtração glomerular, reabsorção tubular, secreção hormonal, reatividade vascular e hemodinâmica renal. A presença do sistema antioxidante auxilia para que não ocorra o desequilíbrio no estado redox, prevenindo o acúmulo de EROs e outras moléculas pró-oxidantes (RATLIFF et al., 2016).

1.3 Transtorno De Déficit De Atenção E Hiperatividade

O Manual Diagnóstico e Estatístico de Transtornos Mentais (DSM-V) define transtorno mental como uma síndrome que afeta significativamente processos psicológicos e biológicos responsáveis principalmente pelo funcionamento mental, como a cognição, regulação emocional e comportamento do indivíduo. Portanto, esses transtornos são estabelecidos de acordo com questões familiares, culturais e sociais, uma vez que tais valores influenciam e modelam a experiência e a apresentação dos sintomas, contribuindo, posteriormente, para o diagnóstico (AMERICAN PSYCHIATRIC ASSOCIATION, 2013).

No grupo dos transtornos mentais, há os transtornos do neurodesenvolvimento, grupo caracterizado por pessoas que apresentam condições que afetam a função do sistema nervoso central (SNC) nos domínios responsáveis pelas habilidades motoras, cognição, comunicação e/ou comportamento (MULLIN et al., 2013). Geralmente, os sintomas têm início no período do desenvolvimento, ou seja, durante a infância, antes da puberdade ou antes do indivíduo chegar aos 22 anos de idade (ISMAIL; SHAPIRO, 2019; THAPAR et al., 2016). Por consequência, há dificuldade no desenvolvimento social, pessoal e educacional desses indivíduos, e

futuramente no âmbito profissional, já que normalmente se trata de um distúrbio crônico, de curso estável (AMERICAN PSYCHIATRIC ASSOCIATION, 2013; ISMAIL; SHAPIRO, 2019).

O Transtorno de Déficit de Atenção e Hiperatividade (TDAH) é o mais comum transtorno do neurodesenvolvimento, sendo caracterizado por sintomas persistentes de desatenção, hiperatividade e impulsividade. Desse modo, trata-se de uma condição prevalente e prejudicial, frequentemente associada a outros transtornos psiquiátricos (AMERICAN PSYCHIATRIC ASSOCIATION, 2013; POSNER et al., 2020). O quadro de desatenção é definido, por exemplo, quando a criança apresenta problemas para prestar atenção e/ou realizar tarefas ou atividades lúdicas, não percebe detalhes e acaba cometendo erros, perde com frequência objetos e se distrai facilmente. Quando é observado que a criança é muito agitada, movimenta-se muito, fala excessivamente e não tem paciência para esperar, caracteriza-se como hiperatividade e impulsividade (AMERICAN PSYCHIATRIC ASSOCIATION, 2013).

Dentre os sintomas que caracterizam o TDAH, há uma subdivisão de acordo com o DSM-V, que auxilia no entendimento da apresentação do TDAH e consequentemente na classificação diagnóstica. Portanto, o indivíduo pode apresentar esta condição como: predominantemente desatento, predominantemente hiperativo/impulsivo ou com esses critérios combinados, além da categoria de remissão parcial (AMERICAN PSYCHIATRIC ASSOCIATION, 2013; WILLCUTT et al., 2012).

Embora o conceito de TDAH seja relativamente novo, introduzido somente em 1980, na terceira edição do DSM (AMERICAN PSYCHIATRIC ASSOCIATION, 1980), diversos pesquisadores se dedicaram a buscar em descrições históricas, científicas e não científicas e a primeira descrição de um caso com sintomas, características, semelhante a definição atual de TDAH (BARKLEY; PETERS, 2012; LANGE et al., 2010; MARTINEZ-BADÍA; MARTINEZ-RAGA, 2015). Não há consenso científico, porém, o crédito normalmente é dado ao médico britânico George Frederic Still (1902), também considerado por muitos o “pai da pediatria britânica” (BARKLEY; PETERS, 2012; LANGE et al., 2010; MARTINEZ-BADÍA; MARTINEZ-RAGA, 2015). Em suas palestras no *Royal College of London*, no ano de 1902, acabou relatando “algumas condições psíquicas anormais em crianças”, após observar um grupo de 43 crianças, que apresentavam problemas de concentração e atenção, e a esta condição foi dado o nome de “defeito anormal de controle moral”

(STILL, 1902).

A partir da introdução do termo TDAH, fez-se necessário estimar o número de indivíduos acometidos por este transtorno neurocomportamental, para assim auxiliar no diagnóstico e tratamento, além de contribuir no entendimento da fisiopatologia (POLANCZYK et al., 2015; POSNER et al., 2020). De acordo com meta-análise realizada por Polanczyk et al. (2007), que compreendeu uma revisão sistemática de 102 estudos, abrangendo mais de 171.000 indivíduos, estima-se que a prevalência mundial de TDAH em crianças e adolescentes seja de 5,29% (IC 95% = 5,01–5,56), não diferindo significativamente entre os continentes (POLANCZYK et al., 2015). A variabilidade nas informações referentes a prevalência mundial ou continental dessa condição em relação a outros artigos, se dá aos fatores metodológicos aplicados em cada um dos artigos (Polanczyk et al., 2007). Além disso, Polanczyk et al. (2015) também demonstraram que a prevalência mundial se mostrou estável ao longo de três décadas (1985 a 2012). Outro fator importante a se destacar, é que juntamente com essas informações epidemiológicas, Polanczyk et al. (2007) relataram que a incidência de TDAH é maior em indivíduos do sexo masculino.

O TDAH pode persistir até a vida adulta, quando se estima que a prevalência entre 19 e 45 anos seja de 2,5% (IC 95% 2,3–3,1) (SIMON et al., 2009). Portanto, pode-se dizer que aproximadamente 50% das crianças diagnosticadas com TDAH continuam a manifestar sintomas desse transtorno durante a vida adulta (AMERICAN PSYCHIATRIC ASSOCIATION, 2013). Porém, há uma discussão em relação à veracidade desses dados. Simon et al. (2009) acreditam que os critérios diagnósticos do DSM-IV para essa condição em adultos não são totalmente claros e específicos, o que pode levar a essas taxas reduzidas de prevalência de TDAH em adultos, necessitando uma melhor compreensão deste transtorno.

Embora a sua etiologia ainda seja discutível, há evidências convincentes sobre o papel dos genes como fator de risco para o transtorno (FARAONE; LARSSON, 2019), visto que o TDAH infantil é fortemente hereditário, com herdabilidade estimada de 75% (FARAONE; MICK, 2010). Grande parte das alterações genômicas observadas estão estritamente relacionadas com o funcionamento da sinalização neuronal, afetando transportadores e receptores de neurotransmissores (BRALTEN et al., 2013). Entretanto, este fato não exclui os fatores ambientais como fonte associada de etiologia, uma vez que podem resultar em alterações epigenéticas (FARAONE; LARSSON, 2019). Riscos ambientais como

exposição a toxinas (ex. mercúrio e manganês), complicações durante a gravidez e no parto (ex. sofrimento fetal, pré-eclâmpsia e idade materna), exposição fetal ao cigarro e/ou álcool, têm sido associados ao TDAH (BANERJEE et al., 2007).

Diversas alterações nas regiões do cérebro e nas vias neurais já foram observadas em pacientes com TDAH, as quais auxiliaram a elucidar este transtorno e entender o porquê dos principais sintomas. Entretanto, há necessidade de mais estudos para entender integralmente os fundamentos neuroanatômicos e neurofisiológicos do TDAH (FRIEDMAN; RAPOPORT, 2015). Durston et al. (2004), após realizarem ressonância magnética em meninos com TDAH, observaram alterações corticais nas imagens obtidas, quais como redução na substância cinzenta, nas regiões pré-frontal direita e occipital esquerda, além da diminuição da substância branca nessa última; e redução do volume cerebelar direito. À vista disso, Durston et al. (2004) relataram atenuação do volume intracraniano nesses indivíduos (4%).

Corroborando com o entendimento neuroanatômico de indivíduos com TDAH, em uma meta-análise realizada por Valera et al. (2007), jovens com TDAH apresentaram, em imagens estruturais, alterações volumétricas principalmente no cerebelo, em particular o vérmis inferior posterior, bem como o esplênio do corpo caloso, volume cerebral total e direito e caudado direito. Provavelmente essas são as regiões mais afetadas pelo transtorno. Porém, não se descartam alterações em outras regiões. Importante salientar que essas regiões descritas acima, quando afetadas, resultam em sintomas do TDAH, visto que são áreas cerebrais responsáveis por funções fundamentais no processo cognitivo, tais como processamento emocional e atenção (HOOGMAN et al., 2019). O controle da coordenação do movimento e a aprendizagem motora já foi associado exclusivamente à função cerebelar, porém, há evidências de função na cognição e na emoção (D'ANGELO; CASALI, 2012).

Outro fator importante na fisiopatologia do TDAH, é o entendimento dos sistemas dopaminérgico e serotoninérgico, responsáveis normalmente pela função neural, porém que nesta condição estão alterados (DUNN et al., 2019). A dopamina e seu derivado, a norepinefrina, ajudam nos processos cognitivos e nas atividades motoras (FARAONE et al., 2015). Porém, em indivíduos com TDAH, já foram observados polimorfismos em genes que codificam transportadores e receptores de dopamina (CAMPO et al., 2011). A serotonina está envolvida na modulação do sistema dopaminérgico, além de apresentar função importante em questões comportamentais e emocionais (DUNN et al., 2019), e sabe-se que cada vez

está mais claro a desregulação emocional em casos de TDAH, retirando o foco somente nas alterações cognitivas (SHAW et al., 2014). Ainda são recentes e limitados os estudos científicos e o entendimento do sistema GABAérgico e glutamatérgicos no TDAH, mas futuramente esperam-se relatos científicos mais consistentes na relação desses neurotransmissores com esta condição (DUNN et al., 2019).

Considerando estas características abordadas, principalmente as neurofuncionais, os tratamentos farmacológicos do TDAH visam agir na distribuição/liberação destes neurotransmissores, a fim de amenizar os sintomas (CAMPO et al., 2011; DUNN et al., 2019).

1.3.1 Tratamento: Farmacológico e Não Farmacológico

Para o TDAH, normalmente é necessário um tratamento multimodal, ou seja, uma combinação de abordagens terapêuticas farmacológicas e não farmacológicas, que juntos reduzem os resultados negativos desta condição e melhoram os aspectos psicossociais. Esse tratamento será determinado de acordo com a necessidade individual de cada paciente (CRESCENZO et al., 2017).

Os tratamentos não farmacológicos são importantes pois: dependendo da situação social e financeira do indivíduo e de sua família, podem não ter acesso aos medicamentos; a combinação do tratamento farmacológico e não farmacológico pode apresentar uma melhora ainda maior nos sintomas; nem todos os pacientes com TDAH respondem as medicações; e dependendo da idade ou sintomatologia do paciente, o médico pode não encontrar justificativas para prescrever algum medicamento (FARAONE et al., 2015). Alguns exemplos dessas abordagens não farmacológicas são terapias dietéticas, como suplementação com ácidos graxos e exclusão de aditivos artificiais; terapias comportamentais, que são as mais utilizadas e com resultados positivos na resolução de problemas parentais e na conduta das crianças com TDAH em diferentes esferas da vida (FARAONE et al., 2015); e terapias neurocognitivas, que fazem uso do neurofeedback, visando abordar os déficits desta condição mental fazendo uso da plasticidade do cérebro (HOLTMANN et al., 2014).

Em relação ao tratamento farmacológico para o TDAH, este dependerá de orientação médica, que irá considerar a gravidade dos sintomas apresentados, a presença de comorbidades e o ambiente psicossocial que esta

pessoa vive (FARAONE et al., 2015). Portanto, após essas observações, o médico responsável avaliará a necessidade da recomendação do uso de medicamentos, psicoestimulantes ou não psicoestimulantes (CRESCENZO et al., 2017). Essa triagem é muito importante pois o uso dos medicamentos para esta condição costuma ser de longo prazo. Por isso, a recomendação deve ser muito precisa visando o melhor efeito frente aos sintomas (FARAONE et al., 2015; LANGBERG; BECKER, 2012).

Dentre os exemplos de não psicoestimulantes, há atomoxetina, guanfacine e clonidina, normalmente prescritos quando os pacientes não apresentam uma resposta muito eficaz aos estimulantes ou apresentam efeitos adversos ao uso deles. Portanto, estes medicamentos são considerados tratamentos de segunda linha para o TDAH (POSNER et al., 2020).

Para o tratamento de primeira linha, é recomendado o uso dos medicamentos estimulantes do sistema nervoso, ou seja, utilizar um produto com metilfenidato ou com anfetaminas (FARAONE et al., 2015). De acordo com um estudo observacional e retrospectivo realizado por Raman et al. (2018), observou-se nos dados de registro populacional um aumento mundial nos últimos anos no uso de psicoestimulantes para o TDAH.

Piper et al. (2018), relataram aumento na utilização de anfetaminas e do seu pró-fármaco, dimesilato de lisdexanfetamina (LDX), entre 2006-2016 nos Estados Unidos (EUA). Em relação ao metilfenidato, houve um crescimento expressivo principalmente no ano de 2012, mas que nos últimos anos de avaliação o consumo foi reduzido. Provavelmente a alta no uso de estimulantes se deve ao aumento de diagnósticos de TDAH durante essa década nos EUA

São semelhantes os mecanismos de ação do metilfenidato e anfetaminas, pois ambos têm como principal ação inibir os transportadores de dopamina e os transportadores de norepinefrina, resultando no aumento da disponibilidade sináptica de dopamina e norepinefrina (FARAONE, 2018). Esse excesso de neurotransmissores nos terminais sinápticos será catabolizado pela monoamina oxidase (MAO) (HEAL et al., 2013). Alguns isômeros de anfetaminas possuem a capacidade de inibir a MAO, o que contribui também para o aumento nos níveis das catecolaminas para retro-transporte para a sinapse, porém essa inibição é relativamente fraca (MANTLE et al., 1976; MILLER et al., 1980; HEAL et al., 2013). Importante ressaltar, que as principais alterações na atividade da dopamina e norepinefrina ocorrem onde já é relatado cientificamente haver alterações

morfofisiológicas e funcionais encefálicas em pacientes com TDAH, incluindo a região cortical e o corpo estriado (FARAONE et al., 2015; FARAONE, 2018).

Atualmente, há diferentes formulações de anfetaminas disponíveis para o TDAH, dentre elas a dextroanfetamina (d-anfetamina), sais de anfetaminas mistos e o LDX (PUNJA et al., 2016).

1.4 Dimesilato De Lisdexanfetamina

O dimesilato de lisdexanfetamina (LDX), com nome comercial do medicamento de referência Venvanse®, é um pró-fármaco inativo da d-anfetamina que tem sido amplamente prescrito para o tratamento do TDAH, e transtorno de compulsão alimentar (COMIRAN et al., 2016). Este é o primeiro pró-fármaco psicoestimulante de ação prolongada destinado para o tratamento do TDAH, que consiste em uma d-anfetamina covalentemente ligada ao aminoácido essencial L-lisina, como representado na Figura 1 (GOODMAN, 2010). Por ser um fármaco de ação prolongada, sua liberação no organismo é lenta, reduzindo a necessidade da administração mais de uma vez ao dia (COMIRAN et al., 2016), o que consequentemente diminui o potencial de abuso do fármaco (BUKSTEIN; HORNER, 2010). Entretanto, sabendo do histórico de abuso e dependência de anfetaminas, a caixa do medicamento contém uma tarja de cor preta, sendo uma substância de venda controlada no Brasil (ANVISA, 2022) e em outros países (BLICK; KEATING, 2007).

Figura 5. Estrutura do dimesilato de lisdexanfetamina e seus metabólitos imediatos

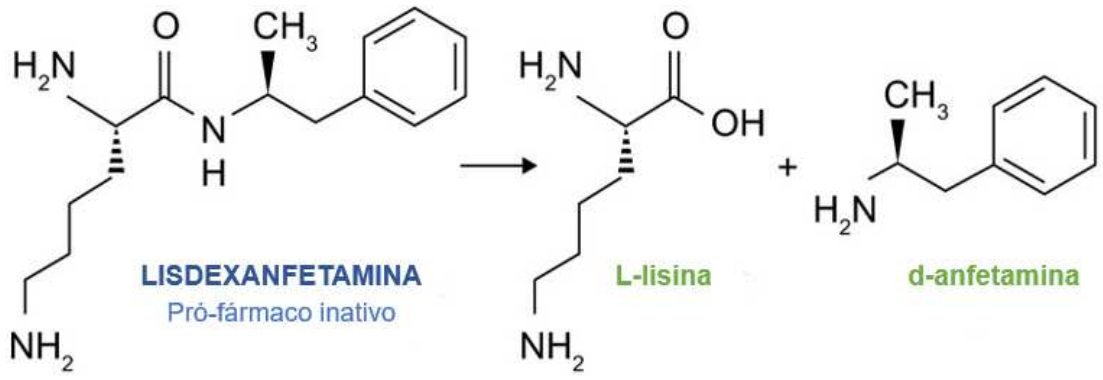

Fonte: Modificado de Ermer et al. (2016)

A dosagem diária inicial de LDX é de 30 mg, entretanto, conforme a necessidade, alterações na posologia podem ser realizadas para obtenção de melhor resposta frente aos sintomas do TDAH, podendo chegar até 70 mg por dia (STEER et al., 2012). Como este medicamento é vendido principalmente em cápsulas, a administração normalmente é via oral, e pode ser dissolvido em água ou suco para ingestão ou misturado à iogurte (ERMER et al., 2016; STEER et al., 2012). Outras vias de administração do LDX são via intranasal e intravenosa, porém menos comuns, uma vez que há preocupação no risco de abuso. Entretanto alguns estudos já demonstraram ausência de efeitos psicoativos significativos quando o medicamento é administrado por estas vias (ERMER et al., 2011; JASINSKI; KRISHNAN, 2009).

A administração do fármaco deve ser feita preferencialmente no período da manhã, pois a insônia pode ser um dos possíveis efeitos adversos (BIEDERMAN et al., 2007). O tratamento sendo feito no início da manhã (07:00h) também apresentou uma duração até o fim da tarde (18:00h; último horário de avaliação), melhorando os sintomas do TDAH durante todo o dia quando comparado a quem recebeu o placebo (COGHILL et al., 2014).

Diversos ensaios clínicos randomizados foram realizados para avaliar a eficácia, tolerabilidade e a segurabilidade do LDX em crianças e adolescentes com TDAH, recebendo uma dose fixa do fármaco, podendo ser de 30, 50 ou 70 mg, uma vez ao dia durante um período. Estes apresentaram uma resposta eficaz do fármaco quando comparado ao placebo, além de um perfil de segurança e tolerabilidade consistente e semelhante ao de outros psicoestimulantes (BIEDERMAN et al., 2007; COGHILL et al., 2013; FINDLING et al., 2011; FINDLING et al., 2013).

Quando abordada as características de um fármaco, faz-se necessário relatar seu mecanismo de ação no organismo (farmacodinâmica) e suas propriedades farmacocinéticas, como por exemplo as etapas de absorção, distribuição, biotransformação e eliminação/excreção (COMIRAN et al., 2016).

Após a administração oral, o LDX será absorvido principalmente por meio do transportador de peptídeos 1 (PEPT1) (ERMER et al., 2012), que são proteínas transmembranas responsáveis pelo transporte de aminoácidos no formato de peptídeos, além de auxiliar na absorção de diversos compostos farmacológicos (VIENNOIS et al., 2018). O PEPT1 é especialmente expresso no trato gastrointestinal, sendo abundantemente encontrado no intestino (VIENNOIS et al., 2018). Em estudo com ratos Sprague Dawley expostos ao LDX, foi observada uma absorção

consistente, rápida e eficiente do fármaco intacto no lúmen de determinadas regiões intestinais, como o duodeno, jejuno e íleo (PENNICK, 2010). Como o LDX inclui a L-lisina em sua estrutura, esta servirá como substrato para o PEPT1, e aparentemente sua função não é afetada pela ingestão do medicamento com alimentos, não sendo necessário estar em jejum para a administração do LDX, pois o estado alimentado não afeta a biodisponibilidade dele (KRISHNAN; ZHANG, 2008; PENNICK, 2010).

Ao ser absorvido no trato gastrointestinal, o LDX chegará à circulação sanguínea e portal e rapidamente será hidrolisado enzimaticamente, liberando a L-lisina e a d-anfetamina, que é o fármaco ativo (ERMER et al., 2016). Esta metabolização ocorre no sangue total e não no plasma. Foi observado metabolização do LDX em homogenatos de fígado e rins, devido ao sangue residual presente nesses tecidos (PENNICK, 2010), uma vez que já se sabe que essa conversão em d-anfetamina é feita no citosol dos eritrócitos por uma aminopeptidase ainda desconhecida (SHARMAN; PENNICK, 2014). Portanto, diferente de outros fármacos, o LDX intacto não é metabolizado pelas enzimas do citocromo P450 (FRAMPTON, 2018).

A d-anfetamina atravessará a barreira hematoencefálica, chegando ao SNC, onde irá agir aumentando a neurotransmissão noradrenérgica e dopaminérgica, ação importante para reduzir os sintomas do TDAH (NAJIB et al., 2020). O LDX, por ser um estimulante de ação prolongada, apresentou melhora dos sintomas das 1,5h até as 13h (último horário de avaliação) em crianças de 6 a 12 anos (WIGAL et al., 2009) e em adultos foram avaliados de 2 a 14h após a administração oral da dose (WIGAL et al., 2011).

A principal via de eliminação do LDX, da d-anfetamina e dos outros metabólitos gerados é por excreção renal, sendo então eliminado na urina, dentro de um período de 120h após a administração. A excreção fecal de LDX é ínfima, menor que 0,3% (KRISHNAN et al., 2008).

1.4.1 Toxicologia do Dimesilato de Lisdexanfetamina - Fígado e Rins

Em razão das anfetaminas serem amplamente utilizadas como tratamento farmacológico para diversas doenças há muito tempo, suas propriedades farmacológicas e ação toxicológica são bem conhecidas (CARVALHO et al., 2012). Contudo, faz-se necessária uma avaliação mais extensa sobre o perfil toxicológico do

LDX, por estar há pouco mais de dez anos no mercado o que, em relação a outras moléculas, pode ser considerado novo no mercado. Além disso, ele apresenta um perfil farmacológico diferente das outras anfetaminas, sendo o primeiro pró-fármaco anfetamínico (HEAL et al., 2013).

Um dos principais estudos experimentais presente nas bases de dados, informando o perfil de toxicidade do LDX, é o estudo de Krishnan e Montcrief (2007), no qual foi verificada a exposição aguda de dose única, além de dois estudos de exposição subcrônica de dose repetida (7 e 28 dias). Esses autores utilizaram ratos Sprague-Dawley, tanto machos como fêmeas, com aproximadamente 7 semanas de idade, com peso entre 204-274 g para ratos e 155-221 g para ratas. Para o experimento foram determinadas diferentes concentrações do LDX (>99% puro) para a avaliação em cada estudo, e utilizando d-anfetamina para ser usada como controle ativo e água deionizada para controle negativo.

No estudo de dose única, por administração oral, Krishnan e Montcrief (2007) sugerem que a DL50 (dose necessária da droga para causar a morte de 50% dos animais dentro de um período de observação estipulado) do LDX é provavelmente 5x maior que a do sulfato de d-anfetamina, parecendo ser maior que 1000mg/kg de LDX. Sinais toxicológicos não foram observados em ratos tratados com doses menores ou igual a 10mg/kg. Entretanto, nas dosagens de 60, 100 e 1000 mg/kg, houve aumento da atividade motora, cromodacriorreia e cromorrinorreia nos primeiros dias de observação. Na dose maior, de 1000 mg/kg também foi relatado nos primeiros dias a morte de uma rata e um rato foi submetido à eutanásia devido a feridas abertas autoinfligidas graves, lesões cutâneas e pouca ou nenhuma produção fecal/urinária até o dia 4.

Os estudos de exposição subcrônica de dose oral repetida, mostrou que no estudo de 7 dias, alguns ratos e todas as ratas precisaram ser sacrificados devido a lesões causadas por automutilação, que foram consideradas relacionadas aos efeitos comportamentais do LDX na dose 300 mg/kg. A maioria dos sinais clínicos avaliados foram somente observados nas doses de 100 e 300 mg/kg. Além de também relatarem nessas mesmas doses uma redução no peso corporal médio dos ratos, no ganho de peso, no consumo de ração e no peso absoluto e relativo de determinados órgãos (fígado, cérebro e baço). Com isso, o NOAEL (Nível Sem Efeitos Adversos Observáveis) para o LDX após esse período foi <30mg/kg/dia (KRISHNAN; MONTCRIEF, 2007).

No estudo de 28 dias, utilizando as doses de 20, 40 e 80 mg/kg/dia, foram observados efeitos como aumento da atividade, pelos arrepiados e manchas pretas nos olhos. Houve, assim como no estudo de 7 dias, uma redução no peso corporal médio e no ganho de peso médio, nos ratos e ratas tratados com 40 e 80mg/kg/dia de LDX. Os animais não apresentaram alterações nos parâmetros hematológicos e de coagulação. Ainda, não foram verificadas mudanças importantes no peso dos órgãos, e nem alterações histopatológicas significativas. Em vista disso, o NOAEL para o LDX após esse período foi <40 mg/kg/dia (KRISHNAN; MONTCRIEF, 2007).

Muito se tem discutido sobre a hepatotoxicidade causada pelo uso de anfetaminas, sendo esta já bem descrita (CARVALHO et al., 2012), porém, sabe-se pouco sobre as possíveis alterações que o uso do pró-fármaco LDX pode causar na morfofisiologia hepática.

Krishnan e Montcrief (2007), demonstraram que em ratos tratados com 30 mg/kg de LDX por 7 dias, não foram encontradas alterações em parâmetros bioquímicos destinados a avalição de função hepática, porém houve aumento na fosfatase alcalina e na glicose, além de redução nos triglicerídeos nos ratos tratados com 100 mg/kg. Algumas dessas alterações também foram relatadas no grupo que recebeu 300 mg/kg, além do aumento sanguíneo de albumina e marcadores de lesão hepática, como o aspartato aminotransferase (AST) e alanina aminotransferase (ALT). Alterações bioquímicas semelhantes foram observadas em ratas na dosagem de 100 mg/kg.

Ao avaliar esses mesmos parâmetros bioquímicos, porém no período de tratamento de 28 dias, e com dosagens diferentes, Krishnan e Montcrief (2007) relataram que a dose de 20 mg/kg/dia de LDX não provocou nenhuma alteração bioquímica significativa em ratos e ratas. No entanto, ao avaliar o uso da dose de 40 e 80 mg/kg/dia de LDX, ambos sexos apresentaram aumento de ALT, e especialmente em ratas, o aumento da glicose também. Tais observações podem indicar alterações morfofuncionais hepáticas, mesmo que não tenha sido encontrada alterações histopatológicas.

Considerando o desequilíbrio no estado redox das células, frente ao uso de d-anfetamina, foi demonstrado que o estresse oxidativo induzido pela droga apresenta papel importante em seu potencial efeito hepatotóxico (CARVALHO et al., 2001; EL-TAWIL et al., 2011).

Assim também, uma resposta inflamatória desregulada pode ser causada em resposta a um composto tóxico, e levar a injúria tecidual (CHEN et al., 2018a). Contudo, na literatura, há somente um relato de caso relatando a associação entre o uso do LDX e hepatite. Um adolescente de 14 anos de idade, fazendo uso de LDX (30 mg/dia) para o tratamento do TDAH, prescrito por seu médico 5 meses antes do ocorrido, foi diagnosticado com hepatite eosinofílica devido ao uso da droga, mas que após 2 meses sem o uso deste e com o devido tratamento, houve melhora dos sintomas e uma normalização nos níveis das aminotransferases (HOOD; NOWICKI, 2010).

Tendo em vista que os rins são responsáveis pela excreção do LDX e seus metabólitos (FRAMPTON, 2018), também se faz necessária uma avaliação mais aprofundada sobre os possíveis efeitos tóxicos deste fármaco na morfofisiologia renal.

Krishnan e Montcrief (2007) observaram aumento do nitrogênio da ureia no sangue em ratos (100 e 300 mg/kg/dia durante 7 dias de tratamento) e ratas (30 e 100 mg/kg/dia durante 7 dias de tratamento). No estudo de 28 dias, a mesma condição foi observada em ratos e ratas, ambos na dose de 80 mg/kg/dia. Estas informações são importantes pois levantam a discussão de uma possível falha na função renal, visto que o nitrogênio da ureia no sangue é utilizado para avaliar a função renal, uma vez que este é filtrado pelos rins e deve ser eliminado na urina. Entretanto, tal alteração no nitrogênio da ureia no sangue também pode estar relacionada a disfunção hepática, sendo necessárias maiores avaliações (TRAYNOR et al., 2006).

Em estudo com ratos Wistar, para avaliar os efeitos de doses repetidas de d-anfetamina (20 mg/kg) por 14 dias na resposta antioxidante no fígado e rins, os autores observaram que a d-anfetamina altera as funções destes órgãos e seu sistema oxidante. Nos rins houve aumento de NAG (N-acetil-β-D-glucosaminidase) urinária e diminuição da creatinina urinária, indicando injúria renal, mesmo que pequena. Entretanto, ao final do experimento a resposta antioxidante renal foi efetiva, com aumento da GST (glutationa-S-transferase), CAT e Gred (glutationa redutase), evidenciando uma adaptação do órgão frente a lesão (CARVALHO et al., 1999). Em relação ao fígado, Carvalho et al. (1999) perceberam um aumento no ALT e AST após a administração de d-anfetamina, e aumento nos níveis de GSH, e redução nos níveis de GST, CAT e SOD2.

2 JUSTIFICATIVA

O TDAH é um dos transtornos de neurodesenvolvimento mais comumente diagnosticado em crianças, de curso estável, onde geralmente os sintomas podem continuar até a vida adulta. Seus sintomas de desatenção, desorganização e hiperatividade/impulsividade, afetam profundamente o desenvolvimento pessoal, social, educacional e profissional.

Para o tratamento desta condição, recomenda-se um tratamento multimodal, ou seja, uma combinação de abordagens terapêuticas farmacológicas e não farmacológicas. Entre as abordagens farmacológicas, tem sido observado um aumento nos últimos anos, na prescrição médica do fármaco LDX, um pró-fármaco da dextroanfetamina, com tempo de ação farmacológica prolongada e aparentemente menos reações adversas e risco de abuso, quando comparado a outros anfetamínicos. Esse fármaco é metabolizado na corrente sanguínea, especialmente na circulação portal, é e excretado via urinária.

Portanto, levando em conta a alta prescrição do fármaco para crianças com TDAH, as características farmacocinéticas, e a falta de informações detalhadas na literatura sobre os efeitos do LDX na morfofisiologia hepática e renal, faz-se necessário uma melhor avaliação deste utilizando uma metodologia aplicável e eficaz para responder nossos objetivos, e assim contribuir, com os resultados obtidos, na compreensão dos possíveis efeitos do fármaco sobre a morfofisiologia hepática e renal de ratos durante a peripuberade.

3 OBJETIVOS

3.1 GERAL

Devido à relevância clínica do tema e à falta de informações específicas sobre o assunto na literatura especializada, o objetivo deste presente trabalho foi avaliar se a administração de dimesilato de lisdexanfetamina pode gerar prejuízos para a morfofisiologia hepática e renal de ratos Wistar na peripuberdade, imediatamente após o término de sua administração.

3.2 ESPECÍFICOS

- Determinar se esse tratamento promove alterações histológicas e morfométricas no fígado e nos rins;

- Avaliar se este fármaco altera a fisiologia renal e hepática através da avaliação do perfil bioquímico, dosando creatinina, ureia, alanina aminotransferase, aspartato aminotransferase e marcadores de metabolismo lipídico;

- Analisar possíveis mecanismos de toxicidade do fármaco nestes órgãos através da avaliação do perfil inflamatório e de marcadores de estresse oxidativo;

- Contribuir com dados na literatura sobre os efeitos imediatos da administração de dimesilato de lisdexanfetamina sobre a morfofisiologia hepática e renal de ratos;

- Inferir a segurança do dimesilato de lisdexanfetamina para o fígado e rim durante a fase de peripuberdade.

4 ARTIGO 1

Effects of exposure to lisdexamfetamine dimesylate on hepatic parameters of pubertal rats

Artigo será submetido à revista – “Toxicology”

ISSN: 0300-483X

Fator de impacto (2020): 4.221

Qualis CAPES 2019 (Medicina II) = A2

Effects of exposure to lisdexamfetamine dimesylate on hepatic parameters of pubertal rats

João V. H. Silva[1,2], Letícia C. Santos[3], Rafaela P. Erthal[1,2], Dayane P. Santos[1,2], Camila R. Ferraz[2], Camila F. Souza[4], Waldiceu A. Verri Jr[2], Ernane T. Uchôa[4], Fábio G. Andrade[3], Glaura S. A. Fernandes[1*].

1 - Department of General Biology, Biological Sciences Center, State University of Londrina – UEL, Londrina, Paraná, Brazil

2 - Department of Pathology, Biological Sciences Center, State University of Londrina – UEL, Londrina, Paraná, Brazil

3 - Department of Histology, Biological Sciences Center, State University of Londrina – UEL, Londrina, Paraná, Brazil

4 - Department of Physiological Sciences, Biological Sciences Center, State University of Londrina – UEL, Londrina, Paraná, Brazil

***Corresponding author**

Tel.: +55 43 33714417
E-mail address: glaura@uel.br (G.S. A. Fernandes)

ABSTRACT

Lisdexamfetamine dimesylate (LDX) is a psychostimulant of the central nervous system, which has been widely recommended in recent years for the treatment of Attention-Deficit/Hyperactivity Disorder (ADHD). ADHD is a neurobehavioral disorder characterized by symptoms such as inattention, hyperactivity, or impulsivity, causing damage to people's quality of life. Therefore, the present study aims to evaluate the effects of LDX administration on the hepatic morphophysiology of puberal Wistar rats, since the liver is an organ involved in several functions of the organism. For this, 20 male Wistar rats were distributed randomly into two experimental groups: LDX group (LDX) - received 11,3 mg/kg/day of LDX diluted in tap water; and Control group (C) - received tap water. Animals were treated by gavage (oral route) during puberty, from postnatal day (PND) 25 to 65. At PND 66, the animals were anaesthetized and euthanized by inferior vena cava puncture. Blood was collected and plasma obtained was destined for biochemical dosage of liver damage and lipid metabolism markers. The liver and white adipose tissue were collected and weighed. The liver was used for determinations of the inflammatory profile, oxidative stress status, and for histochemical, and morphometric analyses. The results showed that the administration of LDX decreased in white adipose tissue weight, without altering weight gain. Plasmatic biochemical analysis demonstrated increase in plasmatic total cholesterol and in concentration of AST and ALT in LDX rats when compared with control, suggesting liver damage. In addition, in LDX animals there was an increase in NAG activity, indirectly indicating a macrophage recruitment to the liver in comparison with control. Also, in the LDX group the GST activity was reduced when compared with control. In conclusion, these results show that LDX causes liver inflammation and injury.

Keywords: Attention Deficit Hyperactivity Disorder; pharmacological treatment; hepatotoxicity; inflammation

1. Introduction

Amphetamine is a synthetic substance that acts as a central nervous system stimulant, being available for sale since the 1930s (HEAL et al., 2013). The main mechanism of action is to inhibit dopamine and norepinephrine transporters, causing increased levels of these catecholamines in the synaptic cleft (FARAONE, 2018). It is known that physiologically, dopamine helps in cognitive processes and motor activities (FARAONE et al., 2015), and serotonin is involved in modulating the dopaminergic system and emotional issues (DUNN et al., 2019).

The first report of the effectiveness of amphetamine was by Bradley (1937), using it in children with behavior problems. From this, and with the accomplishment of more scientific studies, amphetamines and their derivatives began to be used for several disorders, among them Attention-Deficit/Hyperactivity Disorder (ADHD) (CONNOLLY et al., 2015). ADHD is the most common neurodevelopmental disorder, characterized by persistent symptoms of inattention, hyperactivity, and impulsivity (AMERICAN PSYCHIATRIC ASSOCIATION, 2013). The estimated worldwide prevalence of ADHD in children and adolescents is 5.29%, with a higher incidence in men (POLANCZYK et al., 2007).

One of the amphetamines that is widely recommended to treat ADHD is lisdexamfetamine dimesylate (LDX) an inactive prodrug of dextroamphetamine (D-AMPH) (COMIRAN et al., 2016). According to Goodman (2010), LDX is the first long-acting psychostimulant prodrug intended for the treatment of ADHD and it consists of a D-AMPH covalently linked to the essential amino acid L-lysine.

LDX is mainly sold in capsule, so its main route of administration is oral (ERMER et al., 2016; STEER et al., 2012). This drug is mainly absorbed via peptide transporter 1 (PEPT1) (ERMER et al., 2012), which is abundantly expressed in the gut (VIENNOIS

et al., 2018). When absorbed, LDX will reach the portal bloodstream where will be quickly enzymatically hydrolyzed (ERMER et al., 2016). This metabolism occurs in plasma and is carried out in the cytosol of erythrocytes by an unknown aminopeptidase (SHARMAN; PENNICK, 2014). Najib et al., (2020) reported D-AMPH crosses the blood-brain barrier, reaches the central nervous system, and acts by increasing noradrenergic and dopaminergic neurotransmission. Afterwards, their metabolites are eliminated by renal excretion (KRISHNAN et al., 2008).

Evidence shows that LDX can produce some adverse effects on the organism. Krishnan and Montcrief (2007) evaluated the sub chronic repeated-dose (7 and 28 days) treatment of LDX in male and female Sprague-Dawley rats. In both periods evaluated, 7 (at doses of 100 and 300 mg/kg) and 28 days (at doses of 40 and 80 mg/kg), it was observed a reduction in weight gain and body weight of the animals. Further, these authors evaluated the biochemical parameters: in 7 days, the male rats that received 30 mg/kg showed an increase in both alkaline phosphatase and glucose levels. The 100 mg/kg dosage also caused a reduction in triglyceride levels. Furthermore, there was also an increase in blood albumin and liver injury markers in male rats that received 300 mg/kg LDX. The same biochemical parameters were evaluated over a period of 28 days, but with different dosages of the drug. Krishnan and Montcrief (2007) reported that the dose of 20 mg/kg did not cause any significant hepatic alteration. However, when evaluating the doses of 40 and 80 mg/kg, male and female rats showed increased alanine aminotransferase (ALT), and especially in female rats, increased the glucose. It is important to report that, this is the most detailed study on the effects of LDX use on the body, however there is still a lack of information in the scientific literature about the effects of LDX on hepatic morphophysiology.

There is a lot of both clinical and experimental evidence (EL-TAWIL et al., 2011; MONTIEL-DUARTE et al., 2002; SILVA et al., 2013) and case reports (HOOD; NOWICKI, 2010; VANGA et al., 2013) demonstrating hepatotoxicity caused by exposure to amphetamines in general, but not about LDX at this dosage. It is noteworthy that LDX is used in the developmental phase in humans, but there is no study of LDX hepatotoxicity in that phase, the puberty. Thus, as LDX is a relatively new drug and has a pharmacological profile different from other amphetamines (HEAL et al., 2013), it is necessary an extensive evaluation of the toxicological profile of LDX on different organs and tissues, evaluating possible changes in inflammatory, oxidative status, and morphological parameters. According to the explanation given and extensive study of the current scientific literature, the aim of the present study was to evaluate whether the administration of LDX causes damage to the liver morphophysiology of pubertal Wistar rats.

2. Material and methods

2.1. Animals and experimental conditions

Twenty male Wistar rats on postnatal day 22 (PND 22) were obtained from the Central Animal House of the Londrina State University (CCB - UEL), Paraná, Brazil. These animals were acclimated to the new environment (at the Animal House of the Laboratory of Toxicology and Metabolic Dysfunction of Reproduction) for three days before to the beginning of the experiment. During the experimental period (PND 25 to 65), the rats were accommodated into polypropylene cages (5 rats per cage) with laboratory-grade pine shavings as bedding. They were kept under controlled light conditions (12 h light/dark cycle, with lights on at 07:00 am), kept at a constant temperature (23 ± 2°C), and had access to standard commercial laboratory chow and

tap water *ad libitum*, throughout the experiment period. The body weight of all rats was measured three times a week throughout the experimental period and expressed in grams (g). All animal care and handling procedures were conducted in conformity with the National Institutes of Health guide for the care and use of laboratory animals (NIH Publications No. 8023, revised 1978), and this research was approved by the Ethics Committee on Animal Use of Londrina State University (OF. CIRC. CEUA N° 82/2019 and addendum OF. CIRC. CEUA N° 004/2021). All experimental procedures were performed by the same evaluators.

2.2. LDX exposure and experimental design

The animals were randomly assigned to two experimental groups of 10 animals each: control (C) and lisdexamfetamine (LDX). The animals in the LDX group received lisdexamfetamine dimesylate by gavage with 11.3 mg/kg b.w. (body weight) diluted in tap water. The calculation used was the conversion of animal doses (rat) to human equivalent doses based on body surface area (FOOD and DRUG ADMINISTRATION, 2005). This dose was selected considering that it is equivalent to administering a 70 mg capsule of the drug and corresponds to 1.13% of the oral LD50 for rats (oral LD50 for rats > 1000 mg/kg) (KRISHNAN; MONTCRIEF, 2007). Control group received only the vehicle (tap water). All groups were treated daily, by oral gavage, during forty consecutive days (between PND 25 and 65). This time corresponds to the juvenile and peripubertal phase of Wistar rats (OJEDA et al., 1980). This life stage of rats is like the recommended life stage for humans to use LDX, in childhood and puberty (NAJIB et al., 2020).

2.3. Preparation of lisdexamfetamine dimesylate solution

Lisdexamfetamine dimesylate (Venvanse®, Phateon Pharmaceuticals Inc., Ohio, USA) was daily diluted in the corresponding volume of tap water.

2.4. Blood and liver collection

On the 40th day of the experiment (PND 65), rats had their food removed at 9:00 pm, and the animals were subjected to blood glucose test at 9:00 am, when a drop of blood from the tail was collected for the determination of glycemia tested in the tape of the Accu-Chek Active (Roche, Taquara, RJ, Brazil).

In the PND 66, rats were intraperitoneally anaesthetized with a combination of ketamine 75 mg/kg b.w. (Sedomin® 10%, Avellaneda, Argentina) and xylazine 10 mg/kg b.w. (Anasedan®, Paulínia, Brazil), weighed and euthanized by inferior vena cava puncture. Blood samples was collected in the presence of heparin (Hemofol®, São Paulo, Brazil) and plasma was stored at -20°C for the determination of plasmatic aspartate aminotransferase (AST), ALT, cholesterol, triglycerides, and free fatty acids concentrations (n=10 rats per group).

The liver and white adipose tissue (retroperitoneal, perigonadal and perirenal) were removed, and the weights (absolute and relative to body weights) were determined (n=10 per group). Relative weight was determined by the ratio of organ weight to animal body weight multiplied by 100.

The largest lobe of the liver (large right middle lobe) was selected, and from it, divided into 3 parts for each analysis: histologic and histochemical analysis (n=6 per group); inflammatory profile (n=10 per group); and redox balance status assay (n=10 per group).

2.5. Biochemical analyses

2.5.1 Evaluation plasmatic cholesterol and triglycerides concentration

The spectrophotometric determination of cholesterol and triglycerides plasmatic concentrations was performed using the BioLiquid Cholesterol Commercial Kit (Laborclin, PR) and BioLiquid Tryglicérides GPO-Trinder Commercial Kit (Laborclin, PR), respectively, according to the manufacturer protocol and the values were expressed as mg/dL.

2.5.2 Measurement of plasmatic free fatty acids concentration

The spectrophotometric determination (wavelength of 550 nm) of plasmatic free fatty acids concentration was performed according to the methodology of Souza et al. (2019), and the values were expressed in μmoles/dL. For this, 100 μl of the plasma samples were used to perform two extractions, followed by shaking, aspiration of the upper phase and centrifugation. For the standard, 50 μl of palmitic acid (2 mM) was used in 1.0 ml of phosphate buffer (pH 6.4) and 6.0 ml of extractive solution, and the blank had only the extractive solution.

2.5.3 Assessment of liver injury

Plasmatic levels of AST and ALT were measured using the commercially available AST/GOT and ALT/GTP Liquiform kits (Labtest Diagnóstica SA, Brazil), respectively. All samples were measured in duplicates and were included in the same assay to avoid inter-assay errors. Results were presented as U/L.

2.6. Processing and morphometric and histological evaluation

Liver samples were fixed in aqueous Bouin for 48 h. The samples were embedded in paraffin and sectioned at 7 µm (2 non-serial sections per animal). The sections were stained with hematoxylin and eosin (HE) evaluated in a Moticam® image capture system coupled to a photomicroscope (Motic, Xiamen, China) and analyzed using the Motic Image Plus 3.0® software.

For measurement of morphometric parameters, 20 photomicrographs of each animal were obtained at 400x magnification: 10 images of the portal region and 10 of the central regions. The average diameter of portal vein, hepatic artery, bile duct, and central vein were performed. In each image, the diameter of 5 sinusoids next to the veins was also measured, and the count of leukocytes adhered to the vessel lumen.

Histological changes were evaluated based on previous studies (SAMELO et al., 2020; TEKTEMUR et al., 2021). In the sections, the following parameters of liver damage were observed: necrosis, hydropic degeneration, foci of defense cells, steatosis, vascular congestion, and sinusoidal congestion. The frequency of each parameter of liver injury was observed and scored as absent (0), mild (1), moderate (2) and severe (3).

2.7. Histochemical analyzes

2.7.1 Azan Heidenhain trichrome stain

This is a histochemical technique that evidence connective tissue. The slides (with 2 non-serial sections per animal) were first deparaffinized and rehydrated. The dyes used were Azo-Carmin G (20 min), phosphotungstic acid as catalyst (25 min) and Aniline blue (20 min), respectively. Using the Moticam® image capture system coupled to a photomicroscope (Motic, Xiamen, China), at 400x magnification, 5 images from each region (central and portal) were captured per animal. Using Image-Pro PLUS®

software version 4.5, the blue pixels which indicate collagen in each image were quantified according to Taatjes et al. (2019). The data were compared to define the distribution of these tissue components between the regions of the groups.

The regions close to the vessels were chosen for evaluation in the histochemical analyzes, because of the hemodynamic and functional scheme of the liver. As there is a difference in the blood that leaves the portal triad and reaches the central vein, the function of hepatocytes will also be different according to their location in the hepatic lobe (FREITAS-LOPES et al., 2017; TREFTS et al., 2017). For this reason, the lobe is divided into 3 metabolic zones (GRIJALVA; VAKILI, 2013).

2.7.2 Picrosirius-polarization method

Picrosirius red is a histochemical technique used to differentiate between mature (type I) and newly synthesized (type III) collagen fibers when observed under polarized light, so it is possible to determine the percentage of each type of collagen in tissues (GOWDA et al., 2017). In short, the slides (with 2 non-serial sections per animal) were deparaffinized, rehydrated, and immersed in Picrosirius solution (0.2 g of Sirius red in 200 ml of saturated picric acid) for 1 h, after being dehydrated and clarified. Using the Moticam® image capture system coupled to a polarized light microscope (Motic® BA410), at 400x magnification, 5 images from each region (central and portal) were captured per animal. Image-Pro PLUS® software version 4.5 was used to quantify the red pixels for type I collagen fibers and green pixels for type III collagen fibers (PUPIM et al. 2017). The data were compared to define the distribution of these tissue components between the regions of the groups.

2.7.3 Toluidine blue stain

This stain is mainly used to stain the metachromatic granules of the mast cells, and thus to be able to quantify the mast cells in tissues (RIBATTI, 2018). Tissue sections were stained with 1% toluidine blue to identify mast cells. Mast cells were classified with the aid of a light microscope into intact and degranulated mast cells. The analysis of the count of these cells was performed analyzing the entire length of the section (2 non-serial sections per animal) using a light microscope and quantifying and classifying each observed mast cell (PUNHAGUI et al., 2016).

2.8. Inflammatory profile

2.8.1 Myeloperoxidase activity

Myeloperoxidase (MPO) activity is a method of indirect assessment of neutrophil recruitment, since MPO is an abundant enzyme in the azurophilic granules of neutrophils. This assay was performed as previously described by Ferraz et al. (2021). Approximately 100 mg liver samples were removed and stored in a cryotube with 200 µL of 50 mM K_2PO_4 buffer solution (pH 6.0), composed of hexadecyl trimethylammonium bromide (HTAB; 0.5%), at -80 °C. On the day of the assay, these samples were homogenized in ice condition using a Tissue-Tearor (Biospec®). Subsequently, the homogenates were centrifuged (16,100 g, 2 min, 4◦C), and the resulting supernatants (15 µL) were blended with 200 µL 50 mM K_2PO_4 buffer, pH 6.0, containing 0.167 mg/mL of o-dianisidine dihydrochloride and 0.015% hydrogen peroxide. The absorbance of MPO activity was determined spectrophotometrically at 450 nm (Multiskan GO Microplate, Thermo Fischer Scientific, Vantaa, Finland). The results of the MPO activity assay are expressed as the number of neutrophils per mg of protein using a standard curve of neutrophils (196–400.000 neutrophils).

2.8.2 N-acetyl-β-D-glucosaminidase activity

N-acetyl-β-D-glucosaminidase (NAG) activity is a colorimetric method to assess macrophages recruitment. This assay was performed as previously described by Ferraz et al. (2021). Firstly, 10 µL of the supernatant obtained from the MPO activity procedure was separated and added to a 96-well plate followed by the addition of 40 µL of 50 mM phosphate buffer, pH 6.0. The reaction was initiated by the addition of 2.24 mM 4-nitrophenyl NAG. The plate was incubated at 37°C for 10 min, and the reaction was stopped by the addition of 100 µL of 0.2 M glycine buffer, pH 10.6. NAG enzymatic activity was determined spectrophotometrically at 400 nm (Multiskan GO Microplate, Thermo Fischer Scientific, Vantaa, Finland). The results of the NAG activity are expressed as the number of macrophages per mg of protein using a standard curve of macrophages (196–400.000 macrophages).

2.9. Oxidative stress status assay

2.9.1 Tissue preparation and protein determination

Liver samples were first homogenized in 1 mL PBS (pH 7.4) for 45 seconds using an Ultra-turrax (IKA Works, Wilmington, USA), and then centrifuged at 9.500 g for 10 min. The supernatant was used to determine the protein concentration by the Bradford method, using bovine serum albumin as a standard (BRADFORD, 1976). Afterwards, the samples were normalized to 1 mg/mL protein and used for the following analyses:

2.9.2 Determination of lipid peroxidation

Lipid peroxidation was measured to indirectly quantify the peroxides produced, which are thiobarbituric acid reactive substances (TBARS) (LUSHCHAK et al., 2009).

To prepare the test, 50 µL of each normalized sample was pipetted in duplicate in a microplate, and the following substances were added to the sample: 5 µL of 1M $FeCl_3$, 5 µL of 0.5 M ascorbic acid, 50 µL of TCA 2.8%, and 50 µL of 1% thiobarbituric acid (TBA). Afterwards, the samples were shaken and placed in a water bath at 90°C for 15 minutes. The microplate was allowed to cool, to stop the reaction, and finally read. The intermediate product of lipid peroxidation, malondialdehyde (MDA) was determined by subtracting the absorbance at 535 nm and 572 nm (BUEGE; AUST, 1978). Lipid peroxidation was estimated correcting for the amount of protein, and the results are expressed in nmol of MDA per mg of protein.

2.9.3 Catalase activity

Catalase activity was determined based on Aebi (1984). Catalase converts hydrogen peroxide (H_2O_2) into 2 H_2O + 1 O_2. To prepare the test, 3 µL of each normalized sample was pipetted in duplicate in a UV4 microplate, and 297 µL of reaction medium were added to the sample. Reading was performed immediately at 240 nm for 1 min, at 15 second intervals. The catalase values were expressed as units of catalase mM formed.min^{-1}.mg of $protein^{-1}$.

2.9.4 Glutathione S-transferase activity

This analysis evaluates the enzymatic activity of glutathione S-transferase (GST) in catalyzing the conjugation of GSH with the synthetic substrate CDNB, causing the formation of a thioether. This assay was performed as described by Keen et al. (1976) with some modifications. The increase in absorbance through the formation of the thioether was monitored at 340 nm (RS: 100 mM potassium phosphate buffer pH

6.5; 1.5 mM GSH; 2 mM CDNB) for 160 seconds at 40 second intervals. Values were expressed as μM thioether formed.min^{-1}.mg of protein^{-1}.

2.9.5 Glutathione quantification

Reduced glutathione (GSH) levels in the liver homogenate supernatant were determined as proposed by Rahman et al. (2006), with some modifications. For this, was used 10 μL of the normalized sample, 180 μL of the mix solution, and 360 uL CDNB, pipetted into a microplate, and evidenced by a yellow color formation. After 15 min, reading was measured at 412 nm. The amount of GSH was estimated from a GSH standard curve, and the results are expressed in μM/mg of protein^{-1}.

2.9.6 Superoxide dismutase activity

The evaluation of the activity of the enzyme superoxide dismutase (SOD) was performed as described by Senthilkumar et al. (2021) with some adaptations. The enzyme comes from homogenates normalized to 1mg/ml. A reaction mixture was prepared containing sodium carbonate buffer (50mM, pH 10.2), nitroblue tetrazoilium (NBT) (96 uM) and Triton X-100 (0.6%), which was incubated for 2 minutes with sodium hydrochloride. hydroxylamine (NH2OH·HCl) (20 mM, pH 6.0). The final volume was adjusted to 200 μL. The reaction consists of the quantification of complexes formed by superoxide anions with the addition of NBT and NH2OH·HCl of yellowish color with the reduction of NBT, forming a bluish color read at 560 nm for 2 minutes at intervals of 15 seconds. Results are expressed in U formed.min^{-1}.mg of protein^{-1}.

2.10. Statistical analysis

The parameters were submitted to the Shapiro-Wilk test to verify the normal distribution of the data and classify them into parametric and non-parametric data. The homogeneity of the variance between the groups was assessed by the Levene test. Comparisons of data between two groups were performed using Student's unpaired t test or the Mann-Whitney test. Data are presented as mean ± S.E.M. (standard error of the mean), with $P<0.05$ considered statistically significant. The statistical analyses and graph design for results were performed by GraphPad Prism for Windows version 8.2.1 (San Diego, CA, USA).

3. Results

3.1. Body and organs weights

The body weight (gain, initial and final) and relative and absolute organ weights (liver and white adipose tissue) are shown in Table 1. There were no significant differences between groups for body weight parameters. However, it was observed a reduction in the weight of the white adipose tissue (absolute and relative weight) in the animals of the LDX group when compared to the Control group.

3.2. Assessment of liver injury and lipid metabolism

Plasmatic concentrations of AST and ALT, which are markers of liver injury, increased in animals that received LDX compared to Control group (Figure 1).

In the assessment of lipid metabolism, no significant difference was observed in the plasmatic concentration of triglycerides (Figure 2B), free fatty acids (Figure 2C) and glycemia (Figure 2D). However, the plasmatic concentration of total cholesterol was significantly higher in the animals that received LDX (Figure 2A).

3.3. Morphometric and histopathological analyses of the liver

Morphometric analysis (Table 2) showed that the dose used of LDX did not changes the mean diameter of the main hepatic structures, which are the central vein, portal vein, hepatic artery, and bile duct. The average diameter of the lumen of sinusoids near to the main vessels were also not significantly different.

Histopathological analysis of the liver, as shown in Figure 3, revealed moderate vascular congestion and mild vacuolization of hepatocytes, with similar frequency in animals from both experimental groups. On the other hand, in both groups, sinusoidal congestion, focus of defense cells in the parenchyma, steatosis and necrosis were not observed.

3.4. Liver inflammatory profile

With the toluidine blue technique, it was possible to count the number of mast cells in the extent of the cut, and differentiate them as intact or degranulated, but there was no difference between the control and LDX groups (Table 3). Furthermore, in the HE stains, leukocytes adhered to the main vessels were counted, but there was also no significant difference between the groups (Table 3).

In Figure 4, there are the results from the evaluation of MPO and NAG activity. There was no significant difference in MPO activity (Figure 4A) between the LDX and Control groups, however it is possible to observe that LDX increased NAG activity in the liver (Figure 4B). This indirectly indicates that there was an increase in the recruitment of macrophages in the liver, but not neutrophils.

3.5. Hepatic oxidative stress status

LDX administration did not induce an increase in hepatic lipid peroxidation when assessing MDA concentration (Figure 5A). Furthermore, when evaluating enzymes of the antioxidant system, no significant differences were observed in CAT activity (Figure 5C), GSH quantification (Figure 5D), and SOD activity (Figure 5E) between groups. However, there was a reduction in GST activity in the LDX group compared to the control group (Figure 5B).

3.6. Histochemical analyses

The percentage of total collagen (Figure 6) and of the different types of collagens (Figure 7) evidenced that there were no significant differences between the experimental groups for these parameters.

4. Discussion

In the present study, we show that exposure to LDX during peripubertal period impairs the hepatic morphophysiology in pubertal male rats, and that immune and antioxidant systems may to modulate this process.

Interestingly, it was demonstrated that LDX at the dose used reduces white adipose tissue in male Wistar rats without altering significantly gain weight. Corroborating our findings, Krishnan and Montcrief (2007) reported that after 28 days of treatment with LDX (20 mg/kg/day; orally), Sprague-Dawley male rats with approximately seven weeks old at the initiation of treatment, showed minimal toxicological effects, with no change in body assessment parameters. However, the same authors also evidenced rats that received different doses of LDX (40 and 80 mg/kg/day), showed a reduction in mean body weight and weight gain. Oppositely,

Ekstrand et al. (2019) showed a significant decrease in mesenteric, renal and epididymal adiposity and consequently a reduction in body weight in male Long-Evans rats (with approximately five weeks of age at the start of the study) after 1,5 mg/kg LDX oral administration for twenty days and a further nine days of withdrawal period. Therefore, our results indicated that alterations in body parameters are influenced by LDX dose and treatment time since low dose (11,3 mg/kg LDX oral administration) for approximately five weeks caused reduction in adipose tissue without reducing the body weight in male rats.

Liver weight was also assessed, but there was no significant increase or decrease in weight after LDX administration. Other studies evaluating this parameter were also performed, for exposure to LDX (KRISHNAN; MONTCRIEF, 2007) and d-amphetamine (CARVALHO et al., 1999) and none showed a statistically significant change in absolute weight or relative to body weight.

Another significant parameter found altered in our data was the increase in ALT and AST transaminases after LDX administration. Plasmatic dosage of these transaminases has long been used to evaluate liver injury (MCGILL, 2016; SOOKOIAN; PIROLA, 2015), since hepatocellular damage results in increased leakage of these intracellular enzymes into the circulation (KAMIIKE et al., 1989; REICHLING; KAPLAN, 1988). However, it is also known their importance in the functioning of hepatic metabolism, which contributes to the systemic metabolic regulation (SOOKOIAN; PIROLA, 2012; SOOKOIAN; PIROLA, 2015). However, in the present study, despite the increase in ALT and AST levels, no morphological changes were found in the liver. Similarly, to the present results, Krishnan and Montcrief (2007) showed that after 28 days of treatment with LDX (40 and 80 mg/kg), there were no liver histopathological damage in Sprague-Dawley male rats.

On the other hand, methylphenidate, which is another first-line drug for the treatment of ADHD, and with a similar mechanism of action to LDX (MECHLER et al. 2022), did not interfere in increase in ALT and AST (LOUREIRO-VIEIRA et al. 2018). This was observed by Loureiro-Vieira et al. (2018), when using male Wistar rats (PND 40) that received 2 oral doses (at 9 a.m. and 2 p.m.) of 5 mg/kg methylphenidate for 6 days. In addition, qualitative histological analysis showed that the liver structure was preserved.

When the liver is affected by disease or injury, lipid metabolism may be altered (ALANNAN et al., 2020; LIANGPUNSAKUL; CHALASANI, 2019; WILLIS et al., 2021). The liver is the main organ that regulates lipid metabolism (ALVES-BEZERRA; COHEN, 2017), acting, for example, in cholesterol homeostasis (WANG et al., 2018) even as adipose tissue with white adipose tissue being the largest reservoir of free cholesterol (KRAUSE; HARTMAN, 1984). This establishing a balance between cholesterol deposits in adipose tissue and circulating cholesterol (ZHANG et al., 2019). Cholesterol is known to be a structural component of biological membranes where it ensures many of the functions of the membrane (IKONEN, 2008), and can act as a signaling pathway for physiological and pathological processes, modulating cell cycle progression, and aiding in tissue regeneration (DELGADO-COELLO et al., 2011).

Therefore, in the current study, we could hypothesize that the increase in the plasmatic concentration of total cholesterol would be associated with liver damage. However, in a study by Tonomura et al. (2014), where the diagnostic and predictive performance of some biomarkers for drug-induced liver injury in male rats was investigated using an open access database, it was suggested that total cholesterol is not an efficient biomarker for this. In other words, in this case, we believe that the liver injury did not change liver function. Perhaps, more severe liver injury could change

hepatic functional biomarkers (SENIOR, 2012). In addition, it would be necessary to measure the cholesterol fractions, for example the low-density lipoprotein-cholesterol (LDL) and high-density lipoprotein-cholesterol (HDL), to better understand the origin of this increase in plasmatic cholesterol.

According to the inflammatory profile evaluations, the increase in NAG activity indirectly indicated an increase in macrophages in the liver after exposure to LDX. Macrophages are a population of leukocytes that can be found in many tissues. These may be monocytes that when recruited into the tissue become macrophages, or they may already be tissue resident macrophages (KADOMOTO et al., 2022). There were several macrophage subtypes exist, but it is possible to divide them into two main subsets, M1 and M2, according to their inflammatory signs (SHAPOURI-MOGHADDAM et al., 2018). The M1 are activated by LPS and IFN-γ, and are known to be more pro-inflammatory, producing cytokines such as TNF-α and IL-6 (BASHIR et al., 2016). They mainly have activity against microorganisms and malignant tumor cells (LI; HUA, 2017). M2 macrophages can be activated by IL-4 and IL-13 (MURRAY et al., 2014) and unlike M1 macrophages, they present anti-inflammatory, pro-resolving characteristics, repairing or healing wounds by secreting pro-fibrotic factors (WANG et al., 2019). However, studies have already shown that can promote tumor progression (BELGIOVINE et al., 2016; CHEN et al., 2017).

Resident macrophages in liver are called Kupffer cells. They have several functions, such as eliminating pathogens and other waste, maintaining the metabolism of different substances. Briefly, they act on homeostasis and immune tolerance (KRENKEL; TACKE, 2017). In the literature there is evidence of the importance of macrophages in liver recovery after drug-induced injury. To better understand this, Miura et al. (2021) performed liver macrophage depletion after carbon tetrachloride

(CCl4) induced liver injury. They concluded that the absence of these leukocytes during the hepatic regeneration phase suppresses tissue remodeling for injury repair, by affecting cell proliferation, functional recovery of nutrient metabolism and the carbohydrate metabolic pathway. Also, in a model of acetaminophen-induced liver injury, it was proven that the lack of infiltrating macrophages caused a delay in tissue repair (HOLT et al., 2008; YOU et al., 2013).

MPO activity and number of leukocytes adhered to the vessels were unchanged, indicating that there was no alteration in neutrophil recruitment at this time point of ongoing LDX exposure. This information is important because it is known that when neutrophils arrive at the inflammatory site, they contribute to the inflammatory response. Therefore, stopping neutrophilic activity is necessary for lesion resolution (ZIGMOND et al., 2014). Further, the change of cellular profile from neutrophils to macrophages characterizes chronic inflammation and repair phases (MEDZHITOV, 2008), which is compatible with the enhancement of NAG activity observed.

In addition, even with the increase of macrophages in the liver, no fibrotic process was observed in our analyses. Corroborating our data, Loureiro-Vieira et al. (2018) also demonstrated that twice daily oral exposure (for 6 days) of 5 mg/kg of methylphenidate, did not alter collagen deposition in the liver of male Wistar rats (PND 40).

Liver injuries can cause redox imbalance, resulting in oxidative stress (ZHU et al., 2012). Inflammatory response and drug-induced toxicity are examples of increased production of ROS, since the liver has high metabolic and detoxification activity and therefore, it generates many pro-oxidant molecules (ANDRADE et al., 2015).

Although, as far as we know, there was no previous studies evaluating the oxidative status in the liver after continuous use of LDX, however, the use of d-amphetamine has been shown promote hepatotoxicity effects (CARVALHO et al., 2001; EL-TAWIL et al., 2011). Carvalho et al., (1999), in a study with male Wistar rats, using repeated doses of d-amphetamine (20 mg/kg for 14 days), demonstrated that there was an increase in the levels of GSH, and a reduction in the activity of GST, CAT and MnSOD (manganese superoxide dismutase) in the liver. In the current study, the reduction in GST activity evidence that GST seems to be used to protect liver cells against lipid peroxidation, since MDA levels were similar between the experimental groups. GST is a very important enzyme in the detoxification process, because during the oxidative stress process, it acts inactivating secondary metabolites produced (FAUSTINO et al., 2011).

The present study evidenced for the first time that the long-term dose of LDX causes hepatic damage in pubertal rats, such as observed by the increase in ALT and AST. On the other hand, macrophages are recruited for tissue repair in this organ following by reduces adipose tissue weight without significantly alteration in body weight gain.

5. Conclusion

In conclusion, LDX-administration in male rats during the peripubertal period causes liver damage in pubertal age with the involvement of endogenous antioxidant and inflammatory response.

Conflict of interest

The authors declare that there are no conflicts of interest.

Acknowledgements

The authors are grateful to CAPES - PROEX (Coordinating Body for the Improvement of Postgraduate Studies in Higher Education) for providing a Master's scholarship to JVH da Silva, and partially financial support (Finance Code 001). This paper represents part of the Master's thesis by JVH da Silva (Experimental pathology – State University of Londrina - Brazil) under the supervision of GSA Fernandes. WA Verri Jr reports the research fellowship from CNPq (#309633/2021-4).

References

Aebi, H., 1984. Catalase *in vitro*. Methods Enzymol. 105, 121–126. https://doi.org/10.1016/s0076-6879(84)05016-3.

Alannan, M., Fayyad-Kazan, H., Trézéguet, V. & Merched, A., 2020. Targeting Lipid Metabolism in Liver Cancer. Biochemistry, 59, 3951–3964. https://doi.org/10.1021/acs.biochem.0c00477.

American Psychiatric Association, 2013. Diagnostic and statistical manual of mental disorders: DSM-5. Arlington, VA: American Psychiatric Association. https://doi.org/10.1176/appi.books.9780890425596.

Andrade, K. Q., Moura, F. A., Santos, J. M., Araújo, O. R., Santos, J. C. F. & Goulart, M. O., 2015. Oxidative Stress and Inflammation in Hepatic Diseases: Therapeutic Possibilities of N-Acetylcysteine. Int. J. Mol. Sci. 16, 30269–30308. https://doi.org/10.3390/ijms161226225.

Bashir, S., Sharma, Y., Elahi, A. & Khan, F., 2016. Macrophage polarization: the link between inflammation and related diseases. Inflamm. Res. 65, 1–11. https://doi.org/10.1007/s00011-015-0874-1.

Belgiovine, C., D'Incalci, M., Allavena, P. & Frapolli, R., 2016. Tumor-associated macrophages and anti-tumor therapies: complex links. Cell. Mol. Life Sci. 73, 2411–2424. https://doi.org/10.1007/s00018-016-2166-5.

Bradford, M. M., 1976. A rapid and sensitive method for the quantitation of microgram quantities of protein utilizing the principle of protein-dye binding. Anal. Biochem. 72, 248–254. https://doi.org/10.1016/0003-2697(76)90527-3.

Bradley, C., 1937. The Behavior of Children Receiving Benzedrine. Am. J. Psychiatry. 94, 577–581.

Buege, J. A. & Aust, S. A., 1978. Microsomal lipid peroxidation methods. Enzymol 52, 302–310.

Carvalho, F., Fernandes, E., Remião, F. & Bastos, M. L., 1999. Effect of d-amphetamine repeated administration on rat antioxidant defences. Arch. Toxicol. 73, 83–89. https://doi.org/10.1007/s002040050591.

Carvalho, F., Duarte, J. A., Neuparth, M. J., Carmo, H., Fernandes, E., Remião, F. & Bastos, M. L., 2001. Hydrogen peroxide production in mouse tissues after acute d-amphetamine administration. Influence of monoamine oxidase inhibition. Arch. Toxicol. 75, 465–469. https://doi.org/10.1007/s002040100264.

Chan, Y. H., 2003. Biostatistics 104: correlational analysis. Singapore Med. J. 44, 614–619.

Chen, Y., Zhang, S., Wang, Q. & Zhang, X., 2017. Tumor-recruited M2 macrophages promote gastric and breast cancer metastasis via M2 macrophage-secreted CHI3L1 protein. J. Hematol. Oncol. 10, 36. https://doi.org/10.1186/s13045-017-0408-0.

Comiran, E., Kessler, F. H., Fröehlich, P. E. & Limberger, R. P., 2016. Lisdexamfetamine: A pharmacokinetic review. Eur. J. Pharm. Sci. 89, 172–179. https://doi.org/10.1016/j.ejps.2016.04.026.

Connolly, J. J., Glessner, J. T., Elia, J. & Hakonarson, H., 2015. ADHD & Pharmacotherapy: Past, Present and Future: A Review of the Changing Landscape of Drug Therapy for Attention Deficit Hyperactivity Disorder. Ther. Innov. Regul. Sci. 49, 632–642. https://doi.org/10.1177/2168479015599811.

Delgado-Coello, B., Briones-Orta, M. A., Macías-Silva, M. & Mas-Oliva, J., 2011. Cholesterol: recapitulation of its active role during liver regeneration. Liver Int. 31, 1271–1284. https://doi.org/10.1111/j.1478-3231.2011.02542.x.

Dunn, G. A., Nigg, J. T. & Sullivan, E. L., 2019. Neuroinflammation as a risk factor for attention deficit hyperactivity disorder. Pharmacol. Biochem. Behav. 182, 22–34. https://doi.org/10.1016/j.pbb.2019.05.005.

Ekstrand, E., Murphy, H. M. & Wideman, C. H., 2019. The effects of the prodrug Vyvanse on spatial working memory and adiposity in rats. Pharmacol. Biochem. Behav. 186, 172765. https://doi.org/10.1016/j.pbb.2019.172765.

El-Tawil, O. S., Abou-Hadeed, A. H., El-Bab, M. F. & Shalaby, A. A., 2011. d-Amphetamine-induced cytotoxicity and oxidative stress in isolated rat hepatocytes. Pathophysiology 18, 279–285. https://doi.org/10.1016/j.pathophys.2011.04.001.

Ermer, J. C., Haffey, M. B., Doll, W. J., Martin, P., Sandefer, E. P., Dennis K., Corcoran M., Trespidi L. & Page R. C., 2012. Pharmacokinetics of lisdexamfetamine dimesylate after targeted gastrointestinal release or oral administration in healthy adults. Drug Metab. Dispos. 40, 290–297. https://doi.org/10.1124/dmd.111.040691.

Ermer, J. C., Pennick, M. & Frick, G., 2016. Lisdexamfetamine Dimesylate: Prodrug Delivery, Amphetamine Exposure and Duration of Efficacy. Clin. Drug Investig. 36, 341–356. https://doi.org/10.1007/s40261-015-0354-y.

Faraone, S. V., Asherson, P., Banaschewski, T., Biederman, J., Buitelaar, J. K., Ramos-Quiroga, J. A., Rohde, L. A., Sonuga-Barke, E. J., Tannock, R. & Franke, B., 2015. Attention-deficit/hyperactivity disorder. Nat. Rev. Dis. Prim. 1. https://doi.org/10.1038/nrdp.2015.20.

Faraone, S. V., 2018. The pharmacology of amphetamine and methylphenidate: Relevance to the neurobiology of attention-deficit/hyperactivity disorder and other psychiatric comorbidities. Neurosci. Biobehav. Rev. 87, 255–270. https://doi.org/10.1016/j.neubiorev.2018.02.001.

Faustino, L. C., Pires, R. M., Lima, A. C., Cordeiro, A., Souza, L. L. & Ortiga-Carvalho, T. M., 2011. Liver glutathione S-transferase expression is decreased by 3,5,3-triiodothyronine in hypothyroid but not in euthyroid mice. Exp. Physiol. 96, 790–800. https://doi.org/10.1113/expphysiol.2011.058172.

Ferraz, C. R. et al., 2021. Toxicon Peripheral mechanisms involved in Tityus bahiensis venom-induced pain. Toxicon 200, 3–12. https://doi.org/10.1016/j.toxicon.2021.06.013.

Food and Drug Administration, 2013. Guidance for Industry: Estimating the Maximum Safe Starting Dose in Initial Clinical Trials for Therapeutics in Adult Healthy Volunteers. Rockville, EUA, Food and Drug Administration, 2005.

Freitas-Lopes, M. A., Mafra, K., David, B. A., Carvalho-Gontijo, R. & Menezes, G. B., 2017. Differential Location and Distribution of Hepatic Immune Cells. Cells, 6, 48. https://doi.org/10.3390/cells6040048.

Goodman, D. W., 2010. Lisdexamfetamine Dimesylate (Vyvanse), A Prodrug Stimulant for Attention-Deficit / Hyperactivity Disorder. Pharmacy & Therapeutics 35.

Gowda, B. C., Kokila, G., Gopinathan, P. A. & Praveen, K. S., 2017. Picrosirius red and polarization microscopy – a tool for gender differentiation. J. Clin. Diagnostic Res. 11, ZC107–ZC109. https://doi.org/10.7860/JCDR/2017/22863.9296.

Grijalva, J. & Vakili, K., 2013. Neonatal liver physiology. Semin. Pediatr. Surg. 22, 185–189. https://doi.org/10.1053/j.sempedsurg.2013.10.006.

Heal, D. J., Smith, S. L., Gosden, J. & Nutt, D. J., 2013. Amphetamine, past and present – a pharmacological and clinical perspective. J. Psychopharmacol. 27, 479–496. https://doi.org/10.1177/0269881113482532.

Holt, M. P., Cheng, L. & Ju, C., 2008. Identification and characterization of infiltrating macrophages in acetaminophen-induced liver injury. J. Leukoc. Biol. 84, 1410–1421. https://doi.org/10.1189/jlb.0308173.

Hood, B. & Nowicki, M. J., 2010. Eosinophilic hepatitis in an adolescent during lisdexamfetamine dimesylate treatment for ADHD. Pediatrics 125, e1510–e1513. https://doi.org/10.1542/peds.2009-1835.

Ikonen, E., 2008. Cellular cholesterol trafficking and compartmentalization. Nat. Rev. Mol. Cell Biol. 9, 125–138. https://doi.org/10.1038/nrm2336.

Kadomoto, S., Izumi, K. & Mizokami, A., 2022. Macrophage Polarity and Disease Control. Int. J. Mol. Sci. 23, 144. https://doi.org/10.3390/ijms23010144.

Kamiike, W., Fujikawa, M., Koseki, M., Sumimura, J., Miyata, M., Kawashima, Y., Wada, H., & Tagawa, K., 1989. Different patterns of leakage of cytosolic and mitochondrial enzymes. Clin. Chim. Acta 185, 265–270. https://doi.org/10.1016/0009-8981(89)90216-7.

Keen, J. H., Habig, W. H. & Jakoby, W. B., 1976. Mechanism for the several activities of the glutathione S-transferases. J. Biol. Chem. 251, 6183–6188. https://doi.org/10.1016/S0021-9258(20)81842-0.

Krause, B. R. & Hartman, A. D., 1984. Adipose tissue and cholesterol metabolism. J. Lipid. Res. 25, 97–110.

Krenkel, O. & Tacke, F., 2017. Liver macrophages in tissue homeostasis and disease. Nat. Rev. Immunol. 17, 306–321. https://doi.org/10.1038/nri.2017.11.

Krishnan, S. & Montcrief, S., 2007. Toxicity profile of lisdexamfetamine dimesylate in three independent rat toxicology studies. Basic Clin. Pharmacol. Toxicol. 101, 231–240. https://doi.org/10.1111/j.1742-7843.2007.00093.x.

Krishnan, S. M., Pennick, M. & Stark, J. G., 2008. Metabolism, Distribution and Elimination of Lisdexamfetamine Dimesylate: open-label, single-centre, phase I study in healthy adult volunteers. Clin. Drug. Invest. 28, 745–755. https://doi.org/10.2165/0044011-200828120-00002.

Li, N. & Hua, J., 2017. Immune cells in liver regeneration. Oncotarget 8, 3628–3639. https://doi.org/10.18632/oncotarget.12275.

Liangpunsakul, S. & Chalasani, N., 2019. Lipid mediators of liver injury in nonalcoholic fatty liver disease. Am. J. Physiol. Gastrointest. Liver Physiol. 316, G75–G81. https://doi.org/10.1152/ajpgi.00170.2018.

Loureiro-Vieira, S., Costa, V. M., Duarte, J. A., Duarte-Araújo, M., Gonçalves-Monteiro, S., Maria de Lourdes, B., Carvalho, F. & Capela, J. P., 2018. Methylphenidate clinically oral doses improved brain and heart glutathione redox status and evoked renal and cardiac tissue injury in rats. Biomed. Pharmacother. 100, 551–563. https://doi.org/10.1016/j.biopha.2018.02.017.

Lushchak, O. V., Kubrak, O. I., Lozinsky, O. V., Storey, J. M., Storey, K. B. & Lushchak, V. I., 2009. Chromium(III) induces oxidative stress in goldfish liver and kidney. Aquat. Toxicol. 93, 45–52. https://doi.org/10.1016/J.AQUATOX.2009.03.007.

McGill, M. R., 2016. The past and present of serum aminotransferases and the future of liver injury biomarkers. EXCLI J. 15, 817–828. https://doi.org/10.17179/excli2016-800.

Mechler, K., Banaschewski, T., Hohmann, S. & Häge, A., 2022. Evidence-based pharmacological treatment options for ADHD in children and adolescents. Pharmacol. Ther. 230, 107940. https://doi.org/10.1016/j.pharmthera.2021.107940.

Medzhitov, R., 2008. Origin and physiological roles of inflammation. Nature, 454, 428–435. https://doi.org/10.1038/nature07201.

Miura, A., Hosono, T. & Seki, T., 2021. Macrophage potentiates the recovery of liver zonation and metabolic function after acute liver injury. Sci. Rep. 11, 9730. https://doi.org/10.1038/s41598-021-88989-9.

Montiel-Duarte, C., Varela-Rey, M., Osés-Prieto, J. A., López-Zabalza, M. J., Beitia, G., Cenarruzabeitia, E. & Iraburu, M., 2002. 3,4-Methylenedioxymethamphetamine (“Ecstasy”) induces apoptosis of cultured rat liver cells. Biochimica et Biophysica Acta 1588, 26-32. https://doi.org/10.1016/S0925-4439(02)00112-6.

Murray, P. J., et al., 2014. Macrophage activation and polarization: nomenclature and experimental guidelines. Immunity 41, 14–20. https://doi.org/10.1016/j.immuni.2014.06.008.

Najib, J., Didenko, E., Meleshkina, D., Yusupov, K., Maw, K., Ramnarain, J. & Tabassum, M., 2020. Review of lisdexamfetamine dimesylate in children and adolescents with attention deficit/hyperactivity disorder. Curr. Med. Res. Opin. 36, 1717–1735. https://doi.org/10.1080/03007995.2020.1815002.

Ojeda, S. R., Andrews, W. W., Advis, J. P. & White, S. S., 1980. Recent advances in the endocrinology of puberty. Endocr Rev. 1, 228-257. https://doi.org/10.1210/edrv-1-3-228.

Polanczyk, G., Lima, M. S., Horta, B. L., Biederman, J. & Rohde, L. A., 2007. The Worldwide Prevalence of ADHD: A Systematic Review and Metaregression Analysis. Am. J. Psychiatry 164, 942–948. https://doi.org/10.1176/ajp.2007.164.6.942.

Punhagui, A. P. F., Vieira, H. R., Siervo, G. E. M. L., Rosa, R. & Fernandes, G. S. A., 2016. Ethanol exposure during peripubertal period increases the mast cell number and impairs meiotic and spermatic parameters in adult male rats. Microsc. Res. Tech. 79, 541–549. https://doi.org/10.1002/jemt.22664.

Pupim, A. C. E., Campois, T. G., Araújo, E. J. A., Svidizinski, T. I. E. & Felipe, I., 2017. Infection and tissue repair of experimental cutaneous candidiasis in diabetic mice. J. Med. Microbiol. 66, 808–815. https://doi.org/10.1099/jmm.0.000496.

Rahman, I., Kode, A. & Biswas, S. K., 2006. Assay for quantitative determination of glutathione and glutathione disulfide levels using enzymatic recycling method. Nat. Protoc. 1, 3159–3165. https://doi.org/10.1038/nprot.2006.378.

Reichling, J. J., & Kaplan, M. M., 1988. Clinical use of serum enzymes in liver disease. Dig. Dis. Sci. 33, 1601–1614. https://doi.org/10.1007/BF01535953.

Ribatti, D., 2018. The Staining of Mast Cells: A Historical Overview. Int. Arch. Allergy Immunol. 176, 55–60. https://doi.org/10.1159/000487538.

Samelo, R. R., Medeiros, P. C., Cavalcante, D. N. C., Aranha, M., Duarte, F. A., Castro, Í. B., Ribeiro, D. A. & Perobelli, J. E., 2020. Low concentrations of sodium arsenite induce hepatotoxicity in prepubertal male rats. Environ. Toxicol. 35, 553–560. https://doi.org/10.1002/tox.22890.

Senior J. R., 2012. Alanine aminotransferase: a clinical and regulatory tool for detecting liver injury-past, present, and future. Clin. Pharmacol. Ther. 92, 332–339. https://doi.org/10.1038/clpt.2012.108.

Senthilkumar, M., Amaresan, N. & Sankaranarayanan, A., 2021. Plant-Microbe Interactions, Springer Protocols Handbooks. Springer US, New York, NY. https://doi.org/10.1007/978-1-0716-1080-0.

Shapouri-Moghaddam, A., Mohammadian, S., Vazini, H., Taghadosi, M., Esmaeili, S. A., Mardani, F., Seifi, B., Mohammadi, A., Afshari, J. T., & Sahebkar, A., 2018. Macrophage plasticity, polarization, and function in health and disease. J. Cell. Physiol. 233, 6425–6440. https://doi.org/10.1002/jcp.26429.

Sharman, J. & Pennick, M., 2014. Lisdexamfetamine prodrug activation by peptidase-mediated hydrolysis in the cytosol of red blood cells. Neuropsychiatr. Dis. Treat. 20, 2275–2280. https://doi.org/10.2147/NDT.S70382.

Silva, D. D., Carmo, H., Lynch, A. & Silva, E., 2013. An insight into the hepatocellular death induced by amphetamines, individually and in combination: the

involvement of necrosis and apoptosis. Arch. Toxicol. 87, 2165–2185. https://doi.org/10.1007/s00204-013-1082-9.

Sookoian, S. & Pirola, C. J., 2012. Alanine and aspartate aminotransferase and glutamine-cycling pathway: their roles in pathogenesis of metabolic syndrome. World J. Gastroenterol. 18, 3775–3781. https://doi.org/10.3748/wjg.v18.i29.3775.

Sookoian, S. & Pirola, C. J., 2015. Liver enzymes, metabolomics and genome-wide association studies: From systems biology to the personalized medicine. World J. Gastroenterol. 21, 711–725. https://doi.org/10.3748/wjg.v21.i3.711.

Souza, C. F., Stopa, L. R. S., Santos, G. F., Takasumi, L. C. N., Martins, A. B., Garnica-Siqueira, M. C., Ferreira, R. N., Andrade, F. G., Leite, C. M., Zaia, D. A. M., Zaia, C. T. B. V. & Uchoa, E. T., 2019. Estradiol protects against ovariectomy-induced susceptibility to the anabolic effects of glucocorticoids in rats. Life Sci. 218, 185–196. https://doi.org/10.1016/j.lfs.2018.12.037.

Steer, C., Froelich, J., Soutullo, C. A., Johnson, M. & Shaw, M., 2012. Lisdexamfetamine Dimesylate: A New Therapeutic Option for ADHD. CNS Drugs 26, 691–705. https://doi.org/10.2165/11634340-000000000-00000.

Taatjes, D. J., Bouffard, N. A., Barrow, T., Devitt, K. A., Gardner, J. A. & Braet, F., 2019. Quantitative pixel intensity- and color-based image analysis on minimally compressed files: implications for whole-slide imaging. Histochem. Cell Biol. 152, 13–23. https://doi.org/10.1007/s00418-019-01783-7.

Tektemur, N. K., Güzel, E. E., Gül, M., Tektemur, A., Yıldırım, S. O., Balgetir, M. K., Kocamüftüoğlu, G. O., Yalçın, T. & Ozan, İ. E., 2021. The combination of N-acetylcysteine and cyclosporin A reduces acetaminophen-induced hepatotoxicity in mice. Ultrastruct. Pathol. 45, 19–27. https://doi.org/10.1080/01913123.2020.1850964.

Tonomura, Y., Kato, Y., Hanafusa, H., Morikawa, Y., Matsuyama, K., Uehara, T., Ueno, M. & Torii, M., 2015. Diagnostic and predictive performance and standardized threshold of traditional biomarkers for drug-induced liver injury in rats. J. Appl. Toxicol. 35, 165–172. https://doi.org/10.1002/jat.3053.

Trefts, E., Gannon, M. & Wasserman, D. H., 2017. The liver. Curr. Biol. 27, R1147–R1151. https://doi.org/10.1016/j.cub.2017.09.019.

Vanga, R. R., Bal, B. & Olden, K. W., 2013. Adderall induced acute liver injury: a rare case and review of the literature. Case Rep. Gastrointest. Med. 2013. https://doi.org/10.1155/2013/902892.

Viennois, E., Pujada, A., Zen, J. & Merlin, D., 2018. Function, Regulation, and Pathophysiological Relevance of the POT Superfamily, Specifically PepT1 in Inflammatory Bowel Disease. Compr. Physiol. 8, 731–760. https://doi.org/10.1002/cphy.c170032.

Wang, L. X., Zhang, S. X., Wu, H. J., Rong, X. L. & Guo, J., 2019. M2b macrophage polarization and its roles in diseases. J. Leukoc. Biol. 106, 345–358. https://doi.org/10.1002/JLB.3RU1018-378RR.

Wang, Y., Ding, W. X. & Li, T., 2018. Cholesterol and bile acid-mediated regulation of autophagy in fatty liver diseases and atherosclerosis. Biochim. Biophys. Acta. Mol. Cell Biol. Lipids, 1863, 726–733. https://doi.org/10.1016/j.bbalip.2018.04.005.

Willis, S. A., Bawden, S. J., Malaikah, S., Sargeant, J. A., Stensel, D. J., Aithal, G. P. & King, J. A., 2021. The role of hepatic lipid composition in obesity-related metabolic disease. Liver Int., 41, 2819–2835. https://doi.org/10.1111/liv.15059.

You, Q., Holt, M., Yin, H., Li, G., Hu, C. J. & Ju, C., 2013. Role of hepatic resident and infiltrating macrophages in liver repair after acute injury. Biochem. Pharmacol. 86, 836–843. https://doi.org/10.1016/j.bcp.2013.07.006.

Zhang, T., Chen. J., Tang, X., Luo, Q., Xu, D. & Yu, B., 2019. Interaction between adipocytes and high-density lipoprotein: new insights into the mechanism of obesity-induced dyslipidemia and atherosclerosis. Lipids Health Dis. 18, 223. https://doi.org/10.1186/s12944-019-1170-9.

Zhu, R., Wang, Y., Zhang, L. & Guo, Q., 2012. Oxidative stress and liver disease. Hepatol. Res. 42, 741–749. https://doi.org/10.1111/j.1872-034X.2012.00996.x.

Zigmond, E., Samia-Grinberg, S., Pasmanik-Chor, M., Brazowski, E., Shibolet, O., Halpern, Z., & Varol, C., 2014. Infiltrating monocyte-derived macrophages and resident kupffer cells display different ontogeny and functions in acute liver injury. J. Immunol. 193, 344–353. https://doi.org/10.4049/jimmunol.1400574.

Legend of tables

Table 1

Body and organ weight

Values are expressed as the mean ± S.E.M. (n=10 per group). Unpaired t test. *p<0.05. C - rats received tap water; LDX - rats treated with 11.3 mg/kg b.w. lisdexamfetamine dimesylate.

Table 2

Liver morphometric analysis

Values are expressed as the mean ± S.E.M. (n=6 per group). Unpaired t test. p>0.05. C - rats received tap water; LDX - rats treated with 11.3 mg/kg b.w. lisdexamfetamine dimesylate.

Table 3

Number of leukocytes adhered to the vessel lumen and mast cell count per section

Values are expresses as the mean ± S.E.M. (n=6 per group). Unpaired t test. p>0.05. C - rats received tap water; LDX - rats treated with 11.3 mg/kg b.w. lisdexamfetamine dimesylate.

Legend of figure

Figure 1. Assessment of hepatic transaminases in plasma. (A) ALT concentration (U/L). (B) AST concentration (U/L)

Data are the mean ± S.E.M. (n=10 per group). Unpaired t test. *p<0.05; **p<0.01. C - rats received tap water; LDX - rats treated with 11.3 mg/kg b.w. lisdexamfetamine dimesylate.

Figure 2. Plasmatic levels of total cholesterol (A), triglycerides (B), free fatty acids (C) and blood glucose assessment (D)

Data are the mean ± S.E.M. (n=10 per group). Unpaired t test. *p<0.05. C - rats received tap water; LDX - rats treated with 11.3 mg/kg b.w. lisdexamfetamine dimesylate.

Figure 3. Histopathology of the liver

Photomicrograph of liver section from Control group (A, C) and LDX group (B, D). Histological changes are marked, such as vascular congestion (asterisk) and hydropic degeneration (black circle). H&E staining. Bar 10 μm. C - rats received tap water; LDX - rats treated with 11.3 mg/kg b.w. lisdexamfetamine dimesylate.

Figure 4. Myeloperoxidase (A) and N-acetyl-β-D-glucosaminidase (B) activity in the liver

Data are the mean ± S.E.M. (n=10 per group). Unpaired t test. *p<0.05. C - rats received tap water; LDX - rats treated with 11.3 mg/kg b.w. lisdexamfetamine dimesylate.

Figure 5. Oxidative stress status assay in the liver. MDA concentration (A), GST (B), CAT (C) and SOD activity (E), and quantification of GSH (D)

Data are the mean ± S.E.M. (n=10 per group of graphs A, B, C and D; n=9-7 per group on graph E). Unpaired t test. *p<0.05. C - rats received tap water; LDX - rats treated with 11.3 mg/kg b.w. lisdexamfetamine dimesylate.

Figure 6. Histochemical analysis of the percentage of total collagen (stained in blue) in the central (E) and portal (F) regions in the liver

Photomicrograph of liver section from central region (A, C) and portal region (B, D) staining total collagen in blue (arrow). (A and B) Control group; (C and D) LDX group. Azan Heidenhain trichrome staining. Bar 10 μm. Data are the mean ± S.E.M. (n=6 per group). Unpaired t test. $p>0.05$. C - rats received tap water; LDX - rats treated with 11.3 mg/kg b.w. lisdexamfetamine dimesylate.

Figure 7. Histochemical analysis of the percentage of collagen type I (stained in red) and type III (stained in green) in the central (I) and portal (J) regions in the liver

Non-polarized (A-D) and polarized (E-H) photomicrograph of liver sections from the central (A, B, E, F) and portal regions (C, D, G, H). (A, E, C, G) Control group; (B, F, D, H) LDX group. Picrosirius red staining. Bar 20 μm. Data are the mean ± S.E.M. (n=6 per group). Unpaired t test. $p>0.05$. C - rats received tap water; LDX - rats treated with 11.3 mg/kg b.w. lisdexamfetamine dimesylate.

Table 1. Body and organ weight

Parameters	Control group (C)	LDX group (LDX)	P value
Initial body	61.56 ± 1.05	62.85 ± 1.74	0.5361
Final body	272 ± 4.925	256.2 ± 8.36	0.1204
Weight gain	210.5 ± 4.186	193.4 ± 7.124	0.0531
Absolute weight (g)			
Liver	8.810 ± 0.309	7.957 ± 0.441	0.1306
White adipose tissue	4.532 ± 0.344	3.327 ± 0.355	0.0254*
Relative weight (g/100g)			
Liver	3.232 ± 0.07	3.086 ± 0.093	0.2242
White adipose tissue	1.652 ± 0.104	1.274 ± 0.104	0.0189*

Values are expressed as the mean ± S.E.M. (n=10 per group). Unpaired t test. *p<0.05.

Table 2. Liver morphometric analysis

	Control group (C)	LDX group (LDX)	P value
Mean diameter (μm)			
Central vein	50.59 ± 2.877	56.44 ± 2.578	0.1611
Lumen of sinusoids near the central vein	5.569 ± 0.303	5.588 ± 0.372	0.9689
Portal vein	33.29 ± 0.651	35.04 ± 2.196	0.4610
Lumen of sinusoids near the portal vein	3.757 ± 0.243	3.726 ± 0.306	0.9366
Hepatic artery	12.17 ± 0.487	11.47 ± 0.614	0.3913
Bile duct	14.83 ± 0.975	14.95 ± 0.700	0.9233

Values are expressed as the mean ± S.E.M. (n=6 per group). Unpaired t test. $p>0.05$.

Table 3. Number of leukocytes adhered to the vessel lumen and mast cell count per section

		Control group (C)	LDX group (LDX)	P value
	Leukocytes adhered			
Central vein		0.700 ± 0.118	0.967 ± 0.120	0.1449
Portal vein		0.783 ± 0.191	0.833 ± 0.148	0.8398
	Mast cells			
Intact		1.167 ± 0.477	1.167 ± 0.307	>0.9999
Degranulated		1.167 ± 0.307	0.500 ± 0.224	0.1099
Total		1.167 ± 0.271	0.833 ± 0.207	0.3387

Values are expressed as the mean ± S.E.M. (n=6 per group). Unpaired t test. p>0.05.

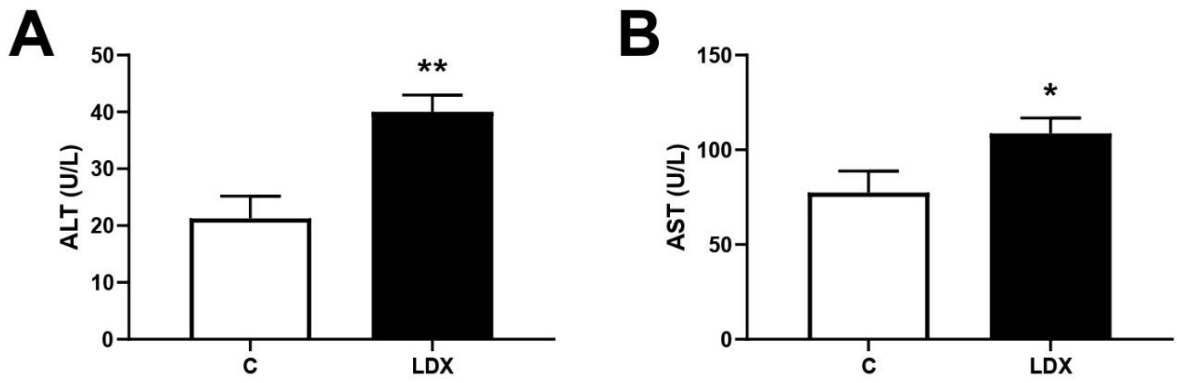

Figure 1. Assessment of hepatic transaminases in plasma. (A) ALT concentration (U/L). (B) AST concentration (U/L). Data are the mean ± S.E.M. (n=10 per group). Unpaired t test. *p<0.05; **p<0.01. C - rats received tap water; LDX - rats treated with 11.3 mg/kg b.w. lisdexamfetamine dimesylate.

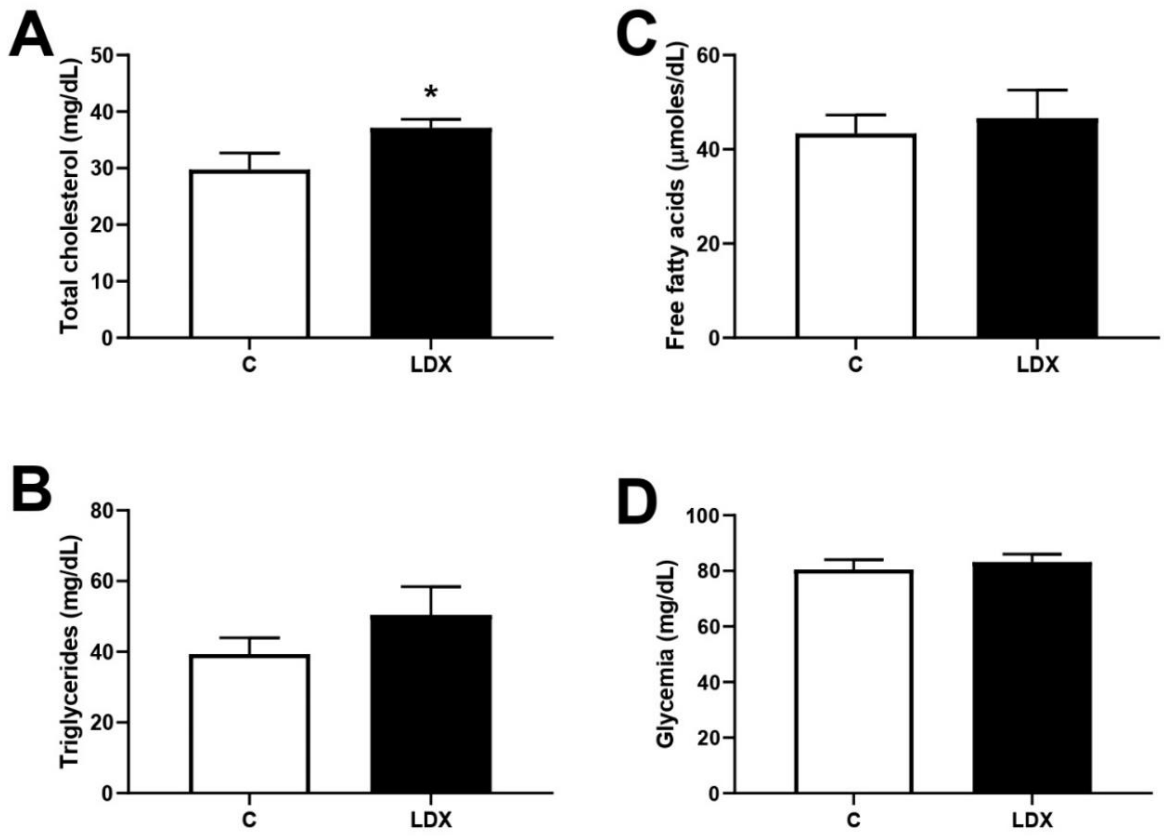

Figure 2. Plasmatic levels of total cholesterol (A), triglycerides (B), free fatty acids (C) and blood glucose assessment (D). Data are the mean ± S.E.M. (n=10 per group). Unpaired t test. *p<0.05. C - rats received tap water; LDX - rats treated with 11.3 mg/kg b.w. lisdexamfetamine dimesylate.

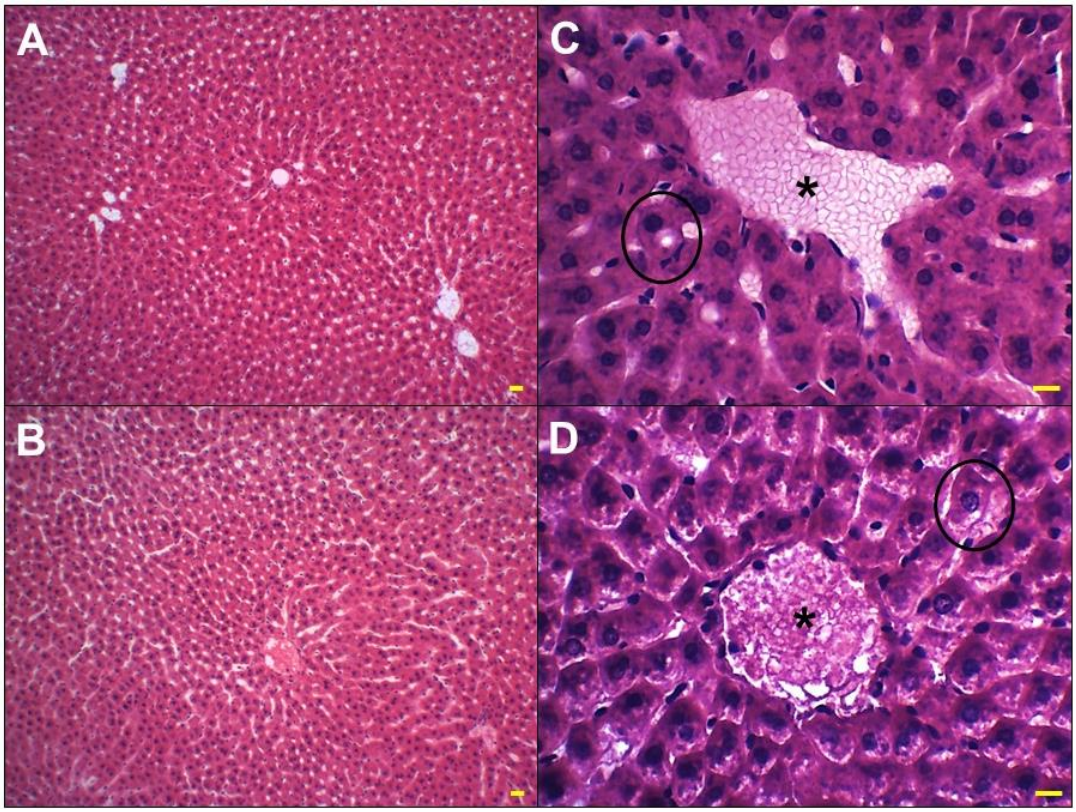

Figure 3. Histopathology of the liver. Photomicrograph of liver section from Control group (A, C) and LDX group (B, D). Histological changes are marked, such as vascular congestion (asterisk) and hydropic degeneration (black circle). H&E staining. Bar 20 μm (A, B) and 10 μm (C, D). C - rats received tap water; LDX - rats treated with 11.3 mg/kg b.w. lisdexamfetamine dimesylate.

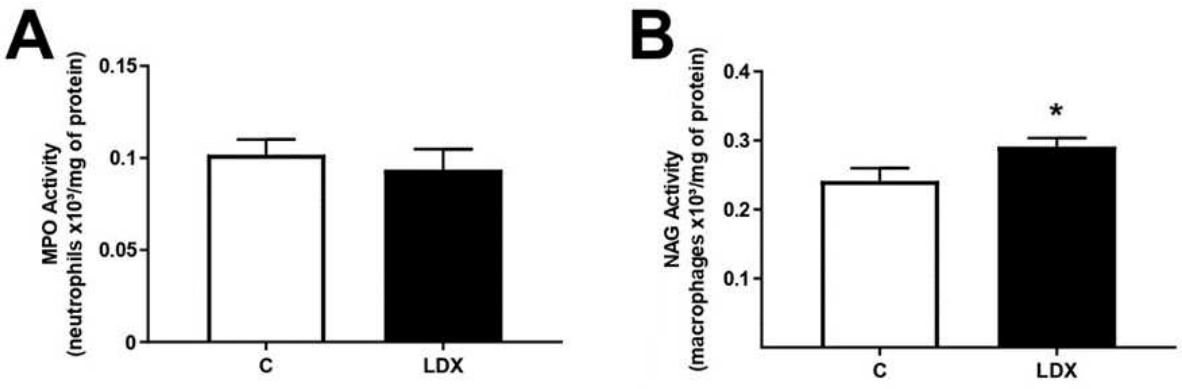

Figure 4. Myeloperoxidase (A) and N-acetyl-β-D-glucosaminidase (B) activity in the liver. Data are the mean ± S.E.M. (n=10 per group). Unpaired t test. *p<0.05. C - rats received tap water; LDX - rats treated with 11.3 mg/kg b.w. lisdexamfetamine dimesylate.

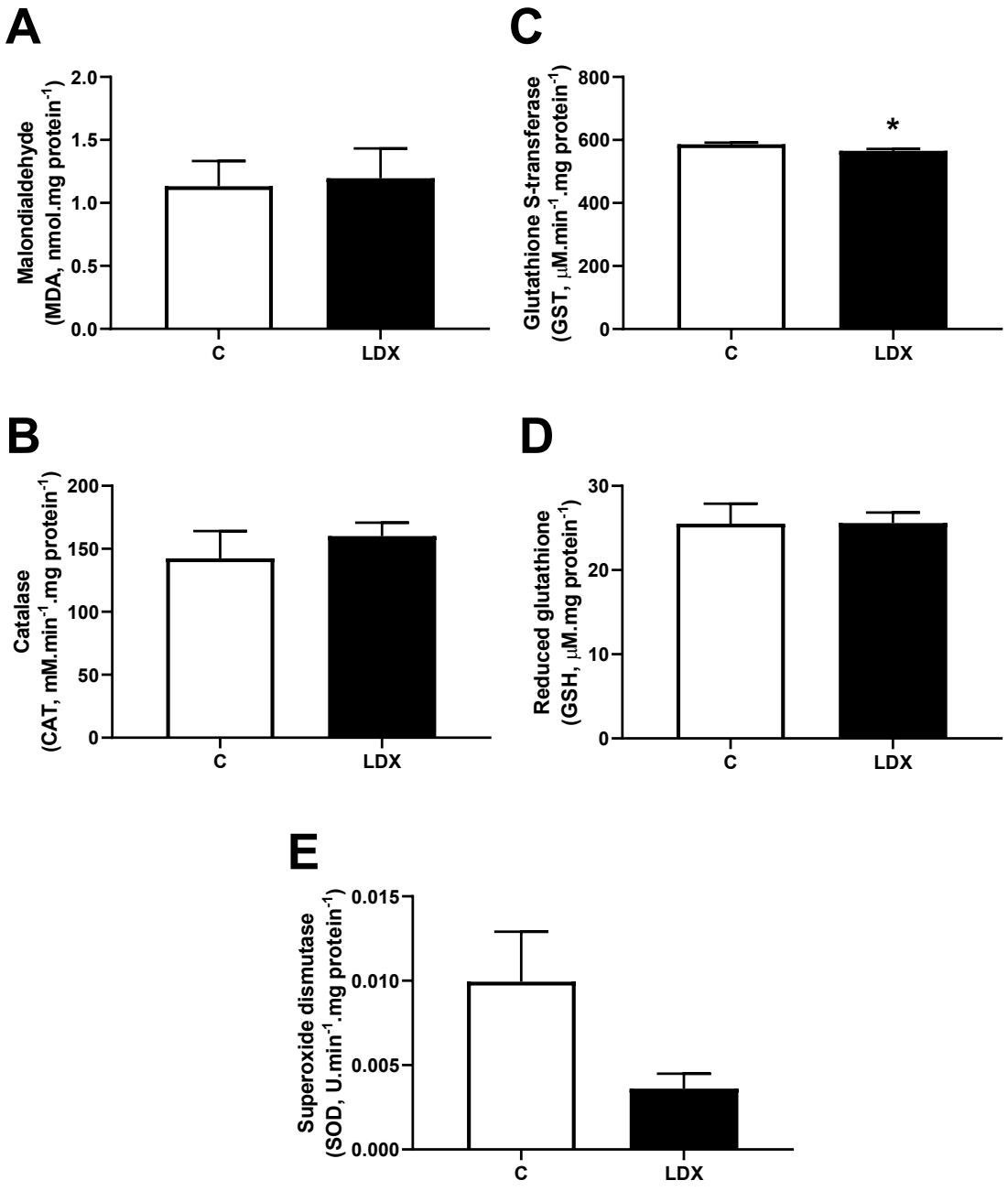

Figure 5. Oxidative stress status assay in the liver. MDA concentration (A), GST (B), CAT (C) and SOD activity (E), and quantification of GSH (D). Data are the mean ± S.E.M. (n=10 per group of graphs A, B, C and D; n=9-7 per group on graph E). Unpaired t test. *p<0.05. C - rats received tap water; LDX - rats treated with 11.3 mg/kg b.w. lisdexamfetamine dimesylate.

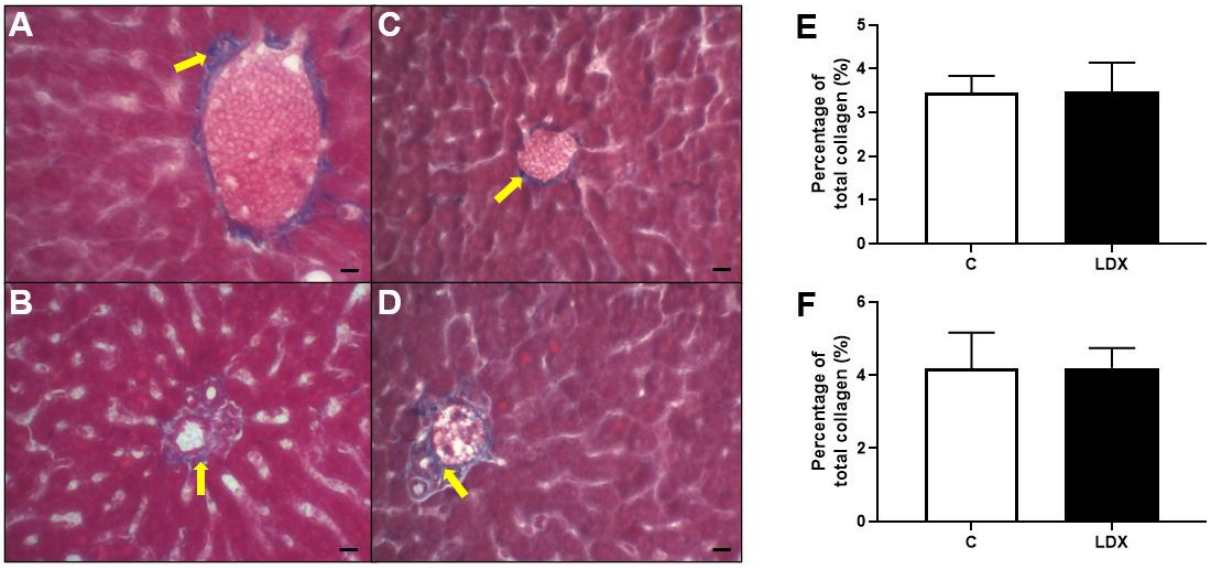

Figure 6. Histochemical analysis of the percentage of total collagen (stained in blue) in the central (E) and portal (F) regions in the liver. Photomicrograph of liver section from central region (A, C) and portal region (B, D) staining total collagen in blue (arrow). (A and B) Control group; (C and D) LDX group. Azan Heidenhain trichrome staining. Bar 10 μm. Data are the mean ± S.E.M. (n=6 per group). Unpaired t test. $p>0.05$. C - rats received tap water; LDX - rats treated with 11.3 mg/kg b.w. lisdexamfetamine dimesylate.

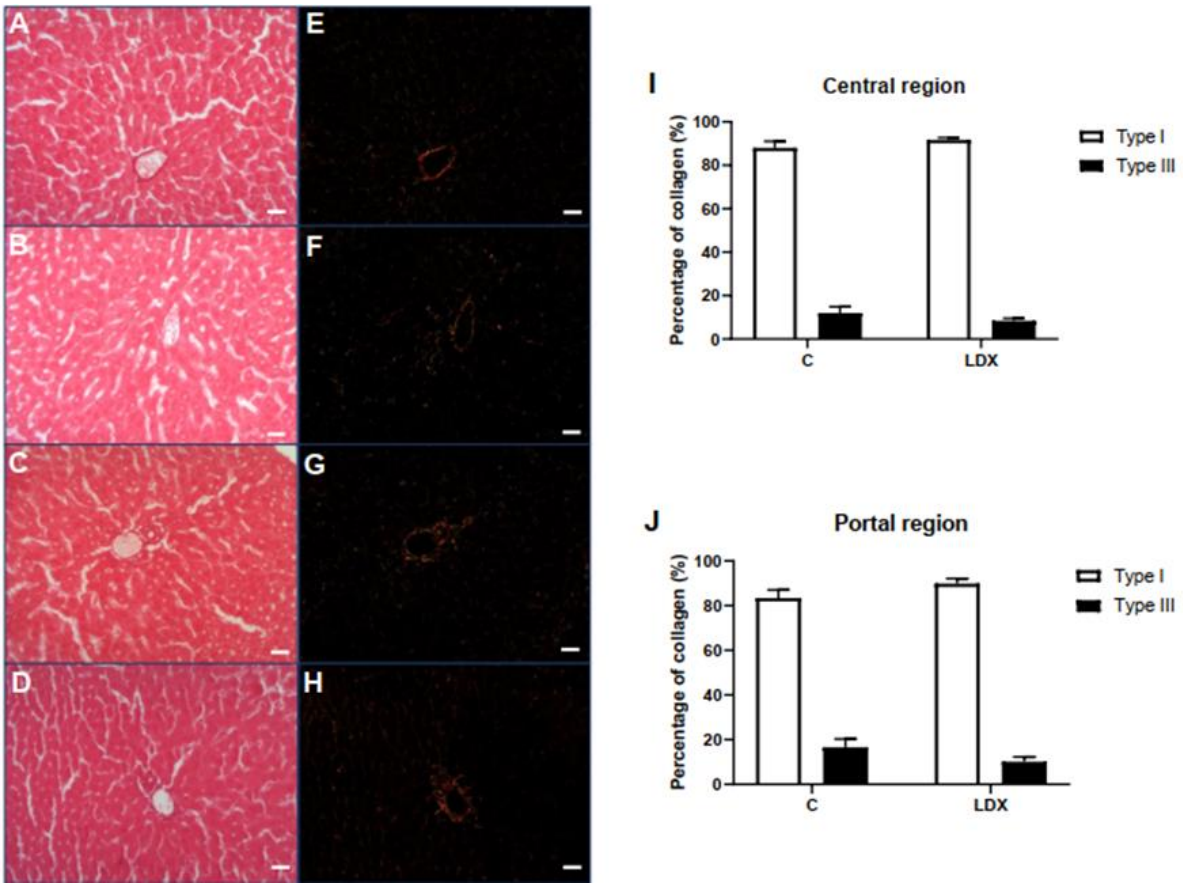

Figure 7. Histochemical analysis of the percentage of collagen type I (stained in red) and type III (stained in green) in the central (I) and portal (J) regions in the liver. Non-polarized (A-D) and polarized (E-H) photomicrograph of liver sections from the central (A, B, E, F) and portal regions (C, D, G, H). (A, E, C, G) Control group; (B, F, D, H) LDX group. Picrosirius red staining. Bar 20 μm. Data are the mean ± S.E.M. (n=6 per group). Unpaired t test. $p>0.05$. C - rats received tap water; LDX - rats treated with 11.3 mg/kg b.w. lisdexamfetamine dimesylate.

5 ARTIGO 2

Lisdexamfetamine dimesylate impair the kidneys of male pubertal rat: morphological, oxidative stress and inflammatory parameters

Artigo será submetido à revista – “Archives of Toxicology”

ISSN: 0340-5761

Fator de impacto (2020): 5.153

Qualis CAPES 2019 (Medicina II) = A1

Lisdexamfetamine dimesylate impair the kidneys of male pubertal rat: morphological, oxidative stress and inflammatory parameters

João V. H. Silva[1,2], Isadora C. Vercellone[3], Rafaela P. Erthal[1,2], Dayane P. Santos[1,2], Camila R. Ferraz[2], Ricardo L. N. Matos[4], Waldiceu A. Verri Jr[2], Ana P. F. R. L. Bracarense[4], Fábio G. Andrade[3], Glaura S. A. Fernandes[1*].

1 - Department of General Biology, Biological Sciences Center, State University of Londrina – UEL, Londrina, Paraná, Brazil

2 - Department of Pathology, Biological Sciences Center, State University of Londrina – UEL, Londrina, Paraná, Brazil

3 - Department of Histology, Biological Sciences Center, State University of Londrina – UEL, Londrina, Paraná, Brazil

4 - Department of Preventive Veterinary Medicine, Agrarian Sciences Center, State University of Londrina – UEL, Londrina, Paraná, Brazil

***Corresponding author**

Tel.: +55 43 33714417
E-mail address: glaura@uel.br (G.S. A. Fernandes)

ABSTRACT

Lisdexamphetamine dimesylate (LDX) is a prodrug of dextroamphetamine, which has been widely recommended for the treatment of Attention-Deficit/Hyperactivity Disorder (ADHD). There are still no data in the literature relating the possible toxic effects of LDX on the kidneys. Therefore, the present study aims to evaluate the effects of exposure to LDX on morphological, oxidative stress, cell death and inflammation parameters in the kidneys of male pubertal Wistar rats, since the kidneys are organs related to the excretion of most drugs. For this, 20 male Wistar rats were distributed randomly into two experimental groups: LDX group (LDX) - received 11,3 mg/kg/day of LDX diluted in tap water; and Control group (C) - received tap water. Animals were treated by gavage from postnatal day (PND) 25 to 65. At PND 66, the animals were anaesthetized and euthanized by inferior vena cava puncture. Plasma was collected and destined to the biochemical dosage of kidney function markers. The kidneys were collected, weighed, and destined for determinations of the inflammatory profile, oxidative stress status, cell death, and for histochemical, and morphometric analyses. Our results show that there was an increase in the number of cells marked for cell death, and a reduction in the mean diameter of proximal and distal convoluted tubules in the group that received LDX. In addition, an increase in MPO and NAG activity, indicating an inflammatory response. The oxidative stress profile showed an increase in CAT and GST activity, and a reduction in the amount of GSH. Antioxidant system is working very well to avoid oxidative stress. In conclusion, LDX-exposition in male rats during the peripubertal period causes renal damage in pubertal age involves inflammatory mechanisms and apoptosis process.

Keywords: Amphetamine; antioxidant system; nephrotoxicity; inflammation

1. Introduction

Lisdexamfetamine dimesylate (LDX) is an inactive prodrug of dextroamphetamine (d-amphetamine) (COMIRAN et al. 2016) that demonstrates efficacy for the treatment of adults with Moderate to Severe Binge-Eating Disorder (HUDSON et al. 2017; MCELROY et al. 2015). However, in the LDX has been widely used mainly for the treatment of symptoms from Attention-Deficit/Hyperactivity Disorder (ADHD) in children (BIEDERMAN et al. 2007), adolescents (FINDLING et al. 2013), and adults (MANEETON et al. 2014).

LDX is usually administered orally and can be dissolved in water or juice for ingestion (ERMER et al. 2011) and it has better efficacy and durability when administered in the morning (BIEDERMAN et al. 2007; COGHILL et al. 2014). Afterwards, LDX is absorbed in the gastrointestinal tract, mainly in the intestine, with the aid of peptide transporter 1 (PepT1) (ERMER et al. 2012). Upon being absorbed, it will reach the bloodstream where it is rapidly enzymatically hydrolyzed (ERMER et al. 2016a). Its conversion is carried out in the cytosol of erythrocytes (SHARMAN; PENNICK, 2014). The structure of LDX consists of a d-amphetamine covalently linked to L-lysine (GOODMAN, 2010). Therefore, its metabolization releases d-amphetamine, the active drug (ERMER et al. 2016a). D-amphetamine acts on the central nervous system, increasing concentrations of dopamine and norepinephrine (HUTSON et al. 2014). Finally, it will be excreted mainly via the kidneys in the urine (KRISHNAN et al. 2008).

The kidneys are components of the urinary tract. They have several important functions for hemostasis, including filtering blood, regulating blood pressure, controlling erythrocyte production, and circulating calcium levels (FARIA et al. 2019; MCMAHON, 2016). They are very susceptible to drug damage (FARIA et al. 2019;

GRIFFIN et al. 2019). Some of the reasons are the large exposure of the kidneys to the drugs and its metabolites, because these organs are responsible for most of the drug clearance (SCHREUDER et al. 2014) and they receive the large blood flow (RADI, 2019). Studies on LDX-induced nephrotoxicity are limited (ERMER et al. 2016b; KRISHNAN; MONTCRIEF, 2007). However, these researches are needed due to the increase in the use of amphetamines for the treatment of ADHD (PIPER et al. 2018), mainly by children and adolescents, given its effectiveness and lower risk of abuse (NAJIB, 2012). However, there is a lack of previous studies evaluating the effect of LDX on the kidneys specifically in this period of life. According to the explanation given, the present study aimed to evaluate the effect of LDX exposure on the renal morphophysiology renal in male pubertal Wistar rats with emphasis in inflammatory and oxidative stress profile, apoptosis cell and plasmatic markers of the renal function.

2. Material and methods

2.1. Animals and experimental conditions

Twenty male Wistar rats on postnatal day 22 (PND 22) were obtained from the Central Animal House of the Londrina State University (CCB - UEL), Paraná, Brazil. These animals were acclimated to the new environment (at the Animal House of the Laboratory of Toxicology and Metabolic Dysfunction of Reproduction) for three days before to the beginning of the experiment. During the experimental period (PND 25 to 65), the rats were accommodated into polypropylene cages (5 rats per cage) with laboratory-grade pine shavings as bedding. They were kept under controlled light conditions (12 h light/dark cycle, with lights on at 07:00 am), kept at a constant temperature (23 ± 2°C), and had access to standard commercial laboratory chow and tap water *ad libitum*, throughout the experiment period. Furthermore, during the

experimental period, the animals were observed to show any signs of toxicity (tearing, dripping nose, blood in the nose, frightened during handling, ruffled fur, diarrhea, and wet cage). All animal care and handling procedures were conducted in conformity with the National Institutes of Health guide for the care and use of laboratory animals (NIH Publications No. 8023, revised 1978), and this research was approved by the Ethics Committee on Animal Use of Londrina State University (OF. CIRC. CEUA N° 82/2019 and addendum OF. CIRC. CEUA N° 004/2021). All experimental procedures were performed by the same evaluators.

2.2. LDX exposure and experimental design

The animals were randomly assigned to two experimental groups of 10 animals each: control (C) and lisdexamfetamine (LDX). The animals in the LDX group received lisdexamfetamine dimesylate by gavage with 11.3 mg/kg b.w. (body weight) diluted in tap water. Every two days, the animals were weighed to adjust the dose according to the average weight of the group, and to assess the animal's general welfare. The calculation used was the conversion of animal doses (rat) to human equivalent doses based on body surface area (FOOD and DRUG ADMINISTRATION, 2005). This dose was selected considering that it is equivalent to administering a 70 mg capsule of the drug and corresponds to 1.13% of the oral LD50 for rats (oral LD50 for rats > 1000 mg/kg) (KRISHNAN; MONTCRIEF, 2007). Control group received only the vehicle (tap water) in the same volume as the LDX group (0.2mL). All groups were treated daily, by oral gavage, during forty consecutive days (between PND 25 and 65). This time corresponds to the juvenile and peripubertal phase of Wistar rats (OJEDA et al., 1980). This life stage of rats is like the recommended life stage for humans to use LDX, in childhood and puberty (NAJIB et al., 2020).

2.3. Preparation of lisdexamfetamine dimesylate solution

Lisdexamfetamine dimesylate (Venvanse®, Phateon Pharmaceuticals Inc., Ohio, USA) was daily diluted in the corresponding volume of tap water.

2.4. Blood and kidneys collection

The animals were fasted for 12 hours before euthanasia (food removed at 9:00 pm). In PND 66, rats were intraperitoneally anaesthetized with a combination of ketamine 75 mg/kg b.w. (Sedomin® 10%, Avellaneda, Argentina) and xylazine 10 mg/kg b.w. (Anasedan®, Paulínia, Brazil), weighed and euthanized by inferior vena cava puncture. Blood samples was collected in the presence of heparin (Hemofol®, São Paulo, Brazil) and plasma was stored at -20°C for the determination of plasmatic creatinine, and urea concentrations (n=10 rats per group).

The kidneys (left and right) were removed, and the weights (absolute and relative to body weights) (n=10 per group). The right kidney was selected, and from it, divided into two parts for each analysis: stereological and histochemical analysis (n=6 per group); and immunohistochemistry (n=6 per group). The left kidney was divided into two parts for each analysis: inflammatory profile (n=10 per group); and redox balance status assay (n=10 per group).

2.5. Assessment of organ function

Plasmatic levels of creatinine and urea were measured using the commercially available diagnostic Liquiform kits (Labtest Diagnóstica SA, Brazil). All samples were measured in duplicates and were included in the same assay to avoid inter-assay errors. Results were presented as mg/dL.

2.6. Processing and stereological and histological evaluation

Kidney samples were fixed in aqueous Bouin for 48 h. The samples were embedded in paraffin and sectioned at 7 µm (2 non-serial sections per animal). The sections were stained with hematoxylin and eosin (HE), evaluated in a Moticam® image capture system coupled to a photomicroscope (Motic, Xiamen, China) and analyzed using the Motic Image Plus 3.0® software.

For measurement of stereological parameters, 20 photomicrographs of each animal were obtained at 400x magnification: 10 images of the cortex (with one glomerulus in the center of image, and this glomerulus must have an evident vascular pole) and 10 of the medulla (with evident collecting tubules). In the renal cortex images, the mean diameter of 10 glomerulus, 10 proximal convoluted tubules and 10 distal convoluted tubules were determined. The mean size of Bowman's space of 10 renal corpuscles was also determined. In the images of the renal medulla, the determination of the average diameter of 10 collecting tubules was performed.

Histological changes were evaluated based on previous studies (SAMELO et al., 2020; MI et al., 2018). The following parameters of renal injury in the cortical and medullary region were observed: necrosis, foci of defense cells and congestion. The frequency of each kidney injury parameter was observed and scored as absent (0), mild (1), moderate (2) and severe (3).

2.7. Histochemical analyzes

2.7.1 Azan Heidenhain trichrome stain

The slides, with 2 non-serial sections per animal, were first deparaffinized and rehydrated. The dyes used were Azo-Carmin G (20 min), phosphotungstic acid as

catalyst (25 min) and Aniline blue (20 min), respectively, they evidence the collagen. Using the Moticam® image capture system coupled to a photomicroscope (Motic, Xiamen, China), at 400x magnification, 5 images from each region (cortex and medulla) were captured per animal. Using Image-Pro PLUS® software version 4.5, the blue pixels which indicate collagen in each image were quantified according to Taatjes et al. (2019). The data were compared to define the distribution of these tissue components between the regions of the groups.

2.7.2 Picrosirius-polarization method

It is a histochemical technique used to differentiate between mature (type I) and newly synthesized (type III) collagen fibers when observed under polarized light, so it is possible to determine the percentage of each type of collagen in tissues (GOWDA et al. 2017). The slides, with 2 non-serial sections per animal, were submitted to a standard histological routine protocol, however, the dye used was Picrosirius solution (0.2 g of Sirius red in 200 ml of saturated picric acid) for 1 h. Using the Moticam® image capture system coupled to a polarized light microscope (Motic® BA410), at 400x magnification, 5 images from each region (cortex and medulla) were captured per animal. Image-Pro PLUS® software version 4.5.0.29 was used to quantify the pixels of interest in each image. The data were compared to define the distribution of these cellular components between the regions of the groups (PUPIM et al. 2017).

2.7.3 Periodic acid Schiff stain

This stain is used to identify neutral glycoconjugates in the tissues. The slides were left for 15 min in a 0.5% solution periodic acid in distilled water. The slides, with 2 non-serial sections per animal, were washed in distilled water, and then placed in

Schiff's reagent for 1 h and 30 min at room temperature. The usual sulfur water washes followed, and the sections were dehydrated in alcohols and mounted in balm after xylene. Using the Moticam® image capture system coupled to a photomicroscope (Motic, Xiamen, China), at 400x magnification, 5 imagens from each region (cortex and medulla) were captured per animal. Image-Pro PLUS® software version 4.5 was used to quantify the pixels of interest in each image (TAATJES et al. 2019), which indicate positive staining for neutral glycoconjugates (purple or magenta color). The data were compared to define the distribution of these tissue components between the regions of the groups.

2.7.4 Toluidine blue stain

This stain is mainly used to stain the metachromatic granules of the mast cells, and thus to be able to quantify the mast cells in the tissue (RIBATTI, 2018). Tissue sections were stained with 1% toluidine blue to identify mast cells. Mast cells were classified with the aid of a light microscope into intact and degranulated mast cells. The analysis of the count of these cells was performed analyzing the entire length of the section (2 non-serial sections per animal) using a light microscope and quantifying and classifying each observed mast cell (PUNHAGUI et al. 2016).

2.8. Immunohistochemistry

Another part of the right kidney was fixed in paraformaldehyde for 4 h in 0.1 M sodium phosphate buffer (PBS), pH 7.4, and subsequently, they were washed in PBS, pH 7.2, and then stored in 70%. The samples were embedded in paraffin and sectioned at 4 μm thickness. These thin tissue sections were mounted on silanized slides, subsequently, the slides were deparaffinized in xylene, and rehydration with

decreasing alcohol baths. For antigen retrieval, the slides were heated in a pressure cooker for 3 minutes (86-90°C) in citrate buffer (pH 6.0) and cooled at room temperature for 20 minutes. Afterwards, endogenous peroxidase was blocked using 3% of hydrogen peroxide and methanol (8:7) for 30 minutes, followed by unspecific blocking of proteins with Molico's milk 5% for 10 minutes. After blocking the nonspecific background, the slides were washed in PBS and incubated with primary antibodies against cleaved caspase-3 (1:200, Asp175, Cell Signaling Technology, Beverly, MA) for 22 h at 4°C in a humid chamber. The slides were washed twice in PBS for 5 minutes, then, subsequently, the secondary polyclonal antibody was incubated for 30 min, and then was washed twice in PBS for 5 minutes. After that, DAB (3,3′-Diaminobenzidine, Invitrogen, São Paulo, SP, Brazil) was used to be revealed the immunoreactions for 3 min. The sections were counterstained using Harris hematoxylin for 90 seconds, followed by mounting. All immunoreactions were accompanied by a positive control for the tested antibody (anti cleaved caspase-3) and negative control (absent primary antibody). The slides were analyzed under a light microscope using a 40x objective. Were captured 10 images of the renal cortex, which had a single glomerulus at the center of the image. Immunoreactivity was scored based on the number of positive cells per field.

2.9. Inflammatory profile

2.9.1 Myeloperoxidase activity

Myeloperoxidase (MPO) activity is a method of indirect assessment of neutrophil recruitment. This assay was performed as previously described by Ferraz et al. (2021). Approximately 100 mg kidney samples were removed and stored in a cryotube with 200 µL of 50 mM K_2PO_4 buffer solution (pH 6.0), composed of hexadecyl

trimethylammonium bromide (HTAB; 0.5%), at -80 °C. On the day of the assay, these samples were homogenized in ice condition using a Tissue-Tearor (Biospec®). Subsequently, the homogenates were centrifuged (16,100 g, 2 min, 4◦C), and the resulting supernatants (15 µL) were blended with 200 µL 50 mM K_2PO_4 buffer, pH 6.0, containing 0.167 mg/mL of o-dianisidine dihydrochloride and 0.015% hydrogen peroxide. The absorbance of MPO activity was determined spectrophotometrically at 450 nm (Multiskan GO Microplate, Thermo Fischer Scientific, Vantaa, Finland). The results of the MPO activity assay are expressed as the number of neutrophils per mg of protein using a standard curve of neutrophils (196–400.000 neutrophils).

2.9.2 N-acetyl-β-D-glucosaminidase activity

N-acetyl-β-D-glucosaminidase (NAG) activity is a colorimetric method to assess macrophages recruitment. This assay was performed as previously described by Ferraz et al. (2021). Firstly, 10 µL of the supernatant obtained from the MPO activity procedure was separated and added to a 96-well plate followed by the addition of 40 µL of 50 mM phosphate buffer, pH 6.0. The reaction was initiated by the addition of 2.24 mM 4-nitrophenyl NAG. The plate was incubated at 37°C for 10 min, and the reaction was stopped by the addition of 100 µL of 0.2 M glycine buffer, pH 10.6. NAG enzymatic activity was determined spectrophotometrically at 400 nm (Multiskan GO Microplate, Thermo Fischer Scientific, Vantaa, Finland). The results of the NAG activity are expressed as the number of macrophages per mg of protein using a standard curve of macrophages (196–400.000 macrophages).

2.10. Oxidative stress profile assay

2.10.1 Tissue preparation and protein determination

Kidney samples were first homogenized in 1 mL PBS (pH 7.4) for 45 seconds using an Ultra-turrax (IKA Works, Wilmington, USA), and then centrifuged at 9.500 g for 10 min. The supernatant was used to determine the protein concentration by the Bradford method, using bovine serum albumin as a standard (BRADFORD, 1976). Afterwards, the samples were normalized to 1 mg/mL protein and used for the following analyses:

2.10.2 Determination of lipid peroxidation

Lipid peroxidation was measured to indirectly quantify the peroxides produced, which are thiobarbituric acid reactive substances (TBARS) (LUSHCHAK et al. 2009). To prepare the test, 50 µL of each normalized sample was pipetted in duplicate in a microplate, and the following substances were added to the sample: 5 µL of 1M $FeCl_3$, 5 µL of 0.5 M ascorbic acid, 50 µL of TCA 2.8%, and 50 µL of 1% thiobarbituric acid (TBA). Afterwards, the samples were shaken and placed in a water bath at 90°C for 15 minutes. The microplate was allowed to cool, to stop the reaction, and finally read. The intermediate product of lipid peroxidation, malondialdehyde (MDA) was determined by subtracting the absorbance at 535 nm and 572 nm (BUEGE; AUST, 1978). Lipid peroxidation was estimated correcting for the amount of protein, and the results are expressed in nmol of MDA per mg of protein.

2.10.3 Catalase activity

Catalase activity was determined based on Aebi (1984). Catalase converts hydrogen peroxide (H_2O_2) into 2 H_2O + 1 O_2. To prepare the test, 3 µL of each normalized sample was pipetted in duplicate in a UV4 microplate, and 297 µL of reaction medium were added to the sample. Reading was performed immediately at

240 nm for 1 min, at 15 second intervals. The catalase values were expressed as units of catalase mM formed.min^{-1}.mg of protein^{-1}.

2.10.4 Glutathione S-transferase activity

This analysis evaluates the enzymatic activity of glutathione S-transferase (GST) in catalyzing the conjugation of GSH with the synthetic substrate CDNB, causing the formation of a thioether. This assay was performed as described by Keen et al. (1976) with some modifications. The increase in absorbance through the formation of the thioether was monitored at 340 nm (RS: 100 mM potassium phosphate buffer pH 6.5; 1.5 mM GSH; 2 mM CDNB) for 160 seconds at 40 second intervals. Values were expressed as μM thioether formed.min^{-1}.mg of protein^{-1}.

2.10.5 Glutathione quantification

Reduced glutathione (GSH) levels in the liver homogenate supernatant were determined as proposed by Rahman et al. (2006), with some modifications. For this, was used 10 μL of the normalized sample, 180 μL of the mix solution, and 360 uL CDNB, pipetted into a microplate, and evidenced by a yellow color formation. After 15 min, reading was measured at 412 nm. The amount of GSH was estimated from a GSH standard curve, and the results are expressed in μM/mg of protein^{-1}.

2.10.6 Superoxide dismutase activity

The evaluation of the activity of the enzyme superoxide dismutase (SOD) was performed as described by Senthilkumar et al. (2021) with some changes. The enzyme comes from homogenates normalized to 1mg/ml. A reaction mixture was prepared containing sodium carbonate buffer (50mM, pH 10.2), nitroblue tetrazoilium (NBT) (96

uM) and Triton X-100 (0.6%), which was incubated for 2 minutes with sodium hydrochloride. hydroxylamine (NH2OH·HCl) (20 mM, pH 6.0). The final volume was adjusted to 200 µL. The reaction consists of the quantification of complexes formed by superoxide anions with the addition of NBT and NH2OH·HCl of yellowish color with the reduction of NBT, forming a bluish color read at 560 nm for 2 minutes at intervals of 15 seconds. Results are expressed in U formed.min^{-1}.mg of $protein^{-1}$.

2.11. Statistical analysis

The data were submitted to the Shapiro-Wilk test to verify their normal distribution and classify them into parametric and non-parametric data. The homogeneity of the variance between the groups was assessed by the Levene test. Data comparisons between two groups were performed using Student's unpaired t test for parametric data, and the Mann-Whitney test for non-parametric data. Results are presented as mean ± S.E.M. (standard error of the mean), with $P<0.05$ considered statistically significant. The statistical analyses and graph design for results were performed by GraphPad Prism for Windows version 8.2.1 (San Diego, CA, USA).

3. Results

3.1. Kidney weight, assessment of kidney function and signs of toxicity

Absolute and relative kidney weight and plasmatic creatinine and urea levels are shown in Table 1. These evaluations demonstrate there was a significant reduction in the absolute weight of the kidneys of the animal’s exposure to LDX. However, there was no significant difference in the relative weight of the kidneys.

The plasmatic levels of creatinine and urea did not show difference in the LDX group when compared to the Control group.

No signs of toxicity assessed (tearing, dripping nose, blood in the nose, frightened during handling, ruffled fur, diarrhea, and wet cage) were observed during the experimental period.

3.2. Stereological and histopathological analysis

Stereological analysis (Table 2) showed that exposure to LDX caused a reduction in the mean diameter of the proximal convoluted tubules and distal convoluted tubules in LDX group. However, the measures of the other kidney structures (glomerulus, bowman space and collecting duct) was not statically different between the experimental groups.

The histopathological analysis of the kidney, as shown in Figure 1, revealed the absence of necrosis, congestion and focus of defense cells in animals from both experimental groups.

3.3. Cell death

The immunohistochemistry technique for cleaved caspase-3 labeling was used to identify apoptotic cells. This analyze evidenced the number of apoptotic cells was higher in the renal cortex of animals that received LDX (Figure 2). Furthermore, it was possible to observe that the main labeled cells in the LDX group were the cells of the proximal and distal convoluted tubules. In the renal medulla there was no labeling in any of the experimental groups (data not shown).

3.4. Inflammatory profile

MPO and NAG activity is an indirect method for evaluating neutrophil and macrophage recruitment, respectively. These analyses showed that there was a significant increase in the MPO (Figure 3A) and NAG (Figure 3B) activity after LDX administration. It is important evidenced this increase was more significant for NAG ($p=0.0003$) than MPO ($p=0.0210$) in the kidneys.

Through the histochemical staining of Toluidine blue, it is possible to determine the presence of these cells in the tissue, quantify them and differentiate into intact or degranulated mast cells (RIBATTI 2018). In relation to mast cell quantification (Table 3) there was no significant difference in the number of this cellular population (total, intact or degranulated) after LDX-administration being similar between experimental groups.

3.5. Oxidative stress profile

To determine the oxidative stress status, the MDA concentration, and the activity (CAT, GST, and SOD) and amount (GSH) of some antioxidant enzymes were evaluated (Figure 4). The kidneys from LDX group showed an increase in CAT (Figure 4C) and GST (Figure 4D) activity, and a reduction in GSH levels (Figure 4B). However, among the antioxidants evaluated only SOD activity (Figure 4E) remained unchanged. In relation to lipid peroxidation assay, the present results showed the MDA concentration were similar between experimental groups (Figure 4A).

3.6. Histochemical analyses

Periodic acid Schiff histochemical staining was performed to assess the deposition of neutral glycoconjugates. It is possible to observe the labeling (magenta color) in structures present in the renal cortex, such as the glomerular basement

membrane and the luminal wall of the proximal convoluted tubules (Figure 5A and 5E). In the medullary region, the marking is observed mainly on the wall of the collecting ducts (Figure 6A and 6E).

The Azan Heidenhain trichrome stain marks the collagen in dark blue. The labeling was on the glomerular basement membrane in cortical region (Figure 5B and 5F) and on the renal interstitial in medullary region (Figure 6B and 6F). In addition, to determine the type of collagen deposited, the Picrosirius-polarization method was performed. The present results evidenced the percentage of type III collagen was more prevalent than the percentage of type I collagen (Figure 5K and 6K) in cortical and medullary regions. However, there was no difference between the experimental groups for each type of collagen.

Both histochemical techniques were performed to determine possible changes in the renal cortex and renal medulla. However, no significant changes were observed in the location of the labeling or in the percentage of neutral glycoconjugates, total collagen and collagen types I and III between the groups.

4. Discussion

In this study, it was proven that LDX treatment during peripubertal period is nephrotoxic, impairing the renal morphophysiology in male pubertal rats.

The reduction in the absolute weight observed in the kidney seems not to be a harmful change, because its relative weight in relation to body weight did not altered after LDX-administration. This indicates that LDX did not directly affect kidney weight, which could be an independent change. Similarly, to the results described by Fernandes et al. (2007), we reinforce the importance of considering the absolute

weight. This is because a decrease in organ weight does not necessarily indicate an apparent decrease in body weight. Therefore, the relative weight may not show significant differences if the body and organ weights change in the same direction.

Krishnan and Montcrief (2007) also reported a trend of reduction in the absolute renal weight of male Sprague-Dawley rats after 28 days of exposure to 40 and 80 mg/kg/day of LDX while the 20 mg/kg dose of LDX did not change kidney weight. Carvalho et al. (1999) evaluated the administration of d-amphetamine (20 mg/kg, for 14 days) in male Wistar rats (160–180 g) and observed the relative weight of kidneys by body weight did not change. In another study, evaluating the effects of methylphenidate (2 doses per day of 5mg/kg, for 6 days, oral route) in male Wistar rats of PND 40, the authors also reported no significant change in kidney weight after exposure (LOUREIRO-VIEIRA et al. 2018). Methylphenidate is a drug of first choice for the treatment of ADHD, and it has a mechanism of action similar to that of LDX (MECHLER et al. 2022).

The reduction in the mean diameter of proximal and distal convoluted tubules after exposure to LDX from animals LDX group may be related to absolute weight of the kidney. To assess whether the reduction in tubule diameter altered renal function, we performed plasmatic creatinine and urea measurements which forwent this relationship. Determination of the levels of these elements (creatinine and urea) are conventional tests of kidney function (HOKAMP; NABITY, 2016). According to our data, there was no change in the concentration of these markers of renal function. Krishnan and Montcrief (2007) reported that only exposure to LDX at a dose of 80 mg/kg for 28 days caused an increase in blood urea nitrogen in male and female Sprague-Dawley rats. Contributing with our data, Salviano et al. (2015) showed that adult male Wistar rats treated with 10mg/kg of methylphenidate, did not show

significant changes in urea, creatinine, and creatinine clearance values, after 24 and 48h of treatment. Our study is the first to evaluate the effects of this dose of LDX on renal function, during an experimental period of 40 days, in animals in the pubertal phase of life. Therefore, there are no studies with doses close to those used by us, or in the same period of life.

Corroborating the renal injuries reported in the present study, such as reduction in tubule diameter and weight of the kidney, the increase in the number of apoptotic cells evidenced in this cortical region confirms the harmful effect of LDX. Apoptosis is a normal physiological process of cell death, which occurs as a homeostatic mechanism, however this can be activated in front of stimuli (XU et al. 2019) becoming a pathological process. Therefore, once the labeling of cleaved caspase-3 occurred exclusively in cells of the proximal and distal convoluted tubules we evidenced the reduction of these structures with the increase of the cell death process. Cleaved caspase 3 is considered the last member of the common pathway for apoptotic cascade. For this reason, its location in any cell indicates a cell death by apoptosis (CHEN et al. 2018). It is reported that, LDX is a stimulant of the nervous system by increasing noradrenergic and dopaminergic neurotransmission (NAJIB et al. 2020) and norepinephrine induced apoptosis of cultured endothelial cells from neonatal rat heart (FU et al. 2006). From this, we can infer that the excessive stimulation of the sympathetic system caused using LDX may be one of the pathways for the apoptosis process in the renal tubular cells. Also corroborating our hypothesis, Raoofi et al. (2020) showed that methylphenidate, when administered at a dose of 20mg/kg/day (gavage for 21 days) to 10-week-old male Wistar rats, caused an increase in the number of apoptotic cells in the renal cortex and medulla, a fact observed by the method TUNEL. Furthermore, they confirmed by evaluating the expression of pro-

apoptotic genes (caspase-3 and 8, BBC3, BAX, P21, and mTOR) that were increased in the methylphenidate-treated group.

According to present results of this study, it is reasonable to infer that the damages in the diameter of the proximal and distal convoluted tubules added to cell death that occurring mainly in the cells of these structures, can lead to an electrolyte imbalance. The epithelial cells of the proximal convoluted tubules have attributes to carry out most of the reabsorption of water, low molecular weight proteins, and a significant part of Na^+, K^+, Cl^-, HCO_3^-, phosphate and glucose (GUEUTIN et al. 2012; NIESKENS; WILMER, 2016; RADI, 2019). It is also a segment of the nephron that purges unfiltered xenobiotics. Therefore, it can easily be the target of drug-induced renal toxicity (NIESKENS; WILMER, 2016). In relation to distal convoluted tubule, it acts in the reabsorption of Na^+ and Cl^- and has a role in the regulation of systemic calcium and magnesium homeostasis (MCCORMICK; ELLISON, 2015; RADI, 2019). Moore (1966) showed that d-amphetamine-treated mice, with a 'depressed' appearance, showed increased sodium concentration (mEq/kg water) and reduced potassium (mEq/kg water) in the kidneys, and in plasma there was a reduction in calcium concentration, indicating an alteration in electrolyte balance.

Disfunction and damage to renal structures can result in the development of kidney disease, stimulating an inflammatory response (ANDRADE-OLIVEIRA et al. 2019; TECKLENBORG et al. 2018). In our experimental design, indirect methods of assessing leukocyte recruitment indicated increase in the recruitment of neutrophils and macrophages due to increase in the MPO and NAG levels, respectively. Leukocytes and cytokines can exacerbate the injury or repair the tissue damage (MADJENE et al. 2015). The first type of immune cell to arrive at the injury site is the neutrophil. Neutrophils are the most abundant leukocytes in the blood (OLIVEIRA et

al. 2016) and they act predominantly in the acute inflammatory response, eliminating pathogens, producing ROS, and releasing inflammatory mediators (LACY; EITZEN, 2008).

The increase in neutrophils in the tissue can lead to excessive inflammation and severe damage (KOLACZKOWSKA; KUBES, 2013). Moreover, neutrophils recruit monocytes to inflamed tissues (SOEHNLEIN; LINDBOM, 2010). This process can happen, for example, because most neutrophils when they die, release molecules that attract macrophages to carry out their elimination (CHALARIS et al. 2007; SCANNELL et al. 2007). Macrophages can be resident in the kidneys or be recruited, these being derived from monocytes (CAO et al. 2015).

Therefore, this previous information corroborates to increase in the MPO and NAG levels found in the present study, indicating an inflammatory resolution. Furthermore, it is known that local stimuli can induce the development of an M1 phenotype macrophage, and they can activate other leukocytes and produce pro-inflammatory cytokines (TANG et al. 2019). Another phenotype that can be induced in these macrophages is M2 that can act on tissue repair (VINUESA et al. 2008) or renal fibrosis (KUSHIYAMA et al. 2011).

There were no experimental studies reporting the effects of LDX on the inflammatory response in the kidneys. However, Loureiro-Vieira et al. (2018) reported leukocyte infiltrate when performing qualitative histological examination of the kidneys of male Wistar rats after treatment with methylphenidate (oral doses of 5 mg/kg twice daily for 6 days). They suggest that this is due to NF-kB activation in interstitial and tubular cells. Furthermore, Raoofi et al. (2020) reported that methylphenidate (20 mg/kg, oral route for 21 days) also caused in the kidneys of male Wistar rats, an increase in gene expression of IL-6 and IL-1b levels.

Oxidative stress is an imbalance between pro-oxidants and antioxidants, which can result in cell damage (JONES, 2008). Antioxidant molecules help to prevent an imbalance in the redox state, preventing the accumulation of ROS and other pro-oxidants (RATLIFF et al. 2016). Inflammation is sometimes directly related to oxidative stress levels, because of leukocyte recruitment and cytokine release (ELMARAKBY; SULLIVAN, 2012; GRIVEI et al. 2020). Associated with our results, it is possible to predict the increase in leukocytes in the kidneys may be generating an increase in pro-oxidants, resulting in lipid peroxidation. However, we observed the absence of this process since the levels of MDA were similar between the experimental groups. The lipid peroxidation process did not happen because there was an increase in the activity of CAT and GST, and a reduction in the concentration of GSH in kidneys belonging to the LDX group. Therefore, it is evident that, at this moment, the antioxidant system acted to avoid an increased oxidative stress status and consequently this cellular and tissue damage. Corroborating our data, Carvalho et al. (2001) shown that d-amphetamine stimulates the production of H_2O_2 by kidneys, but an adaptation of antioxidant defenses in the kidneys after repeated administration of d-amphetamine has been described (CARVALHO et al. 1999).

Kidney injury and the inflammatory response can cause tissue fibrosis. Leukocytes release cytokines, recruit, and activate other cells, such as macrophages and fibroblasts, which can induce collagen production/transformation (LV et al. 2018). To evaluate a possible tissue fibrosis caused by the recruitment of macrophages and neutrophils in the kidneys after exposure to LDX, we performed Toluidine blue, Azan Heidenhain trichrome and Picrosirius-polarization histochemistry. We could observe that the maintenance on the number of mast cell is an important information because this cell type contributed to the development of kidney diseases, releasing chymases

that contribute to kidney inflammation and worsen fibrosis (BLANK et al. 2007; VIBHUSHAN et al. 2020). Regarding collagen deposition, Gagliano et al. (2000), showed that the gene expression of type III collagen is greater than that of type I collagen under physiological conditions in the kidneys of male Sprague-Dawley rats (two-month-old). However, in a fibrotic process, there would be a change in the collagen pattern and renal function would probably be impaired (GAGLIANO et al. 2000; GENOVESE et al. 2014), because types I and III collagen would accumulate in the renal interstitium and glomeruli, contributing to fibrosis (SOYLEMEZOGLU et al. 1997; STOKES et al. 2000). Therefore, as through our evaluations, we did not observe a significant change in collagen deposition in the renal cortex and renal medulla, we can say that leukocyte recruitment did not cause tissue fibrosis.

Assessing the deposition of neutral glycoconjugates in renal tissue is important because the importance of the kidneys in glucose homeostasis is already known (SULLIVAN; FORBES, 2019). Some diseases, such as diabetes and Glycogen storage disease type I (GSD-I), show that the progressive accumulation of glycogen in the kidneys caused by these conditions alters morphology and function renal (AOUN et al. 2020; KANG et al. 2005; NANNIPIERI et al. 2001). Therefore, it is important to maintain glycogen storage, even if small, in the kidneys in a physiological state to avoid functional changes and kidney damage, contributing to maintain the systemic glucose homeostasis (ALSAHLI; GERICH, 2017).

5. Conclusion

In conclusion, LDX-administration in male rats during the peripubertal period causes renal damage in pubertal age with involvement of inflammatory mechanisms and apoptosis process.

Conflict of interest

The authors declare that there are no conflicts of interest.

Acknowledgements

The authors are grateful to CAPES - PROEX (Coordinating Body for the Improvement of Postgraduate Studies in Higher Education) for providing a Master' s scholarship to JVH da Silva, and partially financial support (Finance Code 001). This paper represents part of the Master' s thesis by JVH da Silva (Experimental pathology - State University of Londrina - Brazil) under the supervision of GSA Fernandes. WA Verri Jr reports the research fellowship from CNPq (#309633/2021-4).

References

Aebi H., 1984. Catalase *in vitro*. Methods Enzymol. 105, 121–126. https://doi.org/10.1016/s0076-6879(84)05016-3.

Alsahli, M. & Gerich, J. E., 2017. Renal glucose metabolism in normal physiological conditions and in diabetes. Diabetes Res. Clin. Pract. 133, 1–9. https://doi.org/10.1016/j.diabres.2017.07.033.

Andrade-Oliveira, V., Foresto-Neto, O., Watanabe, I. K. M., Zatz, R. & Câmara, N. O. S., 2019. Inflammation in Renal Diseases: New and Old Players. Front. Pharmacol. 10, 1192. https://doi.org/10.3389/fphar.2019.01192.

Aoun, B., Sanjad, S., Degheili, J. A., Barhoumi, A., Bassyouni, A. & Karam, P. E., 2020. Kidney and Metabolic Phenotypes in Glycogen Storage Disease Type-I Patients. Front. Pediatr. 8, 591. https://doi.org/10.3389/fped.2020.00591.

Biederman, J., Krishnan, S., Zhang, Y., McGough, J. J. & Findling, R. L., 2007. Efficacy and tolerability of lisdexamfetamine dimesylate (NRP-104) in children with attention-deficit/hyperactivity disorder: a phase III, multicenter, randomized, double-

blind, forced-dose, parallel-group study. Clin. Ther. 29, 450–463. https://doi.org/10.1016/s0149-2918(07)80083-x.

Blank, U., Essig, M., Scandiuzzi, L., Benhamou, M. & Kanamaru, Y., 2007. Mast cells and inflammatory kidney disease. Immunol. Rev. 217, 79–95. https://doi.org/10.1111/j.1600-065X.2007.00503.x.

Bradford M. M., 1976. A rapid and sensitive method for the quantitation of microgram quantities of protein utilizing the principle of protein-dye binding. Anal. Biochem. 72, 248–254. https://doi.org/10.1016/0003-2697(76)90527-3.

Buege J. A. & Aust S. A., 1978. Microsomal lipid peroxidation methods. Enzymol 52, 302–310.

Cao, Q., Harris, D. C. & Wang, Y., 2015. Macrophages in kidney injury, inflammation, and fibrosis. Physiology (Bethesda), 30, 183–194. https://doi.org/10.1152/physiol.00046.2014.

Carvalho, F., Fernandes, E., Remião, F. & de Bastos, M. L., 1999. Effect of d-amphetamine repeated administration on rat antioxidant defences. Arch. Toxicol. 73, 83–89. https://doi.org/10.1007/s002040050591.

Carvalho, F., Duarte, J. A., Neuparth, M. J., Carmo, H., Fernandes, E., Remião, F. & Bastos, M. L., 2001. Hydrogen peroxide production in mouse tissues after acute d-amphetamine administration. Influence of monoamine oxidase inhibition. Arch. Toxicol. 75, 465–469. https://doi.org/10.1007/s002040100264.

Chalaris, A., Rabe, B., Paliga, K., Lange, H., Laskay, T., Fielding, C. A., Jones, S. A., Rose-John, S. & Scheller, J., 2007. Apoptosis is a natural stimulus of IL6R shedding and contributes to the proinflammatory trans-signaling function of neutrophils. Blood, 110, 1748–1755. https://doi.org/10.1182/blood-2007-01-067918.

Chen, Y., Feng, X., Hu, X., Sha, J., Li, B., Zhang, H. & Fan, H., 2018. Dexmedetomidine Ameliorates Acute Stress-Induced Kidney Injury by Attenuating Oxidative Stress and Apoptosis through Inhibition of the ROS/JNK Signaling Pathway. Oxid. Med. Cell. Longev. 2018, 4035310. https://doi.org/10.1155/2018/4035310.

Coghill, D. R., Banaschewski, T., Lecendreux, M., Zuddas, A., Dittmann, R. W., Otero, I. H., Civil, R., Bloomfield, R. & Squires, L. A., 2014. Efficacy of

lisdexamfetamine dimesylate throughout the day in children and adolescents with attention-deficit/hyperactivity disorder: results from a randomized, controlled trial. Eur. Child Adolesc. Psychiatry, 23, 61–68. https://doi.org/10.1007/s00787-013-0421-y.

Comiran, E., Kessler, F. H., Fröehlich, P. E. & Limberger, R. P., 2016. Lisdexamfetamine: A pharmacokinetic review. Eur. J. Pharm. Sci. 89, 172–179. https://doi.org/10.1016/j.ejps.2016.04.026.

Elmarakby, A. A. & Sullivan, J. C., 2012. Relationship between oxidative stress and inflammatory cytokines in diabetic nephropathy. Cardiovasc. Ther. 30, 49–59. https://doi.org/10.1111/j.1755-5922.2010.00218.x.

Ermer, J. C., Dennis, K., Haffey, M. B., Doll, W. J., Sandefer, E. P., Buckwalter, M., Page, R. C., Diehl, B. & Martin, P. T., 2011. Intranasal versus oral administration of lisdexamfetamine dimesylate: a randomized, open-label, two-period, crossover, single-dose, single-centre pharmacokinetic study in healthy adult men. Clin. Drug Investig. 31, 357–370. https://doi.org/10.2165/11588190-000000000-00000.

Ermer, J. C., Haffey, M. B., Doll, W. J., Martin, P., Sandefer, E. P., Dennis, K., Corcoran, M., Trespidi, L. & Page, R. C., 2012. Pharmacokinetics of lisdexamfetamine dimesylate after targeted gastrointestinal release or oral administration in healthy adults. Drug Metab. Dispos. 40, 290–297. https://doi.org/10.1124/dmd.111.040691.

Ermer, J. C., Pennick, M. & Frick, G., 2016a. Lisdexamfetamine Dimesylate: Prodrug Delivery, Amphetamine Exposure and Duration of Efficacy. Clin. Drug Investig. 36, 341–356. https://doi.org/10.1007/s40261-015-0354-y.

Ermer, J., Corcoran, M., Lasseter, K., Marbury, T., Yan, B. & Martin, P. T., 2016b. A Single-Dose, Open-Label Study of the Pharmacokinetics, Safety, and Tolerability of Lisdexamfetamine Dimesylate in Individuals With Normal and Impaired Renal Function. Ther. Drug Monit. 38, 546–555. https://doi.org/10.1097/FTD.0000000000000296.

Faria, J., Ahmed, S., Gerritsen, K., Mihaila, S. M. & Masereeuw, R., 2019. Kidney-based in vitro models for drug-induced toxicity testing. Arch. Toxicol. 93, 3397–3418. https://doi.org/10.1007/s00204-019-02598-0.

Fernandes, G. S., Arena, A. C., Fernandez, C. D., Mercadante, A., Barbisan, L. F. & Kempinas, W. G., 2007. Reproductive effects in male rats exposed to diuron. Reprod. Toxicol. 23, 106–112. https://doi.org/10.1016/j.reprotox.2006.09.002.

Ferraz, C. R. et al., 2021. Toxicon Peripheral mechanisms involved in Tityus bahiensis venom-induced pain. Toxicon 200, 3–12. https://doi.org/10.1016/j.toxicon.2021.06.013.

Findling, R. L., Cutler, A. J., Saylor, K., Gasior, M., Hamdani, M., Ferreira-Cornwell, M. C. & Childress, A. C., 2013. A long-term open-label safety and effectiveness trial of lisdexamfetamine dimesylate in adolescents with attention-deficit/hyperactivity disorder. J. Child Adolesc. Psychopharmacol. 23, 11–21. https://doi.org/10.1089/cap.2011.0088.

Food and Drug Administration, 2013. Guidance for Industry: Estimating the Maximum Safe Starting Dose in Initial Clinical Trials for Therapeutics in Adult Healthy Volunteers. Rockville, EUA, Food and Drug Administration, 2005.

Fu, Y. C., Yin, S. C., Chi, C. S., Hwang, B. & Hsu, S. L., 2006. Norepinephrine induces apoptosis in neonatal rat endothelial cells via a ROS-dependent JNK activation pathway. Apoptosis. 11, 2053–2063. https://doi.org/10.1007/s10495-006-0192-8.

Gagliano, N., Arosio, B., Santambrogio, D., Balestrieri, M. R., Padoani, G., Tagliabue, J., Masson, S., Vergani, C. & Annoni, G., 2000. Age-dependent expression of fibrosis-related genes and collagen deposition in rat kidney cortex. J. Gerontol. A. Biol. Sci. Med. Sci. 55, B365–B372. https://doi.org/10.1093/gerona/55.8.b365.

Genovese, F., Manresa, A. A., Leeming, D. J., Karsdal, M. A. & Boor, P., 2014. The extracellular matrix in the kidney: a source of novel non-invasive biomarkers of kidney fibrosis?. Fibrogenesis Tissue Repair. 7, 4. https://doi.org/10.1186/1755-1536-7-4.

Goodman, D. W., 2010. Lisdexamfetamine dimesylate (vyvanse), a prodrug stimulant for attention-deficit/hyperactivity disorder. P. T. 35, 273–287.

Gowda, B. C., Kokila, G., Gopinathan, P. A. & Praveen, K. S., 2017. Picrosirius red and polarization microscopy – a tool for gender differentiation. J. Clin. Diagnostic Res. 11, ZC107–ZC109. https://doi.org/10.7860/JCDR/2017/22863.9296.

Griffin, B. R., Faubel, S. & Edelstein, C. L., 2019. Biomarkers of Drug-Induced Kidney Toxicity. Ther. Drug Monit. 41, 213–226. https://doi.org/10.1097/FTD.0000000000000589.

Grivei, A., Giuliani, K., Wang, X., Ungerer, J., Francis, L., Hepburn, K., John, G. T., Gois, P., Kassianos, A. J. & Healy, H., 2020. Oxidative stress and inflammasome activation in human rhabdomyolysis-induced acute kidney injury. Free Radic. Biol. Med. 160, 690–695. https://doi.org/10.1016/j.freeradbiomed.2020.09.011.

Gueutin, V., Deray, G. & Isnard-Bagnis, C., 2012. Physiologie rénale [Renal physiology]. Bull. Cancer 99, 237–249. https://doi.org/10.1684/bdc.2011.1482.

Hokamp, J. A. & Nabity, M. B., 2016. Renal biomarkers in domestic species. Vet. Clin. Pathol. 45, 28–56. https://doi.org/10.1111/vcp.12333.

Hudson, J. I., McElroy, S. L., Ferreira-Cornwell, M. C., Radewonuk, J. & Gasior, M., 2017. Efficacy of Lisdexamfetamine in Adults With Moderate to Severe Binge-Eating Disorder: A Randomized Clinical Trial. JAMA Psychiatry 74, 903–910. https://doi.org/10.1001/jamapsychiatry.2017.1889.

Hutson, P. H., Pennick, M. & Secker, R., 2014. Preclinical pharmacokinetics, pharmacology and toxicology of lisdexamfetamine: a novel d-amphetamine pro-drug. Neuropharmacology, 87, 41–50. https://doi.org/10.1016/j.neuropharm.2014.02.014.

Jones, D. P., 2008. Radical-free biology of oxidative stress. Am. J. Physiol. Cell Physiol. 295, C849–C868. https://doi.org/10.1152/ajpcell.00283.2008.

Kang, J., Dai, X. S., Yu, T. B., Wen, B. & Yang, Z. W., 2005. Glycogen accumulation in renal tubules, a key morphological change in the diabetic rat kidney. Acta Diabetol. 42, 110–116. https://doi.org/10.1007/s00592-005-0188-9.

Keen, J. H., Habig, W. H. & Jakoby, W. B., 1976. Mechanism for the several activities of the glutathione S-transferases. J. Biol. Chem. 251, 6183–6188. https://doi.org/10.1016/S0021-9258(20)81842-0.

Kolaczkowska, E. & Kubes, P., 2013. Neutrophil recruitment and function in health and inflammation. Nat. Rev. Immunol. 13, 159–175. https://doi.org/10.1038/nri3399.

Krishnan, S. & Montcrief, S., 2007. Toxicity profile of lisdexamfetamine dimesylate in three independent rat toxicology studies. Basic Clin. Pharmacol. Toxicol. 101, 231–240. https://doi.org/10.1111/j.1742-7843.2007.00093.x.

Krishnan, S. M., Pennick, M. & Stark, J. G., 2008. Metabolism, distribution and elimination of lisdexamfetamine dimesylate: open-label, single-centre, phase I study in healthy adult volunteers. Clin. Drug Investig. 28, 745–755. https://doi.org/10.2165/0044011-200828120-00002.

Kushiyama, T., Oda, T., Yamada, M., Higashi, K., Yamamoto, K., Sakurai, Y., Miura, S. & Kumagai, H., 2011. Alteration in the phenotype of macrophages in the repair of renal interstitial fibrosis in mice. Nephrology (Carlton), 16, 522–535. https://doi.org/10.1111/j.1440-1797.2010.01439.x.

Lacy, P. & Eitzen, G., 2008. Control of granule exocytosis in neutrophils. Front. Biosci. 13, 5559–5570. https://doi.org/10.2741/3099.

Loureiro-Vieira, S., Costa, V. M., Duarte, J. A., Duarte-Araújo, M., Gonçalves-Monteiro, S., Maria de Lourdes, B., Carvalho, F. & Capela, J. P., 2018. Methylphenidate clinically oral doses improved brain and heart glutathione redox status and evoked renal and cardiac tissue injury in rats. Biomed. Pharmacother. 100, 551–563. https://doi.org/10.1016/j.biopha.2018.02.017.

Lushchak, O. V., Kubrak, O. I., Lozinsky, O. V., Storey, J. M., Storey, K. B. & Lushchak, V. I., 2009. Chromium(III) induces oxidative stress in goldfish liver and kidney. Aquat. Toxicol. 93, 45–52. https://doi.org/10.1016/J.AQUATOX.2009.03.007.

Lv, W., Booz, G. W., Wang, Y., Fan, F. & Roman, R. J., 2018. Inflammation and renal fibrosis: Recent developments on key signaling molecules as potential therapeutic targets. Eur. J. Pharmacol. 820, 65–76. https://doi.org/10.1016/j.ejphar.2017.12.016.

Madjene, L. C., Pons, M., Danelli, L., Claver, J., Ali, L., Madera-Salcedo, I. K., Kassas, A., Pellefigues, C., Marquet, F., Dadah, A., Attout, T., El-Ghoneimi, A., Gautier, G., Benhamou, M., Charles, N., Daugas, E., Launay, P. & Blank, U., 2015. Mast cells in renal inflammation and fibrosis: lessons learnt from animal studies. Mol. Immunol. 63, 86–93. https://doi.org/10.1016/j.molimm.2014.03.002.

Maneeton, N., Maneeton, B., Suttajit, S., Reungyos, J., Srisurapanont, M. & Martin, S. D., 2014. Exploratory meta-analysis on lisdexamfetamine versus placebo in adult ADHD. Drug Des. Devel. Ther. 8, 1685–1693. https://doi.org/10.2147/DDDT.S68393.

McCormick, J. A. & Ellison, D. H., 2015. Distal convoluted tubule. Compr. Physiol. 5, 45–98. https://doi.org/10.1002/cphy.c140002.

McElroy, S. L., Hudson, J. I., Mitchell, J. E., Wilfley, D., Ferreira-Cornwell, M. C., Gao, J., Wang, J., Whitaker, T., Jonas, J. & Gasior, M., 2015. Efficacy and safety of lisdexamfetamine for treatment of adults with moderate to severe binge-eating disorder: a randomized clinical trial. JAMA Psychiatry, 72, 235–246. https://doi.org/10.1001/jamapsychiatry.2014.2162.

McMahon, A. P., 2016. Development of the Mammalian Kidney. Curr. Top. Dev. Biol. 117, 31–64. https://doi.org/10.1016/bs.ctdb.2015.10.010.

Mechler, K., Banaschewski, T., Hohmann, S. & Häge, A., 2022. Evidence-based pharmacological treatment options for ADHD in children and adolescents. Pharmacol. Ther. 230, 107940. https://doi.org/10.1016/j.pharmthera.2021.107940.

Mi, X. J., Hou, J. G., Wang, Z., Han, Y., Ren, S., Hu, J. N., Chen, C. & Li, W., 2018. The protective effects of maltol on cisplatin-induced nephrotoxicity through the AMPK-mediated PI3K/Akt and p53 signaling pathways. Sci. Rep. 8, 15922. https://doi.org/10.1038/s41598-018-34156-6.

Moore, K. E., 1966. Effects of d-amphetamine on plasma and tissue electrolyte concentrations of aggregated and of hyperthyroid mice. Proc. Soc. Exp. Biol. Med. 122, 292–295. https://doi.org/10.3181/00379727-122-31116.

Najib, J., 2012. Lisdexamfetamine in the treatment of adolescents and children with attention-deficit/hyperactivity disorder. Adolesc. Health Medicine Ther. 3, 51–66. https://doi.org/10.2147/AHMT.S19815.

Najib, J., Didenko, E., Meleshkina, D., Yusupov, K., Maw, K., Ramnarain, J. & Tabassum, M., 2020. Review of lisdexamfetamine dimesylate in children and adolescents with attention deficit/hyperactivity disorder. Curr. Med. Res. Opin. 36, 1717–1735. https://doi.org/10.1080/03007995.2020.1815002.

Nannipieri, M., Lanfranchi, A., Santerini, D., Catalano, C., Van de Werve, G. & Ferrannini, E., 2001. Influence of long-term diabetes on renal glycogen metabolism in the rat. Nephron. 87, 50–57. https://doi.org/10.1159/000045884.

Nieskens, T. T. & Wilmer, M. J., 2016. Kidney-on-a-chip technology for renal proximal tubule tissue reconstruction. Eur. J. Pharmacol. 790, 46–56. https://doi.org/10.1016/j.ejphar.2016.07.018.

Ojeda, S. R., Andrews, W. W., Advis, J. P. & White, S. S., 1980. Recent advances in the endocrinology of puberty. Endocr Rev. 1, 228-257. https://doi.org/10.1210/edrv-1-3-228.

Oliveira, S., Rosowski, E. E. & Huttenlocher, A., 2016. Neutrophil migration in infection and wound repair: going forward in reverse. Nat. Rev. Immunol. 16, 378–391. https://doi.org/10.1038/nri.2016.49.

Piper, B. J., Ogden, C. L., Simoyan, O. M., Chung, D. Y., Caggiano, J. F., Nichols, S. D. & McCall, K. L., 2018. Trends in use of prescription stimulants in the United States and Territories, 2006 to 2016. PloS One, 13, e0206100. https://doi.org/10.1371/journal.pone.0206100.

Punhagui, A. P. F., Vieira, H. R., Siervo, G. E. M. L., Rosa, R. & Fernandes, G. S. A., 2016. Ethanol exposure during peripubertal period increases the mast cell number and impairs meiotic and spermatic parameters in adult male rats. Microsc. Res. Tech. 79, 541–549. https://doi.org/10.1002/jemt.22664.

Pupim, A. C. E., Campois, T. G., Araújo, E. J. A., Svidizinski, T. I. E. & Felipe, I., 2017. Infection and tissue repair of experimental cutaneous candidiasis in diabetic mice. J. Med. Microbiol. 66, 808–815. https://doi.org/10.1099/jmm.0.000496.

Radi, Z. A., 2019. Kidney Pathophysiology, Toxicology, and Drug-Induced Injury in Drug Development. Int. J. Toxicol. 38, 215–227. https://doi.org/10.1177/1091581819831701.

Rahman, I., Kode, A. & Biswas, S. K., 2006. Assay for quantitative determination of glutathione and glutathione disulfide levels using enzymatic recycling method. Nat. Protoc. 1, 3159–3165. https://doi.org/10.1038/nprot.2006.378.

Raoofi, A., Delbari, A., Mahdian, D., Mojadadi, M. S., Amini, A., Javadinia, S. S., Dadashizadeh, G., Ahrabi, B., Ebrahimi, V. & Mousavi Khaneghah, A., 2020. Toxicology of long-term and high-dose administration of methylphenidate on the kidney tissue - a histopathology and molecular study. Toxicol. Mech. Methods, 30, 611–619. https://doi.org/10.1080/15376516.2020.1805665.

Ratliff, B. B., Abdulmahdi, W., Pawar, R. & Wolin, M. S., 2016. Oxidant Mechanisms in Renal Injury and Disease. Antioxid. Redox Signal. 25, 119–146. https://doi.org/10.1089/ars.2016.6665.

Ribatti, D., 2018. The Staining of Mast Cells: A Historical Overview. Int. Arch. Allergy Immunol. 176, 55–60. https://doi.org/10.1159/000487538.

Salviano, L. H., Linhares, M. I., de Lima, K. A., de Souza, A. G., Lima, D. B., Jorge, A. R., da Costa, M. F., Filho, A. J., Martins, A. M., Monteiro, H. S., de Jesus, T. M. J. P. & de Fonteles, M. M. F., 2015. Study of the safety of methylphenidate: Focus on nephrotoxicity aspects. Life Sci. 141, 137–142. https://doi.org/10.1016/j.lfs.2015.09.014.

Samelo, R. R., Medeiros, P. C., Cavalcante, D. N. C., Aranha, M., Duarte, F. A., Castro, Í. B., Ribeiro, D. A. & Perobelli, J. E., 2020. Low concentrations of sodium arsenite induce hepatotoxicity in prepubertal male rats. Environ. Toxicol. 35, 553–560. https://doi.org/10.1002/tox.22890.

Scannell, M., Flanagan, M. B., deStefani, A., Wynne, K. J., Cagney, G., Godson, C. & Maderna, P., 2007. Annexin-1 and peptide derivatives are released by apoptotic cells and stimulate phagocytosis of apoptotic neutrophils by macrophages. J. Immunol. 178, 4595–4605. https://doi.org/10.4049/jimmunol.178.7.4595.

Schreuder, M. F., Bueters, R. R. & Allegaert, K., 2014. The interplay between drugs and the kidney in premature neonates. Pediatr. Nephrol. 29, 2083–2091. https://doi.org/10.1007/s00467-013-2651-0.

Senthilkumar M., Amaresan N. & Sankaranarayanan A., 2021. Plant-Microbe Interactions, Springer Protocols Handbooks. Springer US, New York, NY. https://doi.org/10.1007/978-1-0716-1080-0.

Sharman, J. & Pennick, M., 2014. Lisdexamfetamine prodrug activation by peptidase-mediated hydrolysis in the cytosol of red blood cells. Neuropsychiatr. Dis. Treat. 10, 2275–2280. https://doi.org/10.2147/NDT.S70382.

Soehnlein, O. & Lindbom, L., 2010. Phagocyte partnership during the onset and resolution of inflammation. Nat. Rev. Immunol. 10, 427–439. https://doi.org/10.1038/nri2779.

Soylemezoglu, O., Wild, G., Dalley, A. J., MacNeil, S., Milford-Ward, A., Brown, C. B. & el Nahas, A. M., 1997. Urinary and serum type III collagen: markers of renal fibrosis. Nephrol. Dial. Transplant. 12, 1883–1889. https://doi.org/10.1093/ndt/12.9.1883.

Stokes, M. B., Holler, S., Cui, Y., Hudkins, K. L., Eitner, F., Fogo, A. & Alpers, C. E., 2000. Expression of decorin, biglycan, and collagen type I in human renal fibrosing disease. Kidney Int. 57, 487–498. https://doi.org/10.1046/j.1523-1755.2000.00868.x.

Sullivan, M. A. & Forbes, J. M., 2019. Glucose and glycogen in the diabetic kidney: Heroes or villains?. EBioMedicine, 47, 590–597. https://doi.org/10.1016/j.ebiom.2019.07.067.

Taatjes, D. J., Bouffard, N. A., Barrow, T., Devitt, K. A., Gardner, J. A. & Braet, F., 2019. Quantitative pixel intensity- and color-based image analysis on minimally compressed files: implications for whole-slide imaging. Histochem. Cell Biol. 152, 13–23. https://doi.org/10.1007/s00418-019-01783-7.

Tang, P. M., Nikolic-Paterson, D. J. & Lan, H. Y., 2019. Macrophages: versatile players in renal inflammation and fibrosis. Nat. Rev. Nephrol. 15, 144–158. https://doi.org/10.1038/s41581-019-0110-2.

Tecklenborg, J., Clayton, D., Siebert, S. & Coley, S. M., 2018. The role of the immune system in kidney disease. Clin. Exp. Immunol. 192, 142–150. https://doi.org/10.1111/cei.13119.

Vibhushan, S., Bratti, M., Montero-Hernández, J. E., El Ghoneimi, A., Benhamou, M., Charles, N., Daugas, E. & Blank, U., 2020. Mast Cell Chymase and Kidney Disease. Int. J. Mol. Sci. 22, 302. https://doi.org/10.3390/ijms22010302.

Vinuesa, E., Hotter, G., Jung, M., Herrero-Fresneda, I., Torras, J. & Sola, A., 2008. Macrophage involvement in the kidney repair phase after ischaemia/reperfusion injury. J. Pathol. 214, 104–113. https://doi.org/10.1002/path.2259.

Xu, X., Lai, Y. & Hua, Z. C., 2019. Apoptosis and apoptotic body: disease message and therapeutic target potentials. Biosc. Rep. 39, BSR20180992. https://doi.org/10.1042/BSR20180992.

Legend of tables

Table 1

Kidney weight and biochemical measurement of renal function

Values are expressed as the mean ± S.E.M. (n=20 per group for kidney weight; n=10 per group for biochemical measurement). Unpaired t test. *p<0.05.

Table 2

Stereological analysis of the kidneys

Values are expressed as the mean ± S.E.M. (n=6 per group). Unpaired t test. *p<0.05 and **p<0.01.

Table 3

Mast cell count

Values are expressed as the mean ± S.E.M. (n=6 per group). Unpaired t test. p>0.05.

Legend of figure

Figure 1. Histopathology of the kidney

Photomicrograph of kidney section from renal cortex (A, C) and renal medulla (B, D). The arrow indicates the proximal convoluted tubule, the arrowhead the distal convoluted tubule, the asterisk the glomerulus, and the hash the normal collecting ducts. Control group (A, B) and LDX group (C, D). H&E staining. Bar 10 μm. C - rats received tap water; LDX - rats treated with 11.3 mg/kg b.w. lisdexamfetamine dimesylate.

Figure 2. Immunohistochemical reaction with antibody against cleaved caspase-3 in the renal cortex

Photomicrograph of kidney section from renal cortex (A and B) and graph with percentage of the number of cells marked for cleaved caspase-3 (C). Arrows indicate some immunoreactive cells. (A) Control group; (B) LDX group. 400x magnification. Bar 10 μm. Data are the mean ± S.E.M. (n=6 per group). Unpaired t test. **p<0.01. C - rats received tap water; LDX - rats treated with 11.3 mg/kg b.w. lisdexamfetamine dimesylate.

Figure 3. Myeloperoxidase (A) and N-acetyl-β-D-glucosaminidase (B) activity in the kidney

Data are the mean ± S.E.M. (n=10 per group). Unpaired t test. *p<0.05 and ***p<0.001. C - rats received tap water; LDX - rats treated with 11.3 mg/kg b.w. lisdexamfetamine dimesylate.

Figure 4. Oxidative stress profile in the kidney. MDA concentration (A), quantification of GSH (B), and CAT (C), GST (D) and SOD (E) activity

Data are the mean ± S.E.M. (n=10 per group). Unpaired t test. *p<0.05, **p<0.01 and ***p<0.001. C - rats received tap water; LDX - rats treated with 11.3 mg/kg b.w. lisdexamfetamine dimesylate.

Figure 5. Histochemical analysis of the percentage of neutral glycoconjugates (I), total collagen (J) and percentage of collagen type I and type III (K) in the renal cortex

Photomicrographs of sections of renal cortex stained with Periodic acid Schiff (A, E), Azan Heidenhain trichrome (B, F) and unpolarized (C, G) and polarized (D, H) picrosirius red. (A-D) Control group; (E-H) LDX group. 400x magnification in a light microscope (A, B, E, F) and in a polarized light microscope (C, D, G, H). Bar 10 μm. Data are the mean ± S.E.M. (n=6 per group). Unpaired t test. *p>0.05. C - rats received tap water; LDX - rats treated with 11.3 mg/kg b.w. lisdexamfetamine dimesylate.

Figure 6. Histochemical analysis of the percentage of neutral glycoconjugates (I), total collagen (J) and percentage of collagen type I and type III (K) in the renal medulla

Photomicrographs of sections of renal medulla stained with Periodic acid Schiff (A, E), Azan Heidenhain trichrome (B, F) and unpolarized (C, G) and polarized (D, H) picrosirius red. (A-D) Control group; (E-H) LDX group. 400x magnification in a light microscope (A, B, E, F) and in a polarized light microscope (C, D, G, H). Bar 10 μm. Data are the mean ± S.E.M. (n=6 per group). Unpaired t test. *p>0.05. C - rats received tap water; LDX - rats treated with 11.3 mg/kg b.w. lisdexamfetamine dimesylate.

Table 1. Kidney weight and biochemical measurement of renal function

	Parameters	Control group (C)	LDX group (LDX)	P value
Absolute weight (g)				
	Kidney	0.993 ± 0.019	0.913 ± 0.022	0.0090**
Relative weight (g/100g)				
	Kidney	0.365 ± 0.006	0.357 ± 0.005	0.2531
Plasmatic levels (mg/dL)				
	Creatinine	1.609 ± 0.154	1.706 ± 0.172	0.6775
	Urea	78.38 ± 1.443	75.62 ± 2.155	0.2997

Values are expressed as the mean ± S.E.M. (n=20 per group for kidney weight; n=10 per group for biochemical measurement). Unpaired t test. *p<0.05.

Table 2. Stereological analysis of the kidneys

	Control group (C)	LDX group (LDX)	P value
Glomerulus	87.59 ± 2.157	85.23 ± 0.398	0.3072
Bowman space	4.816 ± 0.190	4.686 ± 0.186	0.6356
Proximal convoluted tubule	37.51 ± 0.332	35.90 ± 0.437	0.0148*
Distal convoluted tubule	28.07 ± 0.316	25.93 ± 0.409	0.0020**
Collecting duct	28.49 ± 1.643	29.23 ± 1.848	0.7737

Values are expressed as the mean ± S.E.M. (n=6 per group). Unpaired t test. *$p<0.05$ and **$p<0.01$.

Table 3. Mast cell count

Number of mast cells (per cut)	Control group (C)	LDX group (LDX)	P value
Intact	1.50 ± 0.342	1.17 ± 0.307	0.4848
Degranulated	1.00 ± 0.365	0.67 ± 0.211	0.4475
Total	1.25 ± 0.250	0.92 ± 0.193	0.3027

Values are expressed as the mean ± S.E.M. (n=6 per group) Unpaired t test. $p>0.05$.

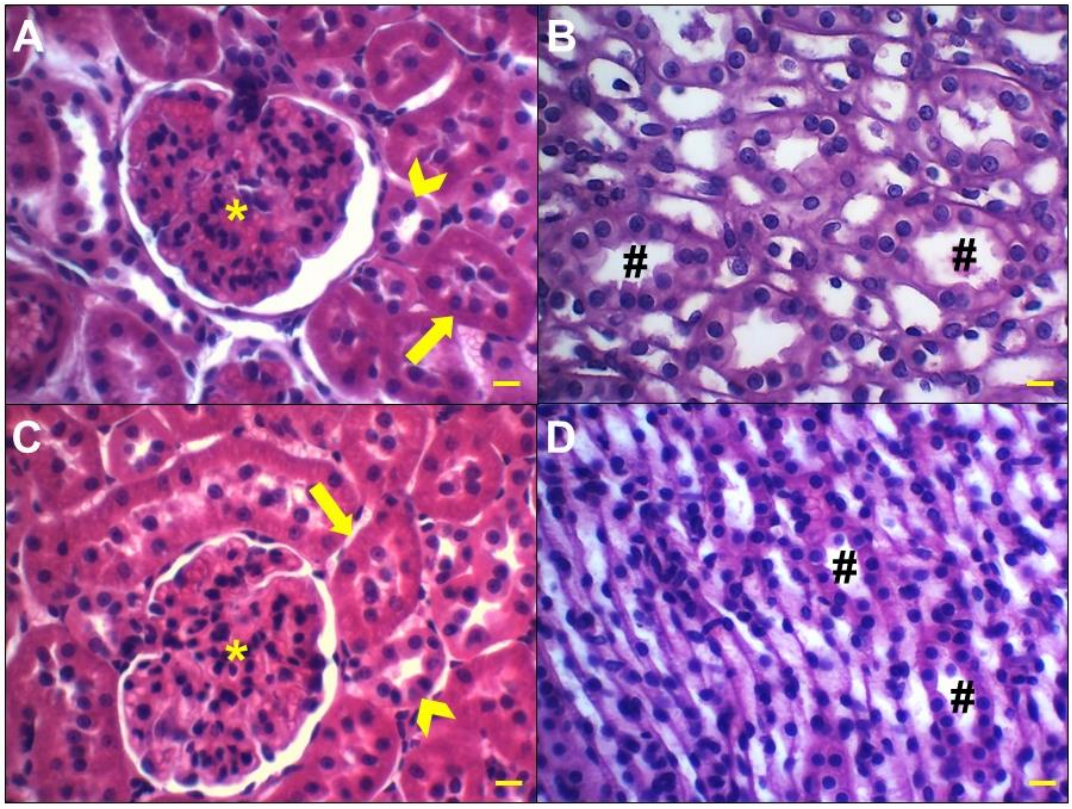

Figure 1. Histopathology of the kidney. Photomicrograph of kidney section from renal cortex (A, C) and renal medulla (B, D). The arrow indicates the proximal convoluted tubule, the arrowhead the distal convoluted tubule, the asterisk the glomerulus, and the hash the normal collecting ducts. Control group (A, B) and LDX group (C, D). H&E staining. Bar 10 μm. C - rats received tap water; LDX - rats treated with 11.3 mg/kg b.w. lisdexamfetamine dimesylate.

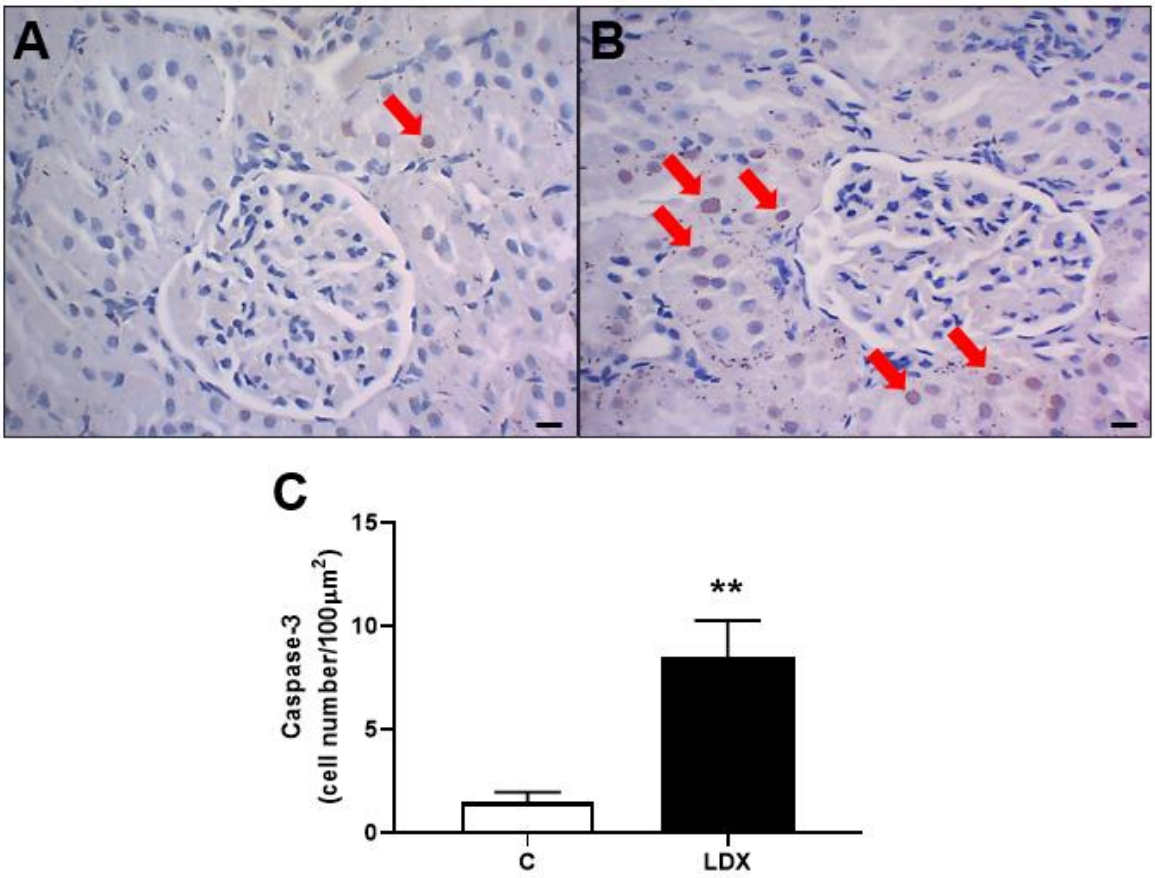

Figure 2. Immunohistochemical reaction with antibody against cleaved caspase-3 in the renal cortex. Photomicrograph of kidney section from renal cortex (A and B) and graph with percentage of the number of cells marked for cleaved caspase-3 (C). Arrows indicate some immunoreactive cells. (A) Control group; (B) LDX group. 400x magnification. Bar 10 µm. Data are the mean ± S.E.M. (n=6 per group). Unpaired t test. **p<0.01. C - rats received tap water; LDX - rats treated with 11.3 mg/kg b.w. lisdexamfetamine dimesylate.

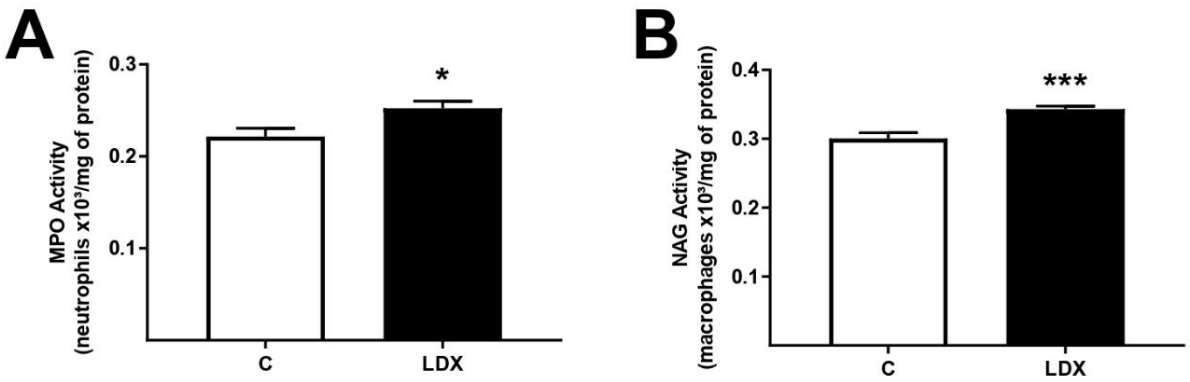

Figure 3. Myeloperoxidase (A) and N-acetyl-β-D-glucosaminidase (B) activity in the kidney. Data are the mean ± S.E.M. (n=10 per group). Unpaired t test. *p<0.05 and ***p<0.001. C - rats received tap water; LDX - rats treated with 11.3 mg/kg b.w. lisdexamfetamine dimesylate.

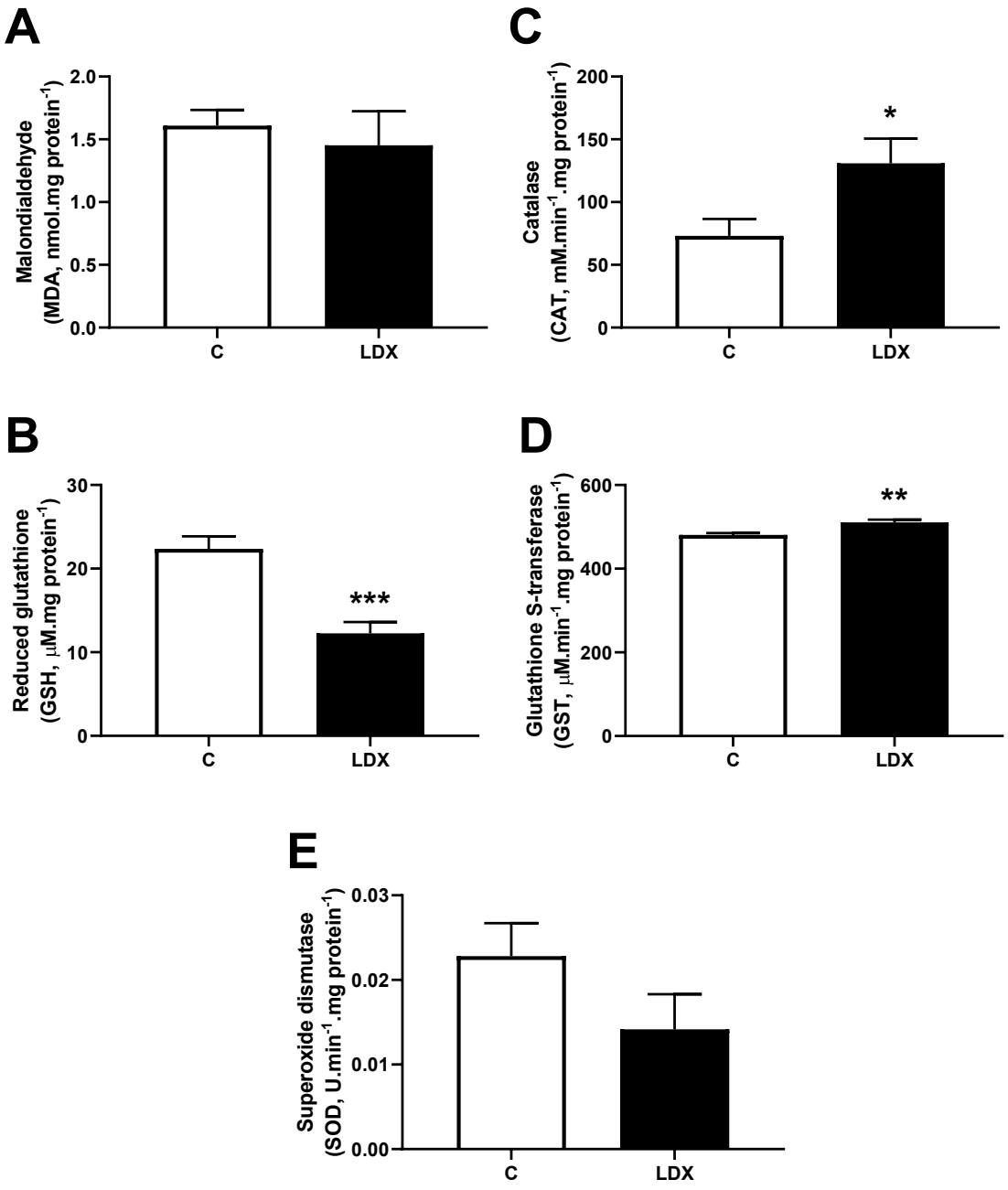

Figure 4. Oxidative stress profile in the kidney. MDA concentration (A), quantification of GSH (B), and CAT (C), GST (D) and SOD (E) activity. Data are the mean ± S.E.M. (n=10 per group). Unpaired t test. *p<0.05, **p<0.01 and ***p<0.001. C - rats received tap water; LDX - rats treated with 11.3 mg/kg b.w. lisdexamfetamine dimesylate.

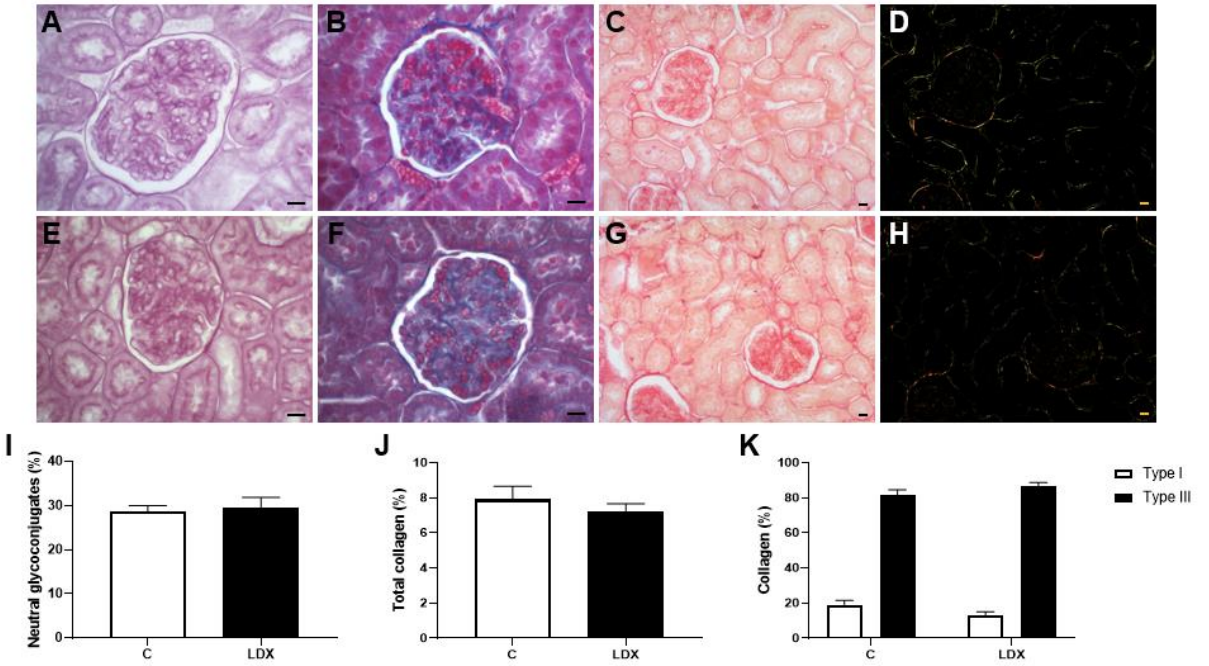

Figure 5. Histochemical analysis of the percentage of neutral glycoconjugates (I), total collagen (J) and percentage of collagen type I and type III (K) in the renal cortex. Photomicrographs of sections of renal cortex stained with Periodic acid Schiff (A, E), Azan Heidenhain trichrome (B, F) and unpolarized (C, G) and polarized (D, H) picrosirius red. (A-D) Control group; (E-H) LDX group. 400x magnification in a light microscope (A, B, E, F) and in a polarized light microscope (C, D, G, H). Bar 10 μm. Data are the mean ± S.E.M. (n=6 per group). Unpaired t test. $p>0.05$. C - rats received tap water; LDX - rats treated with 11.3 mg/kg b.w. lisdexamfetamine dimesylate.

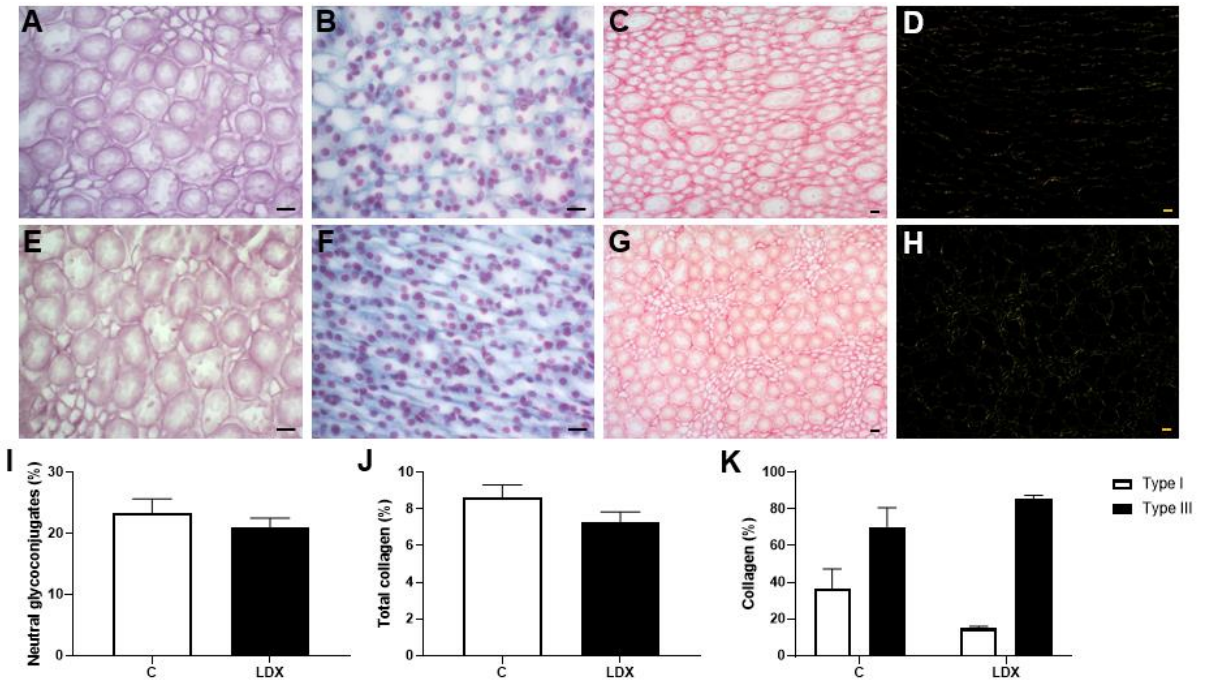

Figure 6. Histochemical analysis of the percentage of neutral glycoconjugates (I), total collagen (J) and percentage of collagen type I and type III (K) in the renal medulla. Photomicrographs of sections of renal medulla stained with Periodic acid Schiff (A, E), Azan Heidenhain trichrome (B, F) and unpolarized (C, G) and polarized (D, H) picrosirius red. (A-D) Control group; (E-H) LDX group. 400x magnification in a light microscope (A, B, E, F) and in a polarized light microscope (C, D, G, H). Bar 10 µm. Data are the mean ± S.E.M. (n=6 per group). Unpaired t test. $p>0.05$. C - rats received tap water; LDX - rats treated with 11.3 mg/kg b.w. lisdexamfetamine dimesylate.

6 CONSIDERAÇÕES FINAIS

Nestas condições experimentais, conclui-se que a exposição ao LDX durante a peripuberdade apresentou hepatotoxicidade e nefrotoxicidade na idade púbere, observado através dos parâmetros avaliados, principalmente de perfil inflamatório. Entretanto, nos rins, foi observado uma resposta efetiva do sistema antioxidante frente as alterações.

Portanto, infere-se que o uso de LDX em crianças e adolescentes deve ser acompanhado de exames clínicos e laboratoriais de modo periódico para o monitoramento de eventuais danos colaterais que possam ocorrer durante o tratamento com este fármaco. Além disso, faz-se necessário a realização de mais estudos e o acompanhamento de pacientes que utilizam outros medicamentos concomitante, devido a possibilidade de uma interação medicamentosa ainda não descrita na literatura.

REFERÊNCIAS

ABDEL-MISIH, Sherif R. Z.; BLOOMSTON, Mark. Liver Anatomy. **Surgical Clinics Of North America**, [s. l], v. 90, n. 4, p. 643-653, 2010.

American Psychiatric Association. **Diagnostic and Statistical Manual of Mental Disorders**. 3rd ed. DSM-III: Washington DC; 1980.

American Psychiatric Association. **Diagnostic and Statistical Manual of Mental Disorders**. 5th ed. DSM V: Washington DC; 2013.

ANDRADE, Kívia Queiroz et al. Oxidative Stress and Inflammation in Hepatic Diseases: Therapeutic Possibilities of N-Acetylcysteine. **International Journal Of Molecular Sciences**, [s. l], v. 16, n. 12, p. 30269-30308, 2015.

Agência Nacional de Vigilância Sanitária - ANVISA. **Lista de substâncias sujeitas a controle especial no Brasil: portaria/svs nº 344, de 12 de maio de 1998**. Disponível em: <http://antigo.anvisa.gov.br/documents/10181/2718376/%2836%29PRT_SVS_344_1998_COMP.pdf/b1453297-c5e8-4349-8ae2-4f2968779c71>. Acesso em: 01 abr. 2022.

ARAUJO, Magali; WILCOX, Christopher S.. Oxidative Stress in Hypertension: Role of the Kidney. **Antioxidants & Redox Signaling**, [s. l], v. 20, n. 1, p. 74-101, 2014.

ARMANDO, Ines et al. Dopamine and renal function and blood pressure regulation. **Comprehensive Physiology**, [s. l], v. 1, n. 3, p. 1075-1170, 2011.

BANERJEE, Tania et al. Environmental risk factors for attention-deficit hyperactivity disorder. **Acta Pædiatrica**, [S.l], v. 96, n. 9, p. 1269-1274, 2007.

BARKLEY, Russell A.; PETERS, Helmut. The Earliest Reference to ADHD in the Medical Literature? Melchior Adam Weikard's Description in 1775 of "Attention Deficit" (Mangel der Aufmerksamkeit, Attentio Volubilis). **Journal Of Attention Disorders**, [S.l], v. 16, n. 8, p. 623-630, 8 fev. 2012.

BASSO, Paulo José et al. Targeting immune cell metabolism in kidney diseases. **Nature Reviews Nephrology**, [s. l], v. 17, p. 465-480, 2021.

BIEDERMAN, Joseph et al. Efficacy and tolerability of lisdexamfetamine dimesylate (NRP-104) in children with attention-deficit/hyperactivity disorder: A Phase III, multicenter, randomized, double-blind, forced-dose, parallel-group study. **Clinical Therapeutics**, [s. l], v. 29, n. 3, p. 450-463, mar. 2007.

BJÖRNSSON, E. et al. The impact of eosinophilia and hepatic necrosis on prognosis in patients with drug-induced liver injury. **Alimentary Pharmacology & Therapeutics**, [s. l], v. 25, n. 12, p. 1411-1421, 2007.

BLICK, Stephanie K. A.; KEATING, Gillian M.. Lisdexamfetamine. **Pediatric Drugs**, [s.l], v. 9, n. 2, p. 129-135, 2007.

BOGDANOS, Dimitrios P. et al. Liver Immunology. **Comprehensive Physiology**, [s. l], v. 3, n. 2, p. 567-598, 2013.

BONNEVILLE, Marc et al. γδ T cell effector functions: a blend of innate programming and acquired plasticity. **Nature Reviews Immunology**, [s. l], v. 10, p. 467-478, 2010.

BRALTEN, Janita et al. Candidate Genetic Pathways for Attention-Deficit/Hyperactivity Disorder (ADHD) Show Association to Hyperactive/Impulsive Symptoms in Children With ADHD. **Journal Of The American Academy Of Child & Adolescent Psychiatry**, [s.l], v. 52, n. 11, p. 1204-1212, 1 nov. 2013.

BRIX, Silke R. et al. CC Chemokine Ligand 18 in ANCA-Associated Crescentic GN. **Journal Of The American Society Of Nephrology**, [s. l], v. 26, n. 9, p. 2105-2117, 2015.

BUKSTEIN, Oscar G.; HORNER, Michelle S.. Management of the Adolescent with Substance Use Disorders and Comorbid Psychopathology. **Child And Adolescent Psychiatric Clinics Of North America**, [s. l], v. 19, n. 3, p. 609-623, jul. 2010.

BURTON, Graham J.; JAUNIAUX, Eric. Oxidative stress. **Best Practice & Research**: Clinical Obstetrics & Gynaecology, [s. l], v. 25, n. 3, p. 287-299, 2011.

CALABRESE, Edward J.; CANADA, Andrew T.. Catalase: its role in xenobiotic detoxification. **Pharmacology & Therapeutics**, [s. l], v. 44, n. 2, p. 297-307, 1989.

CAMPO, Natalia del et al. The Roles of Dopamine and Noradrenaline in the Pathophysiology and Treatment of Attention-Deficit/ Hyperactivity Disorder. **Biological Psychiatry**, [s. l], v. 69, n. 12, p. 145-157, 15 jun. 2011.

CARVALHO, Félix et al. Effect of d-amphetamine repeated administration on rat antioxidant defences. **Archives Of Toxicology**, [s. l], v. 73, p. 83-89, 1999.

CARVALHO, Félix et al. Hydrogen peroxide production in mouse tissues after acute d-amphetamine administration. Influence of monoamine oxidase inhibition. **Archives Of Toxicology**, [s. l], v. 75, p. 465-469, 2001.

CARVALHO, Márcia et al. Toxicity of amphetamines: an update. **Archives Of Toxicology**, [s. l], v. 86, p. 1167-1231, 2012.

CHEN, Linlin et al. Inflammatory responses and inflammation - associated diseases in organs. **Oncotarget**, [s. l], v. 9, n. 6, p. 7204-7218, 2018a.

CHEN, Yongping et al. Dexmedetomidine Ameliorates Acute Stress-Induced Kidney Injury by Attenuating Oxidative Stress and Apoptosis through Inhibition of the ROS/JNK Signaling Pathway. **Oxidative Medicine And Cellular Longevity**, [s. l], v. 2018, 4035310, 2018b.

CICHOŜ-LACH, Halina; MICHALAK, Agata. Oxidative stress as a crucial factor in liver diseases. **World Journal Of Gastroenterology**, [s. l], v. 20, n. 25, p. 8082-8091, 2014.

COGHILL, David et al. European, randomized, phase 3 study of lisdexamfetamine dimesylate in children and adolescents with attention-deficit/hyperactivity disorder.

European Neuropsychopharmacology, [s. l], v. 23, n. 10, p. 1208-1218, out. 2013.

COGHILL, David R. et al. Efficacy of lisdexamfetamine dimesylate throughout the day in children and adolescents with attention-deficit/hyperactivity disorder: results from a randomized, controlled trial. **European Child & Adolescent Psychiatry**, [s. l], v. 23, p. 61-68, 2014.

COMIRAN, Eloisa et al. Lisdexamfetamine: A pharmacokinetic review. **European Journal Of Pharmaceutical Sciences**, [s. l], v. 89, p. 172-179, 2016.

CONTRERAS-ZENTELLA, Martha Lucinda; HERNÁNDEZ-MUÑOZ, Rolando. Is Liver Enzyme Release Really Associated with Cell Necrosis Induced by Oxidant Stress? **Oxidative Medicine And Cellular Longevity**, [s. l], v. 2016, p. 3529149, 2016.

CRESCENZO, Franco de et al. Pharmacological and non-pharmacological treatment of adults with ADHD: a meta-review. **Evidence-Based Mental Health**, [s. l], v. 20, n. 1, p. 4-11, 2017.

CRISPE, Ian Nicholas. The Liver as a Lymphoid Organ. **Annual Review of Immunology**, [s.l], v. 27, p. 147-163, 2009.

CUEVAS, Santiago et al. Renal Dopamine Receptors, Oxidative Stress, and Hypertension. **International Journal Of Molecular Sciences**, [s. l], v. 14, n. 9, p. 17553-17572, 2013.

D'ANGELO, Egidio; CASALI, Stefano. Seeking a unified framework for cerebellar function and dysfunction: from circuit operations to cognition. **Frontiers In Neural Circuits**, [S.l], v. 6, n. 116, p. 1-23, jan. 2012.

DAVIES, Clare; TOURNIER, Cathy. Exploring the function of the JNK (c-Jun N-terminal kinase) signalling pathway in physiological and pathological processes to design novel therapeutic strategies. **Biochemical Society Transactions**, [s. l], v. 40, n. 1, p. 85-89, 2012.

DUNN, Geoffrey A. et al. Neuroinflammation as a risk factor for attention deficit hyperactivity disorder. **Pharmacology Biochemistry And Behavior**, [s. l], v. 182, p. 22-34, jul. 2019.

DURSTON, Sarah et al. Magnetic Resonance Imaging of Boys With Attention-Deficit/Hyperactivity Disorder and Their Unaffected Siblings. **Journal Of The American Academy Of Child & Adolescent Psychiatry**, [s. l], v. 43, n. 3, p. 332-340, mar. 2004.

EL-KORAIE, Ahmed F. et al. Role of stem cell factor and mast cells in the progression of chronic glomerulonephritides. **Kidney International**, [s. l], v. 60, n. 1, p. 167-172, 2001.

EL-TAWIL, Osama S. et al. D-Amphetamine-induced cytotoxicity and oxidative stress in isolated rat hepatocytes**. Pathophysiology**, [s. l], v. 18, n. 4, p. 279-285, set. 2011.

ELMARAKBY, Ahmed A.; SULLIVAN, Jennifer C.. Relationship between oxidative stress and inflammatory cytokines in diabetic nephropathy. **Cardiovascular**

Therapeutics, [s. l], v. 30, n. 1, p. 49-59, 2012.

ERMER, James C. et al. Intranasal versus Oral Administration of Lisdexamfetamine Dimesylate: a randomized, open-label, two-period, crossover, single-dose, single-centre pharmacokinetic study in healthy adult men. **Clinical Drug Investigation**, [s. l], v. 31, p. 357-370, 2011.

ERMER, James C. et al. Pharmacokinetics of Lisdexamfetamine Dimesylate after Targeted Gastrointestinal Release or Oral Administration in Healthy Adults. **Drug Metabolism And Disposition**, [s. l], v. 40, n. 2, p. 290-297, fev. 2012.

ERMER, James C. et al. Lisdexamfetamine Dimesylate: Prodrug Delivery, Amphetamine Exposure and Duration of Efficacy. **Clinical Drug Investigation**, [s. l], v. 36, p. 341-356, 2016.

FARAONE, Stephen V. et al. Attention-deficit/hyperactivity disorder. **Nature Reviews Disease Primers**, [S.l], v. 1, n. 15020, p. 1-23, ago. 2015.

FARAONE, Stephen V. The pharmacology of amphetamine and methylphenidate: Relevance to the neurobiology of attention-deficit/hyperactivity disorder and other psychiatric comorbidities. **Neuroscience & Biobehavioral Reviews**, [s. l], v. 87, p. 255-270, abr. 2018.

FARAONE, Stephen V.; LARSSON, Henrik. Genetics of attention deficit hyperactivity disorder. **Molecular Psychiatry**, [S.l], v. 24, n. 4, p. 562-575, 2019.

FARAONE, Stephen V.; MICK, Eric. Molecular Genetics of Attention Deficit Hyperactivity Disorder. **Psychiatric Clinics Of North America**, [S.l], v. 33, n. 1, p. 159-180, mar. 2010.

FARIA, João et al. Kidney-based in vitro models for drug-induced toxicity testing. **Archives Of Toxicology**, [s. l], v. 93, p. 3397-3418, 2019.

FINDLING, Robert L. et al. Efficacy and Safety of Lisdexamfetamine Dimesylate in Adolescents With Attention-Deficit/Hyperactivity Disorder. **Journal Of The American Academy Of Child & Adolescent Psychiatry**, [s. l], v. 50, n. 4, p. 395-405, abr. 2011.

FINDLING, Robert L. et al. A Long-Term Open-Label Safety and Effectiveness Trial of Lisdexamfetamine Dimesylate in Adolescents With Attention-Deficit/Hyperactivity Disorder. **Journal Of Child And Adolescent Psychopharmacology**, [s. l], v. 23, n. 1, p. 11-21, fev. 2013.

FINKEL, Toren. Signal transduction by reactive oxygen species. **Journal Of Cell Biology**, [s. l], v. 194, n. 1, p. 7-15, 2011.

FRAMPTON, James E.. Lisdexamfetamine Dimesylate: A Review in Paediatric ADHD. **Drugs**, [s. l], v. 78, p. 1025-1036, 2018.

FREITAS-LOPES, Maria Alice et al. Differential Location and Distribution of Hepatic Immune Cells. **Cells**, [s. l], v. 6, n. 4, dez. 2017.

FRIEDMAN, Lisa A.; RAPOPORT, Judith L.. Brain development in ADHD. **Current**

Opinion In Neurobiology, [S.l], v. 30, p. 106-111, fev. 2015.

FU, Yun-Ching et al. Norepinephrine induces apoptosis in neonatal rat endothelial cells via a ROS-dependent JNK activation pathway. **Apoptosis**, [s. l], v. 11, n. 11, p. 2053-2063, 2006.

GAO, Bin et al. Liver natural killer and natural killer T cells: immunobiology and emerging roles in liver diseases. **Journal Of Leukocyte Biology**, [s. l], v. 86, n. 3, p. 513-528, 2009.

GOMEZ, R. Ariel; SEQUEIRA-LOPEZ, Maria Luisa S.. Renin cells in homeostasis, regeneration and immune defence mechanisms. **Nature Reviews Nephrology**, [s. l], v. 14, n. 4, p. 231-245, 2018.

GOODMAN, David W. Lisdexamfetamine Dimesylate (Vyvanse), A Prodrug Stimulant for Attention-Deficit/Hyperactivity Disorder. **Pharmacy And Therapeutics (P&T)**, [s. l], v. 35, n. 5, p. 273-287, maio 2010.

GORDILLO, Miriam et al. Orchestrating liver development. **Development**, [s. l], v. 142, n. 12, p. 2094-2108, jun. 2015.

GREKA, Anna; MUNDEL, Peter. Cell Biology and Pathology of Podocytes. **Annual Review Of Physiology**, [s. l], v. 74, p. 299-323, 2012.

GRIJALVA, James; VAKILI, Khashayar. Neonatal liver physiology. **Seminars In Pediatric Surgery**, [s. l], v. 22, n. 4, p. 185-189, nov. 2013.

GRIVEI, Anca et al. Oxidative stress and inflammasome activation in human rhabdomyolysis-induced acute kidney injury. **Free Radical Biology and Medicine**, [s. l], v. 160, p. 690-695, nov. 2020.

GUEUTIN, Victor et al. Physiologie rénale: renal physiology. **Bulletin Du Cancer**, [s. l], v. 99, n. 3, p. 237-249, 2012.

HAMMERICH, Linda; TACKE, Frank. Role of gamma-delta T cells in liver inflammation and fibrosis. **World Journal Of Gastrointestinal Pathophysiology**, [s. l], v. 5, n. 2, p. 107-113, 2014.

HASTINGS, Kenneth L. et al. Beyond Metabolism: Role of the Immune System in Hepatic Toxicity. **International Journal Of Toxicology**, [s. l], v. 39, n. 2, p. 151-164, 2020.

HEAL, David J. et al. Amphetamine, past and present – a pharmacological and clinical perspective. **Journal Of Psychopharmacology**, [s. l], v. 27, n. 6, p. 479-496, jun. 2013.

HEYMANN, Felix; TACKE, Frank. Immunology in the liver — from homeostasis to disease. **Nature Reviews Gastroenterology & Hepatology**, [s. l], v. 13, p. 88-110, 2016.

HICKLING, Duane R. et al. Anatomy and Physiology of the Urinary Tract: Relation to Host Defense and Microbial Infection. **Microbiology Spectrum**, [s. l], v. 3, n. 4, 2015.

HIJMANS, Brenda S. et al. Zonation of glucose and fatty acid metabolism in the liver: Mechanism and metabolic consequences. **Biochimie**, [s. l], v. 96, p. 121-129, jan. 2014.

HOLT, Michael P. et al. Identification and characterization of infiltrating macrophages in acetaminophen-induced liver injury. **Journal Of Leukocyte Biology**, [s. l], v. 84, n. 6, p. 1410-1421, 2008.

HOLTMANN, Martin et al. Neurofeedback for ADHD: A Review of Current Evidence. **Child And Adolescent Psychiatric Clinics Of North America**, [s. l], v. 23, n. 4, p. 789-806, out. 2014.

HOOD, Brandy; NOWICKI, Michael J.. Eosinophilic Hepatitis in an Adolescent During Lisdexamfetamine Dimesylate Treatment for ADHD. **Pediatrics**, [s. l], v. 125, n. 6, p. 1510-1513, 2010.

HOOGMAN, Martine et al. Brain imaging of the cortex in ADHD: A coordinated analysis of large-scale clinical and population-based samples. **The American Journal Of Psychiatry**, [S.l], v. 176, n. 7, p. 531-542, jul. 2019.

HSU, Cheng-Chin et al. Preventive effect of Ganoderma amboinense on acetaminophen-induced acute liver injury. **Phytomedicine**, [s. l], v. 15, n. 11, p. 946-950, 2008.

HUBER, Sally et al. γδ T Cells Promote a Th1 Response during Coxsackievirus B3 Infection In Vivo: Role of Fas and Fas Ligand. **Journal of Virology**, [s. l], v. 76, n. 13, p. 6487-6494, 2002.

HUSSAIN, Tarique et al. Oxidative Stress and Inflammation: What Polyphenols Can Do for Us? **Oxidative Medicine And Cellular Longevity**, [s. l], v. 2016, p. 9, 2016.

ISHIYAMA, Kohei et al. Difference in cytotoxicity against hepatocellular carcinoma between liver and periphery natural killer cells in humans. **Hepatology**, [s. l], v. 43, n. 2, p. 362-372, 2006.

ISMAIL, Fatima Y.; SHAPIRO, Bruce K.. What are neurodevelopmental disorders? **Current Opinion In Neurology**, [S.l], v. 32, n. 4, p. 611-616, ago. 2019.

JAESCHKE, Hartmut et al. Glutathione peroxidase–deficient mice are more susceptible to neutrophil-mediated hepatic parenchymal cell injury during endotoxemia: importance of an intracellular oxidant stress. **Hepatology**, [s. l], v. 29, n. 2, p. 443-450, 1999.

JAESCHKE, Hartmut. Reactive oxygen and mechanisms of inflammatory liver injury: Present concepts. **Journal Of Gastroenterology And Hepatology**, [s. l], v. 26, n. 1, p. 173-179, 2011.

JAESCHKE, Hartmut et al. Oxidant stress, mitochondria, and cell death mechanisms in drug-induced liver injury: lessons learned from acetaminophen hepatotoxicity. **Drug Metabolism Reviews**, [s. l], v. 44, n. 1, p. 88-106, 2012.

JASINSKI, D. R.; KRISHNAN, S.. Human pharmacology of intravenous

lisdexamfetamine dimesylate: abuse liability in adult stimulant abusers. **Journal Of Psychopharmacology**, [s. l], v. 23, n. 4, p. 410-418, 2009.

JENSEN, Kendal Jay et al. Hepatic Nervous System and Neurobiology of the Liver. **Comprehensive Physiology**, [s. l], v. 3, n. 2, p. 655-665, 2013.

JONES, Dean P.. Radical-free biology of oxidative stress. **American Journal Of Physiology.: Cell physiology**, [s. l], v. 295, n. 4, p. 849-868, 2008.

JOURDE-CHICHE, Noemie et al. Endothelium structure and function in kidney health and disease. **Nature Reviews Nephrology**, [s. l], v. 15, p. 87-108, 2019.

KATO, Yoji. Neutrophil myeloperoxidase and its substrates: formation of specific markers and reactive compounds during inflammation. **Journal Of Clinical Biochemistry And Nutrition**, [s. l], v. 58, n. 2, p. 99-104, 2016.

KEHRER, James P.. Free radicals as mediators of tissue injury and disease. **Critical Reviews In Toxicology**, [s. l], v. 23, n. 1, p. 21-48, 1993.

KRISHNAN, Suma; MONTCRIEF, Scott. Toxicity Profile of Lisdexamfetamine Dimesylate in Three Independent Rat Toxicology Studies. **Basic & Clinical Pharmacology & Toxicology**, [s. l], v. 101, n. 4, p. 231-240, 2007.

KRISHNAN, Suma M. et al. Metabolism, Distribution and Elimination of Lisdexamfetamine Dimesylate: open-label, single-centre, phase I study in healthy adult volunteers. **Clinical Drug Investigation**, [s. l], v. 28, n. 12, p. 745-755, 2008.

KRISHNAN, Suma; ZHANG, Yuxin. Relative Bioavailability of Lisdexamfetamine 70-mg Capsules in Fasted and Fed Healthy Adult Volunteers and in Solution: A Single-Dose, Crossover Pharmacokinetic Study. **The Journal Of Clinical Pharmacology**, [s. l], v. 48, n. 3, p. 293-302, 2008.

KRÜGER, Thilo et al. Identification and Functional Characterization of Dendritic Cells in the Healthy Murine Kidney and in Experimental Glomerulonephritis. **Journal Of The American Society Of Nephrology**, [s. l], v. 15, n. 3, p. 613-621, 2004.

KUBES, Paul; JENNE, Craig. Immune Responses in the Liver. **Annual Review Of Immunology**, [s. l], v. 36, p. 247-277, 2018.

KUBES, Paul; MEHAL, Wajahat Z.. Sterile inflammation in the liver. **Gastroenterology**, [s. l], v. 143, n. 5, p. 1158-1172, 2012.

KÜPELI, Esra et al. Effect of Cistus laurifolius L. leaf extracts and flavonoids on acetaminophen-induced hepatotoxicity in mice. **Journal Of Ethnopharmacology**, [s. l], v. 103, n. 3, p. 455-460, 2006.

KURTS, Christian et al. Kidney dendritic cells: fundamental biology and functional roles in health and disease. **Nature Reviews Nephrology**, [s.l]. v. 16, n. 7, p. 391-407, 2020.

KUSHIYAMA, Taketoshi et al. Alteration in the phenotys.Ipe of macrophages in the repair of renal interstitial fibrosis in mice. **Nephrology (Carlton)**, [s. l], v. 16, n. 5, p.

522-535, 2011.

LANGBERG, Joshua M.; BECKER, Stephen P.. Does Long-Term Medication Use Improve the Academic Outcomes of Youth with Attention-Deficit/Hyperactivity Disorder? **Clinical Child And Family Psychology Review**, [s. l], v. 15, p. 215-233, 2012.

LANGE, Klaus W. et al. The history of attention deficit hyperactivity disorder. **Attention Deficit And Hyperactivity Disorders**, [S.l], v. 4, n. 2, p. 241-255, 30 nov. 2010.

LONNEMAN, Gerhard et al. Cytokines in human renal interstitial fibrosis. I. Interleukin-1 is a paracrine growth factor for cultured fibrosis-derived kidney fibroblasts. **Kidney International**, [s. l], v. 47, n. 3, p. 837-844, 1995.

LU, Shelly C.. Glutathione synthesis. **Biochimica Et Biophysica Acta (Bba) - General Subjects**, [s. l], v. 1830, n. 5, p. 3143-3153, 2013.

MADJENE, Lydia Celia et al. Mast cells in renal inflammation and fibrosis: Lessons learnt from animal studies. **Molecular Immunology**, [s. l], v. 63, n. 1, p. 86-93, 2015.

MAFRA, Kassiana et al. The liver as a nursery for leukocytes. **Journal Of Leukocyte Biology**, [s. l], v. 106, n. 3, p. 687-693, 2019.

MANTLE, Timothy J. et al. Inhibition of monoamine oxidase by amphetamine and related compounds. **Biochemical Pharmacology**, [s. l], v. 25, n. 18, p. 2073-2077, set. 1976.

MANTOVANI, Alberto et al. The chemokine system in diverse forms of macrophage activation and polarization. **Trends In Immunology**: Cell Press, [s. l], v. 25, n. 12, p. 677-686, 2004.

MARIN, José J. G. et al. Bile Acids in Physiology, Pathology and Pharmacology. **Current Drug Metabolism**, [s. l], v. 17, n. 1, p. 4-29, 2015.

MARTÍN-FONTECHA, Alfonso et al. Regulation of Dendritic Cell Migration to the Draining Lymph Node: impact on t lymphocyte traffic and priming. **The Journal Of Experimental Medicine**, [s. l], v. 198, n. 4, p. 615-621, 2003.

MARTINEZ-BADÍA, Jose; MARTINEZ-RAGA, Jose. Who says this is a modern disorder? The early history of attention deficit hyperactivity disorder. **World Journal Of Psychiatry**, [S.l], v. 5, n. 4, p. 379-386, 22 dez. 2015.

MCCORMICK, James A.; ELLISON, David H.. The Distal Convoluted Tubule. **Comprehensive Physiology**, [s. l], v. 5, n. 1, p. 45-98, jan. 2015.

MCDONALD, Braedon et al. Intravascular Danger Signals Guide Neutrophils to Sites of Sterile Inflammation. **Science**, [s. l], v. 330, n. 6002, p. 362-366, 2010.

MCMAHON, Andrew P.. Development of the Mammalian Kidney. **Current Topics In Developmental Biology**, [s. l], v. 117, p. 31-64, 2016.

MENG, Fanli et al. Interleukin-17 signaling in inflammatory, Kupffer cells, and hepatic

stellate cells exacerbates liver fibrosis in mice. **Gastroenterology**, [s. l], v. 143, n. 3, p. 765-776, 2012.

MILLER, Harold H. et al. In vivo monoamine oxidase inhibition by d-amphetamine. **Biochemical Pharmacology**, [s. l], v. 29, n. 10, p. 1347-1354, maio 1980.

MOORE, Sherri M. et al. Emerging roles for lipids in the hepatic innate immune response. **Journal Of Human Nutrition & Food Science**, [s. l], v. 1, p. 1-9, 2013.

MORMONE, Elisabetta et al. Molecular pathogenesis of hepatic fibrosis and current therapeutic approaches. **Chemico-Biological Interactions**, [s. l], v. 193, n. 3, p. 225-231, 2011.

MULLIN, A. P. et al. Neurodevelopmental disorders: mechanisms and boundary definitions from genomes, interactomes and proteomes. **Translational Psychiatry**, [S.l], v. 3, p. 329-334, 3 dez. 2013.

NAJIB, Jadwiga et al. Review of lisdexamfetamine dimesylate in children and adolescents with attention deficit/hyperactivity disorder. **Current Medical Research And Opinion**, [s. l], v. 36, n. 10, p. 1717-1735, 2020.

NAKAMOTO, Nobuhiro; KANAI, Takanori. Role of Toll-like receptors in immune activation and tolerance in the liver. **Frontiers In Immunology**, [s. l], v. 5, n. 221, 2014.

NETEA, Mihai G. et al. A guiding map for inflammation. **Nature Immunology**, [s. l], v. 18, n. 8, p. 826-831, 2017.

NIESKENS, Tom T. G.; WILMER, Martijn J.. Kidney-on-a-chip technology for renal proximal tubule tissue reconstruction. **European Journal Of Pharmacology**, [s. l], v. 790, p. 46-56, 2016.

OLEINIKA, Kristine et al. Effector and regulatory B cells in immune-mediated kidney disease. **Nature Reviews Nephrology**, [s. l], v. 15, n. 1, p. 11-26, 2019.

PENG, Hui et al. Liver natural killer cells: subsets and roles in liver immunity. **Cellular & Molecular Immunology**, [s. l], v. 13, n. 3, p. 328-336, 2016.

PENNICK, Michael. Absorption of lisdexamfetamine dimesylate and its enzymatic conversion to d-amphetamine. **Neuropsychiatric Disease And Treatment**, [s. l], v. 6, p. 317-327, 2010.

PHAM, Bach-Nga et al. Eotaxin expression and eosinophil infiltrate in the liver of patients with drug-induced liver disease. **Journal Of Hepatology**, [s. l], v. 34, n. 4, p. 537-547, 2001.

PIPER, Brian J. et al. Trends in use of prescription stimulants in the United States and Territories, 2006 to 2016. **Plos One**, [s. l], v. 13, n. 11, p. 1-15, nov. 2018.

POLANCZYK, Guilherme et al. The Worldwide Prevalence of ADHD: A Systematic Review and Metaregression Analysis. **The American Journal Of Psychiatry**, [S.l], v. 164, n. 6, p. 942-948, 1 jun. 2007.

POLANCZYK, Guilherme V. et al. Annual Research Review: A meta-analysis of the worldwide prevalence of mental disorders in children and adolescents. **Journal Of Child Psychology And Psychiatry**, [S.l], v. 56, n. 3, p. 345-365, fev. 2015.

PONZIANI, Francesca Romana et al. Physiology and pathophysiology of liver lipid metabolism. **Expert Review Of Gastroenterology & Hepatology**, [s. l], v. 9, n. 8, p. 1055-1067, 2015.

POSNER, Jonathan et al. Attention-deficit hyperactivity disorder. **The Lancet**, [S.l], v. 395, n. 10222, p. 450-462, 8 fev. 2020.

PUNJA, Salima et al. Amphetamines for attention deficit hyperactivity disorder (ADHD) in children and adolescents. **Cochrane Database Of Systematic Reviews**, [s. l], n. 2, p. 1465-1858, 2016.

RADI, Zaher A.. Kidney Pathophysiology, Toxicology, and Drug-Induced Injury in Drug Development. **International Journal Of Toxicology**, [s. l], v. 38, n. 3, p. 215-227, 2019.

RAMAN, Sudha R. et al. Trends in attention-deficit hyperactivity disorder medication use: a retrospective observational study using population-based databases. **Lancet Psychiatry**, [s. l], v. 5, n. 10, p. 824-835, 2018.

RATLIFF, Brian B. et al. Oxidant Mechanisms in Renal Injury and Disease. **Antioxidants & Redox Signaling**, [s. l], v. 25, n. 3, p. 119-146, 2016.

ROBINSON, Mark W. et al. Liver immunology and its role in inflammation and homeostasis. **Cellular & Molecular Immunology**, [s. l], v. 13, n. 3, p. 267-276, 2016.

ROY, Ankita et al. Collecting Duct Intercalated Cell Function and Regulation. **Clinical Journal Of The American Society Of Nephrology**: CJASN, [s. l], v. 10, n. 2, p. 305-324, 2015.

RÜGER, B. M. et al. Mast cells and type VIII collagen in human diabetic nephropathy. **Diabetologia**, [s. l], v. 39, p. 1215-1222, 1996.

RUI, Liangyou. Energy Metabolism in the Liver. **Comprehensive Physiology**, [s. l], v. 4, n. 1, p. 177-197, 2014.

SEDEEK, Mona et al. NADPH Oxidases, Reactive Oxygen Species, and the Kidney: Friend and Foe. **Journal Of The American Society Of Nephrology**, [s. l], v. 24, n. 10, p. 1512-1518, 2013.

SHARMAN, Johannah; PENNICK, Michael. Lisdexamfetamine prodrug activation by peptidase-mediated hydrolysis in the cytosol of red blood cells. **Neuropsychiatric Disease And Treatment**, [s. l], v. 20, p. 2275-2280, 2014.

SHAW, Philip et al. Emotion dysregulation in attention deficit hyperactivity disorder. **The American Journal Of Psychiatry**, [s. l], v. 171, n. 3, p. 276-293, mar. 2014.

SI-TAYEB, Karim et al. Organogenesis and Development of the Liver. **Developmental Cell**, [s. l], v. 18, n. 2, p. 175-189, fev. 2010.

SIMON, Viktória et al. Prevalence and correlates of adult attention-deficit hyperactivity disorder: meta-analysis. **The British Journal Of Psychiatry**, [S.l], v. 194, n. 3, p. 204-211, mar. 2009.

STARUSCHENKO, Alexander. Regulation of transport in the connecting tubule and cortical collecting duct. **Comprehensive Physiology**, [s. l], v. 2, n. 2, p. 1541–1584, 2012.

STEER, Christopher et al. Lisdexamfetamine Dimesylate: a new therapeutic option for attention-deficit hyperactivity disorder. **CNS Drugs**, [s. l], v. 26, p. 691-705, 2012.

STEWART, Benjamin J. et al. Spatio-temporal immune zonation of the human kidney. **Science**, [s. l], v. 365, n. 6460, p. 1461-1466, 2019.

STILL, GF. Some abnormal psychical conditions in children: the Goulstonian lectures. **Lancet**. 1902;1:1008–1012, 1077-1082, 1163-1168.

SURESHBABU, Angara et al. Oxidative stress and autophagy: Crucial modulators of kidney injury. **Redox Biology**, [s. l], v. 4, p. 208-214, 2015.

SVERRISSON, Kristinn et al. Acute reactive oxygen species (ROS)-dependent effects of IL-1β, TNF-α, and IL-6 on the glomerular filtration barrier (GFB) in vivo. **American Journal Of Physiology**: Renal Physiology, [s. l], v. 309, n. 9, p. 800-806, 2015.

TANG, Patrick Ming-Kuen et al. Macrophages: versatile players in renal inflammation and fibrosis. **Nature Reviews Nephrology**, [s. l], v. 15, p. 144-158, 2019.

THAPAR, Anita et al. Neurodevelopmental disorders. **The Lancet Psychiatry**, Elsevier, v. 4, n. 4, p. 339-346, 12 dez. 2016.

TRAYNOR, Jamie et al. How to measure renal function in clinical practice. **BMJ: British Medical Journal**, [s. l], v. 333, p. 733-737, 2006.

TREFTS, Elijah et al. The liver. **Current Biology**, [s. l], v. 27, n. 21, p. 1147-1151, 2017.

TURNER, Jan-Eric et al. Natural Killer Cells in Kidney Health and Disease. **Frontiers In Immunology**, [s. l], v. 587, n. 10, 2019.

UCHIDA, Takahiro et al. Activated natural killer T cells in mice induce acute kidney injury with hematuria through possibly common mechanisms shared by human CD56 + T cells. **American Journal Of Physiology: Renal Physiology**, [s. l], v. 315, n. 3, p. 618-627, 2018.

VALERA, Eve M. et al. Meta-Analysis of Structural Imaging Findings in Attention-Deficit/Hyperactivity Disorder. **Biological Psychiatry**, [s. l], v. 61, n. 12, p. 1361-1369, jun. 2007.

VIENNOIS, Emilie et al. Function, Regulation, and Pathophysiological Relevance of the POT Superfamily, Specifically PepT1 in Inflammatory Bowel Disease. **Comprehensive Physiology**, [s. l], v. 8, n. 2, p. 731-760, 2018.

VINUESA, E. et al. Macrophage involvement in the kidney repair phase after ischaemia/reperfusion injury. **The Journal Of Pathology**, [s. l], v. 214, n. 1, p. 104-113, 2008.

VISARIUS, Theresa M. et al. Pathways of glutathione metabolism and transport in isolated proximal tubular cells from rat kidney. **Biochemical Pharmacology**, [s. l], v. 52, n. 2, p. 259-272, 1996.

WATSON, Walter H. et al. Thioredoxin and its role in toxicology. **Toxicological Sciences**, [s. l], v. 78, n. 1, p. 3-14, 2004.

WIGAL, Sharon B. et al. A 13-hour laboratory school study of lisdexamfetamine dimesylate in school-aged children with attention-deficit/hyperactivity disorder. **Child And Adolescent Psychiatry And Mental Health**, [s. l], v. 3, n. 17, 2009.

WIGAL, Timothy et al. Effect Size of Lisdexamfetamine Dimesylate in Adults with Attention-Deficit/Hyperactivity Disorder. **Postgraduate Medicine**, [s. l], v. 123, n. 2, p. 169-176, 2011.

WILLCUTT, Erik G. et al. Validity of DSM-IV attention–deficit/hyperactivity disorder symptom dimensions and subtypes. **Journal Of Abnormal Psychology**, [S.l], v. 121, n. 4, p. 991-1010, nov. 2012.

YANG, Seung Hee et al. NKT cells inhibit the development of experimental crescentic glomerulonephritis. **Journal Of The American Society Of Nephrology**, [s. l], v. 19, n. 9, p. 1663-1671, 2008.

ZEISBERG, Elisabeth M. et al. Fibroblasts in kidney fibrosis emerge via endothelial-to-mesenchymal transition. **Journal Of The American Society Of Nephrology**, [s. l], v. 19, n. 12, p. 2282-2287, 2008.

ZHANG, Zhu-Xu et al. NK Cells Induce Apoptosis in Tubular Epithelial Cells and Contribute to Renal Ischemia-Reperfusion Injury. **The Journal Of Immunology**, [s. l], v. 181, n. 11, p. 7489-7498, 2008.

ZHANG, H. et al. Hepatic B cells are readily activated by Toll-like receptor-4 ligation and secrete less interleukin-10 than lymphoid tissue B cells. **Clinical & Experimental Immunology**, [s. l], v. 173, n. 3, p. 473-479, 2013.

ZHANG, Cheng et al. Molecular Mechanisms Involved in Oxidative Stress-Associated Liver Injury Induced by Chinese Herbal Medicine: An Experimental Evidence-Based Literature Review and Network Pharmacology Study. **International Journal Of Molecular Sciences**, [s. l], v. 19, n. 9, p. 2745, 2018.

ZHU, Runzhi et al. Oxidative stress and liver disease. **Hepatology Research**, [s. l], v. 42, n. 8, p. 741-749, 2012.

ANEXOS

ANEXO A

Aprovação de Projeto pelo Comitê de Ética (CEUA-UEL)

Universidade Estadual de Londrina

COMISSÃO DE ÉTICA NO USO DE ANIMAIS

OF. CIRC. CEUA Nº 82/2019

Londrina, 24 de junho de 2019.

Prezado (a) professor (a)

Certificamos que o projeto de pesquisa intitulado: **"Efeitos do uso de dimesilato de lisdexanfetamina sobre o desenvolvimento pós natal do sistema genital masculino de ratos"** protocolo CEUA **nº 9633.2019.65** sob a responsabilidade de **Glaura Scantamburlo Alves Fernandes,** que envolve a produção, manutenção e/ou utilização de animais pertencentes ao filo Chordata, subfilo Vertebrata (exceto o homem) para fins de pesquisa científica (ou ensino), encontra-se de acordo com os preceitos da Lei nº 11.794, de 8 de outubro de 2008, do Decreto nº 6.899, de 15 de julho de 2009, e com as normas editadas pelo Conselho Nacional de Controle da Experimentação Animal (CONCEA), e foi **aprovado** pela Comissão de Ética no Uso de Animais da Universidade Estadual de Londrina (CEUA/UEL), em reunião de **18/06/2019.**

Este projeto tem por objetivo analisar a morfologia, funcionalidade, perfil inflamatório e estresse oxidativo do testículo, epidídimo e próstata; avaliar a morfologia e funcionalidade do ducto deferente; qualidade espermática; função hepática e renal; determinar a concentração plasmática de hormônios e investigar o comportamento sexual de ratos *Wistar* submetidos a gavagem com dimesilato de lisdexanfetamina em dois momentos distintos: na peripuberdade (DPN 66), imediatamente após o termino do período de administração do fármaco, e na vida adulta (DPN 131), após um período de 65 dias de recuperação do tratamento. Grau de invasividade:1.

Finalidade	( ) Ensino (x) Pesquisa científica
Vigência da autorização	01/09/2019 a 01/08/2023
Espécie/ linhagem/ raça	Rato heterogênico: Wistar
N° de animais	**80 machos** de 22 dias e **40 fêmeas** de 60 dias
Peso/ Idade	-/ 22 dias -/ 60 dias
Sexo	Machos e Fêmeas
Origem	Biotério Central do CCB
Amostras a serem coletadas	Sangue, testículos, epidídimos, próstatas, ducto deferentes, fígado, rins.

Cumpre orientar que caso pretendam-se quaisquer alterações no protocolo experimental aprovado, deve-se submeter o novo protocolo à apreciação da CEUA/UEL anteriormente à execução das modificações.

Coloco-me à disposição para quaisquer esclarecimentos que se fizerem necessários. Sem mais para o momento, subscrevo-me, cordialmente.

Maria Fernanda R. Graciano

Profa. Dra. Maria Fernanda Rodrigues Graciano
Coordenadora da CEUA/UEL

Profª Drª Maria Fernanda Rodrigues Graciano
Coordenadora da Comissão de Ética no Uso de Animais
Universidade Estadual de Londrina
ceua@uel.br / (43) 3371-5454

Ilmo.(a) Sr.(a)
Prof. (a) Dr (a). Glaura Scantamburlo Alves Fernandes
Responsável pelo projeto
Departamento de Biologia Geral/CCB
C/C para a Chefia do Depto. de Biologia Geral/CCB
C/C para a Direção de Centro do CCB
C/C Biotério Central do CCB

ANEXO B

Adendo referente ao Projeto aprovado pelo Comitê de Ética (CEUA-UEL)

Universidade
Estadual de Londrina

COMISSÃO DE ÉTICA NO USO DE ANIMAIS

OF. CIRC. CEUA Nº 004/2021

Londrina, 05 de fevereiro de 2021.

Prezado(a) professor(a),

Em resposta ao pedido de adendo referente ao processo **9633.2019.65** "**Efeitos do uso de dimesilato de lisdexanfetamina sobre o desenvolvimento pós natal do sistema genital masculino de ratos**" sob a responsabilidade de **Glaura Scantamburlo Alves Fernandes** e previamente aprovado pelo OF. CIR. CEUA 82/2019, a CEUA-UEL certifica que o mesmo teve parecer aprovado em reunião realizada em 02/02/2020.

É solicitado que 20 ratos machos já pertencentes ao projeto sejam submetidos a um período de jejum de 12h para determinar a glicemia de jejum. O sangue será coletado após anestesia por isoflurano e eutanásia do animal por punção cardíaca, conforme protocolo previamente aprovado. Tal solicitação se justifica pelo fato de não existir dado prévio na literatura e que essas informações contribuirão com os demais dados de avaliação sistêmica previamente aprovados. Não haverá alteração do delineamento experimental bem como dos procedimentos de cuidados e bem estar animal previamente aprovados.

Cumpre orientar que caso pretendam-se quaisquer alterações no protocolo experimental aprovado, deve-se submeter o novo protocolo à apreciação da CEUA/UEL anteriormente à execução das modificações. Coloco-me à disposição para quaisquer esclarecimentos que se fizerem necessários. Sem mais para o momento, subscrevo-me, cordialmente,

Profª Drª Maria Fernanda Rodrigues Graciano
Coordenadora da Comissão de Ética no Uso de Animais
Universidade Estadual de Londrina
ceua@uel.br / (43) 3371-5454

Profa. Dra. Maria Fernanda Rodrigues Graciano
Coordenadora da CEUA/UEL

Ilmo.(a) Sr.(a)
Prof. (a) Dr. (a) Glaura Scantamburlo Alves Fernandes
Responsável pelo projeto
Departamento de Biologia Geral/CCB
Centro de Ciências Biológicas/CCB

ANEXO C

Guide for Authors

Toxicology:

https://www.elsevier.com/journals/toxicology/0300-483X/guide-for-authors

Archives of Toxicology:

https://www.springer.com/journal/204/submission-guidelines